Modelling of Coal Devolatilization

Ponugoti Venkata Prakash

A Thesis Submitted to

Indian Institute of Technology Hyderabad

In Partial Fulfillment of the requirements for

The Degree of Master of Technology

भारतीय प्रौद्योगिकी संस्थान हैदराबाद
Indian Institute of Technology Hyderabad

Department of Chemical Engineering

Indian Institute of Technology Hyderabad

July 2016

Declaration

I declare that this written submission represents my ideas in my own words, and where ideas or words of others have been included. I have adequately cited and referenced the original sources. I also declare that I have adhered to all principles of academic honesty and integrity and have not misrepresented or fabricated or falsified any idea/data/fact/source in my submission. I understand that any violation of the above will be a cause for disciplinary action by the Institute and can also evoke penal action from the sources that have thus not been properly cited, or from whom proper permission has not been taken when needed.

P. V. Prakash

(Signature)

Ponugoti Venkata Prakash
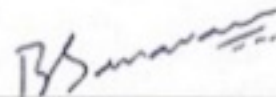(Student Name)

CH14MTECH11017
(Roll No)

Approval Sheet

This thesis entitled Modelling of Coal Devolatilization by **Ponugoti Venkata Prakash** is approved for the degree of Master of Technology from IIT Hyderabad.

_____

Dr Vinod Janardhanan (Adviser)

Department of Chemical Engineering

IIT Hyderabad

_____

Dr Narasimha Mangadoddy (Internal Examiner)

Department of Chemical Engineering

IIT Hyderabad

_____

Dr Saravanan Balusamy (External Examiner)

Department of Mechanical Engineering

IIT Hyderabad

_____

Dr Raja Banerjee (Chairman)

Department of Mechanical Engineering

IIT Hyderabad

Acknowledgments

It gives me an immense pleasure to acknowledge my sincere thanks to the people who have helped me directly or indirectly for making this day possible.

First and foremost, I am indebted to Dr. Vinod M Janardhanan, my adviser, who trusted my abilities and chosen me for this project. I am very much fortunate to work under his guidance and for the support that I received during the course of my project. I express my gratitude to my adviser Dr. Vinod M Janardhanan for his moral support, guidance and encouragement, which inculcated me with the right mind set towards research excellence. From beginning, he created a comfortable environment, which helped me in having fruitful discussions, without which, I could not have finished this dissertation. Those numerous discussions will always be a priceless lectures for which I will remain ever grateful to him.

My devout thanks to K. M. Dakshina Murty and B. Sivaram Pramod of Bharat Heavy Electrical Limited Hyderabad, who showed a great character in clearing my doubts and providing me with the valuable information and suggestions.

I owe to a great extent to the faculty of Chemical Engineering Department for their motivational lectures, unforgettable encouragement and practical experience rendered. I appreciate Dr. Saptarshi Majumdar for his valuable lecture series on non-equilibrium thermodynamics, which had a great impact on research ideologies.

My sincere gratitude to the committee members Dr. Raja Banerjee, Dr. Narasimha Mangadoddy and Dr. Sarvanan Balusamy, whose valuable suggestions and constructive criticism helped in presenting this work of what it is now.

I'm fortunate to have classmates and friends, who showed a great support in times of needy. Especially, I'm grateful to Kunal, who understood me very well and stood with me in tough times. It would be fair to thank Ezra, Akash, Janaki Ram, Alekhya, Monica Sharma, Premlatha, Manohar, Koteswara Rao and Vivek Pawar for giving me memorable moments, which I would cherish for the rest of my life.

Finally, Its my family's unconditional support and infinite love made me what I'm. Their support and encouragement in every stage of my life was and will be precious and valuable.

Dedication

To my beloved parents

Abstract

Pulverized fuel combustor holds a great importance when compared with fluidised bed combustor due to it's high combustion intensities and high heat transfer rates. The science behind pulverized furnace coal combustion is fairly well understood but the crucial interfaces between devolatilisation, secondary gas phase reactions and char combustion makes it difficult to construct a mathematical model. The modelling of coal combustion with some simplifying assumptions, which can be coupled with furnace module and capable of predicting the exit fuel gas concentrations from a pulverized coal furnace is developed as part of this work.

Coal combustion and gasification are complex processes, where devolatilization is always the first step and plays a fundamental role. The key to understanding the phenomena occurring inside the process units thus lies in describing the primary devolatilization and its associated products. It is known that coal devolatilization is a process in which gases, tar, and char are released form coal at elevated temperatures and pressures. Devolatilization is guided by many factors out of which bond strengths of different aromatic and aliphatic molecules plays an important role in formation of tar, gas and char while the stabilization of radicals formed during devolatilization depends the upon amount of hydrogen molecules available, which in turn effects the degradation of coal.

Modelling of coal devolatilization varies from a simple global kinetic model which ignores the structural changes in coal to models like functional-group, depolymerization, vaporization, cross-linking(FG-DVC) and chemical precolation & devolatilization(CPD) which considers the effect of structural changes in coal molecule. The kinetic model used here is based on multi-step global devolatilization kinetics, which accounts for the heating rates on devolatilization process by employing reaction kinetics which are valid both at low and high temperatures.

Starting with the input parameter as ultimate analysis, three reference coal fractions are used to characterize the actual coal. Reference coals participate in the pyrolysis process through a multi-step kinetic mechanism which accounts for the species evolution at low and high temperatures. Finally the pyrolysis of actual coal is assumed to be a linear combination of the reference coals with fractions obtained to characterize the initial coal. Combustion phenomena is accounted by the species $CHAR_C$ and $CHAR_H$ produced during coal pyrolysis. The complete kinetic mechanism for pyrolysis includes 30 reactions with 31 species, while combined pyrolysis and combustion process include 43 reactions and 32 species. As some of the species involved in the mechanisms are lumped compounds, thermodynamic data for those species are developed to implement the energy balance equation.

A single continuous stirred tank reactor (CSTR) system is modelled to implement the reaction mechanism. Model validation has been conducted for 7 different coals with a predefined temperature history. Reasonable prediction in major gas phase species such as CO, CO_2, H_2O and CH_4 has been observed with the developed model, while deviations form the experimental behavior has been observed for the high rank coals due the inaccuracies in prediction of tar species produced during pyrolysis.

List of Tables

List of Figures

Contents

Chapter 1

Fundamentals of Coal Devolatilization

1.1 Introduction

Coal being a metamorphosed product, its molecular configuration continuously changes with geological time. Elucidation of such variation in structure and properties of coal with time helps to look at various means of utilization of different grades of coal. Understanding the basic structures will also help us to understand basic techniques for producing various industry products from coal.

Coal is not homogeneous under the optical microscope and it can be seen to consist of a number of constituents. These are termed as *macerals* and are distinguished on the basis of morphology, optical properties and other properties such as polishing hardness. Macerals recognition is dependent primarily on the morphology and secondarily on the optical properties of the entities. Morphology is the primary criteria for the distinction of macerals, but reflection is also a very important adjunct and in some circumstances may become the determining property. The maceral system developed for coals is useful in understanding the organic matter contribution from each entity to the coal structure. So it is necessary to become familiar with both maceral analysis and vitrinite reflectance of coals.

1.1.1 Classification of coal according to rank

Coals originated through the accumulation of plant debris that were later covered, compacted and changed into the organic rock that we find today. The conversion called *coalification* is based on biological reactions in the first stage, followed by a second phase in which geochemical reactions take place. This phase can be described by a very slow pyrolysis reaction under specially low rates of heating. This transformation successively leads to lignite, bituminous and anthracite coal. The progress in this coalification scale shown in Table 1.1 is called the rank of coal and is suitable for coal classification.

Table 1.1: Rank as parameter of the degree of coalification

Increasing order (Rank)
Peat
Lignite
Sub-bituminous
Bituminous
Anthracite

Coal is chemically and physically heterogeneous rock, mainly containing organic matter. It principally consists of carbon, hydrogen, oxygen and some amounts of sulfur and nitrogen. Coal also contains ash forming inorganic components distributed as discrete particles of mineral matter throughout the coal substance. Its properties like, moisture, carbon content, content of volatile matter, and mean reflectance of vitirinite determining the rank are listed in Table 1.2.

Table 1.2: Classification of rank[1]

Coal property	Relation to rank
Moisture of coal in the seam	Decreasing with rank
Carbon content	Increasing with rank
Volatile matter	Decreasing with rank
Reflectance of Vitirinite	Increasing with rank

1.1.2   Coal petrology

Coals are classified into two groups **Humic** and **Sapropelic**.

- Humic coals are formed from woody substances by a process called *peatification* and they progress in rank from peat to anthracite.

- Sapropelic coals mainly composed of non-woody substances like algae, cuticles, pollen and spores and are formed through a process called *putrefaction* [15].

1.1.3   Structure of coal

Coal macro molecule mainly consists of

- Aromatic clusters.

- Aliphatic and carbonyl side chains and bridges.

Aromatic clusters consists of mainly carbon and less number of hetero atoms such as sulfur, nitrogen and oxygen. They are mostly connected by aliphatic functional groups and rarely with ethers depending upon rank of coal. Bridges which are connected by ethers contain very low bond strength and which are connected by single bond between the aromatic clusters are known as char links. These char links are relatively stable than other bridges in coal molecule.

Side chains in coal molecule are referred as any attachments which do not share the bonds between the aromatic clusters. Mobile phase group in coal are the ones, which are having low bond strength. Schematic of hypothetical structure is shown in Fig. 1.1.

Coal structure can be explained by using different characterization techniques. One such characterization technique, which will not disturb the coal network structure is C NMR spectroscopy.
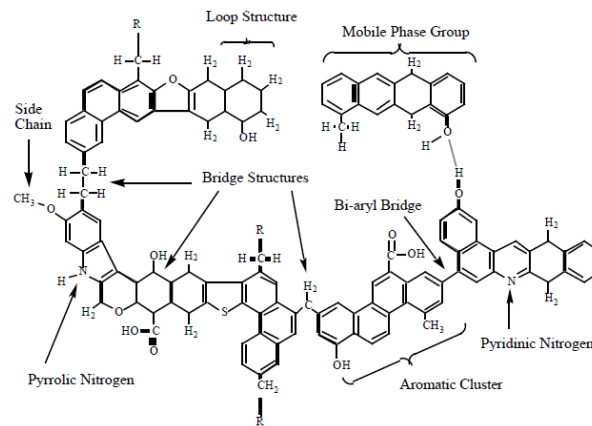
Figure 1.1: Structure of coal molecule[8]

1.2 Coal analysis

The main aim of analyzing coals is to determine whether it will meet the needs for a specific application, and to characterize its quality for future reference. It is useful for obtaining the data of trace elements in coal such as arsenic and also to ascertain whether the pollutants such as sulfur and nitrogen are present in their ore form or not. Coal analysis can be done in different ways and accordingly different types of analytic results can be reported; few of them are dry basis, dry ash-free basis, moist basis.

1.2.1 Proximate analysis

Proximate analysis [16] is used to determine the amount of moisture, volatile matter, ash yields and fixed carbon of a coal sample which can be used to classify rank of coal.

Moisture

Moisture which is readily evaporated in coal is known as *adventitious* moisture and the moisture which is held in coal known as *inherent* moisture. Moisture in coal are classified into four ways

- *Surface moisture*: water held on the surface of coal particles or macerals.

- *Hydroscopic moisture*: water held by capillary action within the micro-fractures of the coal.

- *Decomposition moisture*: water held within the coal's decomposed organic compounds.

- *Mineral moisture*: water that comprises part of the crystal structure of hydrous silicates such as clay.

Volatile matter

Volatile matter analysis is used to determine the amount of gases except moisture which are liberated at high temperatures when coal is heated in the absence of air. The main species considered for volatile matter are hydrogen, carbon monoxide, methane, hydrocarbons and incombustible gases such as carbon dioxide and water vapor. Mineral matter also contribute volatile matter such as water vapor from silicate mineral, sulfur from iron pyrite and carbon dioxide from carbonate minerals.

Fixed carbon

Fixed carbon content is also called as *Carbonaceous* residue yield. It is the carbon left in the coal when the volatile materials are driven off from coal. It differs from ultimate carbon yield of a coal because some amount of carbon in ultimate carbon is driven off as light gases and hydrocarbon species in volatiles.

Ash

It is the non combustible residue left over with the carbonaceous residue after the volatile's are driven off. The components of ash are the bulk mineral matter present in coal. The sum of fixed carbon yield and ash from coal is known is **COKE**. Ash differs from original coal qualitatively and quantitatively due to the loss of water molecules as vapors from clay, sulfur from iron pyrite, carbon dioxide from carbonate mineral and iron oxide from iron pyrite in volatile matter. Moreover ash percentage of a coal determines mineral matter of coal through an empirical formula given by Parr[16]. i.e.,

$$M = 1.08 \text{ A} + 0.55 \text{ S} \tag{1.1}$$

where A is percentage of ash in coal, S is amount of sulfur in coal, M is percentage of mineral matter in coal.

1.2.2 Ultimate analysis

Ultimate analysis [16] of coal is to determine the elemental composition or proportions of chemical elements. So it determines amounts of carbon, hydrogen, oxygen, sulfur and nitrogen compressed in organic portion of coal. It is also used for calculation of heating values, combustion air requirements in coal combustion.

Carbon and hydrogen

Carbon and hydrogen comprises of each 70-95% and 26% dry-ash-free-basis(daf) respectively in organic substance of coal. The results obtained for coal and hydrogen are calculated only for the elements found in organic form. Carbon from mineral carbonates, hydrogen in the form moisture and water in silicate minerals are not included.

Nitrogen

Nitrogen is present in coal only in the form of condensed hetero-cyclic structures such as pyridine and pyrrole. Its determination in coal is based on principles of oxidation, reduction and decomposition.

Sulfur

Sulfur occurs in coal in three different forms

1. Organic sulfur compounds in coal.

2. Iron pyrite.

3. Inorganic sulfates (calcium and iron).

Typical values of organic sulfur is 0.03 w/w and sulfates rarely exceeds 0.001 w/w.

Oxygen

Due the lack of precise methods to determine oxygen in coal, it is has to be determined by subtracting the weight fraction of other elements from 1.

$$O = 1\text{-}(C+H+N+S_{organic}).$$ (1.2)

Other than these elements trace elements such as chlorine and mercury may also be present in coal.

1.2.3 Functional group

Chemical properties of different type of coals changes according to their maceral compositions. So it is hard to describe coal structure under one roof due to large variability in coal maceral composition. Nevertheless, it is possible if the chemical properties are divided into certain number of functional groups which exists in all types of coals. Then the variability in chemical properties are taken care by these functional groups.

Functional group analysis:

Coal can be classified into six functional groups [17]

1. Aromatic nuclei.

2. Hydroaromatic compounds.

3. Alkyl chains.

4. Alkyl bridges.

5. Oxygen groups.

6. Sulfur and Nitrogen.

Aromatic nuclei

Nuclear magnetic resonance spectroscopy analysis of coal shows that 40-75% of carbon is present in aromatic nuclei. Aromatic nuclei are the building blocks coal. Studies on coals mainly consists of two to three condensed ring nuclei such as naphthalene, indene, biphenyl, furan, pyrole, pyridine, benzothiophene, phenanthrene, anthracene and various hetero cyclic structures of oxygen, sulfur and nitrogen rings. Aromatic nuclei which are partly hydrogenated are known as hydroaromatic structures.

Aliphatic structures

Aliphatic structures are divided into

- Aliphatic chains.

- Aliphatic bridges.

- Hydroaromatic structures.

Aliphatic chains include methyl and ethyl where as aliphatic bridges include methylene and ethlyene compounds.

Oxygen

Oxygen containing compounds in coal macro-molecule are

- Phenolic hydroxyl.

- Carboxylic acid groups.

- Aryl-aryl or alkyl-alkyl ether bridges.

- Ring oxygen(Furan-type)

Out of which phenolic hydroxyl constitutes two-third of oxygen in coal. Ether bridges are predominant in bituminous coals. Carboxylic groups are mostly found in sub-bituminous and lignite and furan-type structures are inactive towards reactions.

1.3 Coal properties

Coal physical and thermal properties are important in determining its ability to undergo various conversion processes and also for the design of equipment that is to be employed for various utilization processes such as combustion, gasification and liquefaction.

1.3.1 Physical Properties

Aromaticity

Certain proprieties of coal can be determined by using its aromaticity. The calculation of number liable bridges in coal is used to for predicting the tar forming fraction while coal devolitilization, where liable bridges count depends upon the aromaticity of coal(f_a).

The linear relationship developed by Niksa for predicting the coal structure using NMR parameters used aromaticity equation as given below

$$f_a = (0.0159[C]) - 0.564 \tag{1.3}$$

Aromaticity equation developed by Maroto-Valer et al gives its relationship with H/C atomic ratio

$$f_a = 1.22 - 0.58[H/C] \tag{1.4}$$

Density

X-ray based techniques[18]:

Prakash developed a correlation based on 32 Alberta subbituminous coals.

$$\rho_{g/cc} = 3.5742 - (0.0197[C] + 0.0192[O]) - 0.0691[H] \tag{1.5}$$

Neavel et al. correlation based on 66 high vitrinite content US coals

$$\rho_{g/cc} = 0.023[C] + 0.0292[O] - 0.0261[H] + 0.0225[S] - 0.765 \tag{1.6}$$

Helium based techniques:

Neavel et al. correlation based on 66 sample of lignite to low-volatile bituminous coals

$$\rho_{g/cc} = 0.01556[C] - 0.04117[H] + 0.02247[O] + 0.02049[S] + 0.0208[Ash] \tag{1.7}$$

Density of organic matter on daf basis

$$\rho_{g/cc}^{organic} = 1.534 - 0.05196[H] + 0.007375[O] - 0.02472[N] + 0.003853[S] \tag{1.8}$$

1.3.2 Thermal Properties

Calorific value

Calorific value of coal can be determined by the elemental composition of coal. It can be listed as *Gross calorific* value and *Net calorific* value. Net calorific value does not include water vapor which is formed in coal combustion. An approximate calculation of Calorific value or High heating value is done by the Dulong formula when elemental content in ultimate analysis is weight percentage on dry basis.

$$HHV_{\mathrm{Btu/lb}} = 144.45[C] + 620.28[H] + 40.5[S] - 77.54[O] \tag{1.9}$$

The Dulong-Berthelot formula is used when fuel contents are expressed in % dry ash free basis.

$$HHV_{\mathrm{Btu/lb}} = 81,370 + 345([H]-([O]+[N]-1)/8) + 22.2[S] \tag{1.10}$$

Based on correlations drawn between O/C and O/H atomic ratios to HHV from 160 Indian coals, empirical equation has been developed by Singh and Kakati

$$HHV_{\mathrm{MJ/Kg}} = 37.4541 - 14.204(O/C) - 21.2929(O/H) \tag{1.11}$$

The lower heating value or net heating value can be calculated as

$$LHV_{\mathrm{Btu/lb}} = HHV_{\mathrm{Btu/lb}} - (1,030[H]9)/100 \tag{1.12}$$

Heat capacity

Specific heat of coal increases with increase in moisture, decreases with increase in carbon content increases with increase in volatile matter and ash content. Specific heat can be calculated by using elemental analysis of coal by using

$$C_p = 0.189[C] + 0.874[H] + 0.491[N] + 0.3600 + 0.215[S] \tag{1.13}$$

where C, H, N, O and S are the percentage w/w of respective elements in coal, Where its units in Btu/lb/ °F.

1.4 Gasification fundamentals

Pyrolysis or devolatilization is the first step in coal combustion. Devolatilization occurs when a coal sample is heated in inert or oxidizing environment. Devolatilization is guided by many factors out of which bond strengths of different aromatic and aliphatic molecules plays an important role in formation of tar, gas and char.

Bond energy distribution

The bond energy distribution varies largely in coal, so it is hard to generalize their nature but two rules [2] which are followed by almost all bonds including aromatic and aliphatic bonds are

RULE 1: The rule of least molecular deformation states that "the decomposition by heat will follow that reaction which requires the least possible deformation of molecule"

RULE 2(HABER'S RULE): It states that "the C-C linkage in aromatic series is more stable than the C-H linkage and C-H linkage in aliphatics is more stable than C-C linkage".

The above rule can be explained in the following way. When heat is applied the paraffin's crack instead of forming coke i.e, the C-C bonds are broken but in aromatics condensation of molecule occurs. i.e., carbon-to-carbon combination occurs to form large molecules such as char. Empirical relations are available for the calculations of bond strengths at different temperature in term of free energy. The bond strengths in paraffin and aromatics are given by Eq. 1.14

$$\text{Bond strength} = A + BT\ln(T) + C\,T^2 + DT \tag{1.14}$$

Where A, B, C, D are constants. The constants for paraffins and olefins are given by Table 1.3.

Table 1.3: Respective bond energies in paraffin and olefin series[2]

Bonds	A	B	C	D
C–H:ΔF^0	-3,845	3.0	-0.002	-13.7
C–C:ΔF^0	4,440	0.4	0.002	9.5
C=C:ΔF^0	28,020	2.8	-0.001	-24.9
C–CH$_3$:ΔF^0	-7,620	10.4	-0.006	-36.1

For bond strengths in aromatic linkages we need to consider resonance energy. Resonance energy(ΔF_R^0) creates an extra stability for the molecule due to delocalization of π electrons. So the free energy (ΔF^0) for benzene is given by

$$\Delta F^0 = \text{free energies}(6\text{C-H} + 3\text{C-C} + 3\text{C=C}) + \Delta F_R^0 \tag{1.15}$$

The bond strengths in benzene is given by Eq. 1.14 and Table 1.4. These bond strengths can be tabulated as function of temperature and from Table 1.5 we can say that all aliphtic C-C linkages break before the C-H linkages and from the Table 1.6 we can say that aromatic C-C bonds are much more difficult to break than aliphatic C-C and C-H linkages.

Table 1.4: Respective bond energies in benzene [2]

Bonds	A	B	C	D
$6C\text{–}H:\Delta F^0$	-23,070	18.0	-0.012	-82.2
$3C\text{–}C:\Delta F^0$	13,320	1.2	0.006	28.5
$3C\text{=}C:\Delta F^0$	84,060	8.4	-0.003	-74.7
$C_6H_6:\Delta F_R^0$	-49,910	-8.0	-0.005	41.4
$C_6H_6:\Delta F^0$	24,400	19.6	-0.014	-87.0

Table 1.5: Free energy change of aliphatic bonds at different temperatures [2]

Temperature(K)	C–H	C–C	C=C	C–CH$_3$
600	1281	-12,395	-23,466	-8,477
700	652	-13,904	-22,940	-11,372
800	42	-15,459	-22,433	-15,276
900	-571	-17,058	-21,942	-18,700
1000	-1178	-18,703	-21,462	-22,120

Table 1.6: Free energy change(ΔF_R^0) for resonance version of aromatic compounds at different temperatures[2]

T (K)	Benzene	Xylene	Toulene	Naphthalene
600	55,770	78,780	64,300	110,760
700	57,620	84,000	66,480	114,750
800	59,570	89,280	69,000	118,880
900	61,610	94,570	71,460	123,150
1000	64,720	99,820	73,830	127,540

1.4.1 Coal pyrolysis

Schematic (Fig. 1.2) of coal pyrolysis can be explained in terms of different steps
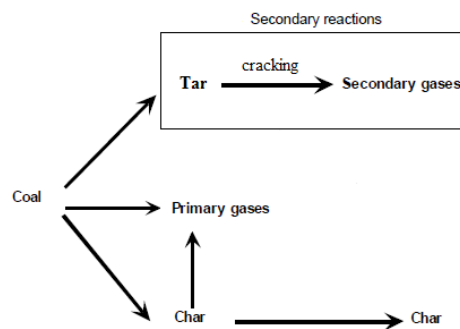
Figure 1.2: Coal pyrolysis

Step 1:

Prior to primary pyrolysis

- Disruption of hydrogen bonds or reduction of hydrogen bonds which leads to melting.

- Light species, which exist as guest molecules, are released by breaking of weak bonds.

Step 2:

- During primary pyrolysis further bond breaking occurs and the weakest bridges labeled as 1, 2 in Fig. 1.3 are broken to produce finite molecular fragments.

- Molecular fragments constitute to form metaplast.
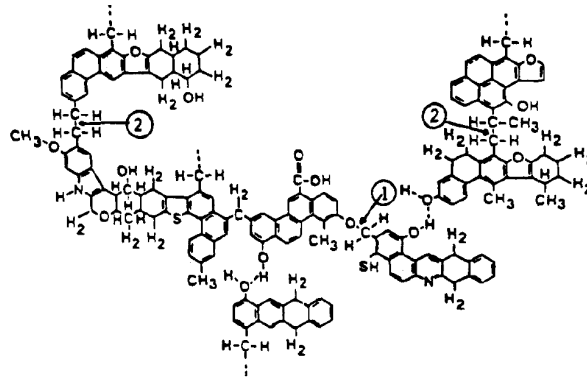
Figure 1.3: Coal[9]
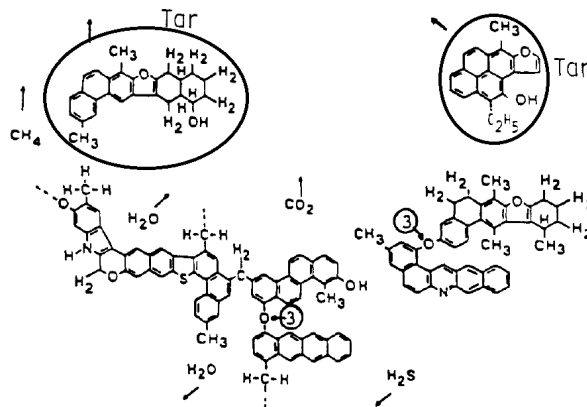
Figure 1.4: Primary pyrolysis[9]

Step 3:

- The fractions or fragments stabilize by abstracting hydrogen from aliphatics and hydro aromatics thus increasing aromatic hydrogen content.

Step 4:

- The fragments which are smaller evaporates and escapes through the pores of coal to produce tar.

- Side chains and broken bridge materials are released as light gas species in the form of light hydrocarbons and oxides.

Step 5:

- The fragments which are large in size formed after devolatilization re-polymerize to form char as their are large enough to pass through the pores of coal.

- Other gases also release during primary pyrolysis by the decomposition of functional groups such as CH_4, CO_2, and H_2O. The release of these gases produces cross-linking to form char

  1. Methane is produced when large molecule release methyl group.
  2. When one large molecules re-polymerize with other molecules at sites where carboxyl groups present they produce carbon dioxide.
  3. When two large molecules re-polymerize at the cost of their two OH groups each from one molecule or one OH and one COOH they produce water-vapor and these are called as condensation reactions.

Cross-linking in low rank and high rank coals have correlation with CO_2 and CH_4 gases released during pyrolysis respectively.

Step 6:

During secondary pyrolysis as shown in Fig. 1.5 additional gas formation occurs.

- CH_4 is released from methyl groups.

- HCN from ring nitrogen.

- CO from ether links.

- H_2 from ring condensation.
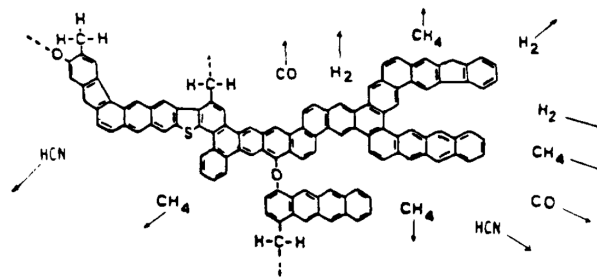
Figure 1.5: Secondary pyrolysis[9]

During devolatilization

- Low rank coals(lignites, sub bituminous) produce large amounts of light gases and less amounts of tar.

- Bituminous coals produce large amount of tar and moderate amount of light gas species.

- High rank coals produces small amounts of tar and light gas species.

1.4.2   Reactions with oxygen

General reaction of volatiles with O_2 [19] can be written as

$$\text{Volatiles} + O_2 \rightarrow CO_2,\ CO,\ H_2,\ H_2S,\ SO_2 \tag{1.16}$$

$$2C(s) + O_2(g) \rightarrow 2CO(g) \quad \Delta H^0_{\text{rxn}} = -221.3\ \text{kJ/gmole} \tag{1.17}$$
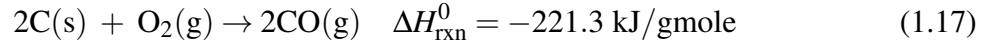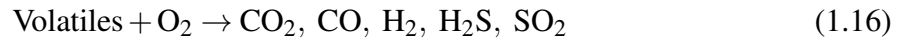
Oxygen reacts with char to produce

$$2C(s) + O_2(g) \rightarrow 2CO(g) \quad \Delta H^0_{\text{rxn}} = -221.3\ \text{kJ/gmole} \tag{1.18}$$

$$C(s) + O_2(g) \rightarrow CO_2(g) \quad \Delta H^0_{\text{rxn}} = -393.98\ \text{kJ/gmole} \tag{1.19}$$
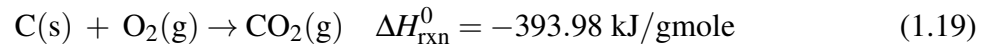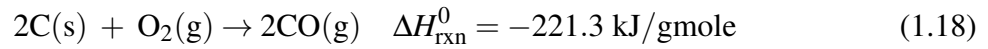
Oxygen reacts with gas species as

$$2CO(g) + O_2(g) \rightarrow 2CO_2(g) \quad \Delta H^0_{\text{rxn}} = -566.65\ \text{kJ/gmole} \tag{1.20}$$

$$2H_2(g) + O_2(g) \rightarrow 2H_2O(g) \quad \Delta H^0_{\text{rxn}} = -484.23\ \text{kJ/gmole} \tag{1.21}$$

$$2CH_4(g) + O_2(g) \rightarrow 2CO(g) + 4H_2(g) \quad \Delta H^0_{\text{rxn}} = -71.44\ \text{kJ/gmole} \tag{1.22}$$
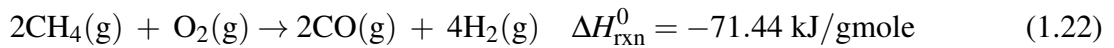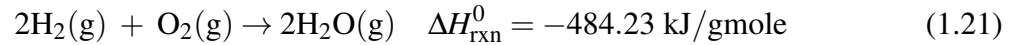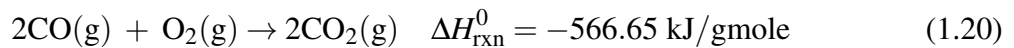
1.4.3   Char reactions

In addition to char combustion, the following reactions also occurs.

Steam gasification

$$C(s) + H_2O(g) \rightarrow CO(g) + H_2(g) \quad \Delta H^0_{\text{rxn}} = +131.46\ \text{kJ/gmole} \tag{1.23}$$

Boudouard reaction

$$C(s) + CO_2(g) \rightarrow 2CO(g) \quad \Delta H^0_{\text{rxn}} = +172.67\ \text{kJ/gmole} \tag{1.24}$$

Methanation reaction

$$C(s) + 2H_2(g) \rightarrow CH_4(g) \quad \Delta H^0_{\text{rxn}} = -74.94\ \text{kJ/gmole} \tag{1.25}$$
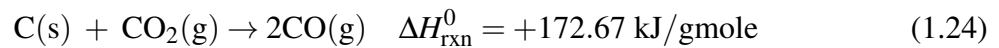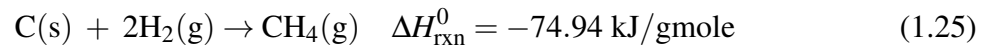
1.4.4   Additional gas phase reactions

If gas temperatures are high the produced light gas species react with each other as given below.

$$CO(g) + H_2(g) \leftrightarrow CO_2(g) + H_2(g) \quad \Delta H^0_{\text{rxn}} = -41.21\ \text{kJ/gmole} \tag{1.26}$$

$$CH_4(g) + H_2(g) \leftrightarrow CO(g) + 3H_2O(g) \quad \Delta H^0_{\text{rxn}} = -206.2\ \text{kJ/gmole} \tag{1.27}$$

Chapter 2

Pyrolysis Models

2.1 Global kinetic model

The devolatilization is a first-order reaction process, with the reaction rate being proportional to the amount of volatile matter still remaining in the coal[20].

$$\frac{dV}{dt} = k(V_\infty - V) \tag{2.1}$$

where

$$k = k_0 \exp(-\frac{E}{RT}) \tag{2.2}$$

Here V_∞ is the total amount of volatile released which is correlated to value obtained from proximate analysis i.e. V_p by

$$V_\infty = Q(1 - V_c)V_p \tag{2.3}$$

Parameters Q, V_c are experimentally determined, where Q, V_c, k_0, E, and V_p are coal specific. This single-step method lacks the flexibility required to describe much of the experimental data available, especially for different heating rates.

2.2 Multi-step model

2.2.1 Two-step model:

Kobayashi model (two-step model) [20] is extension to the single-step model, where single-step is described by the reaction

$$\text{Coal} \xrightarrow{k} (1 - Y)\text{Char} + Y \text{ Volatiles} \tag{2.4}$$

Y is a parameter defined as a fraction of coal devolatilized, which is determined experimentally and is specific to a coal. The single reaction model lacks in fitting the experimental data for wide range of heating rates, whereas the Kobayashi model (two step model) modeled with the following pair of parallel, first-order, irreversible reactions

$$\text{Coal} \xrightarrow{k-1} (1 - Y_1)\,S_1 + Y_1 V_1 \tag{2.5}$$

$$\text{Coal} \xrightarrow{k_2} (1 - Y_2)\,S_2 + Y_2 V_2 \tag{2.6}$$
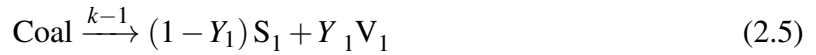
with rate equations

$$\frac{d[\text{coal}]}{dt} = -(k_1 + k_2)[\text{coal}] \tag{2.7}$$

and

$$\frac{dV}{dt} = \frac{dV_1 + dV_2}{dt} = (Y_1 k_1 + Y_2 k_2)[\text{coal}] \tag{2.8}$$

The important feature of this model is $E_1 < E_2$. This approach satisfactorily correlates the data obtained under conditions of transient temperature. This model is limited in its general usability since Y_1, Y_2, k_0^1, k_0^2, E_1, and E_2 are specific to coal.

2.2.2 Multiple-reaction model:

This model [21] assumes that volatiles are released through an numerous independent chemical reactions. These reactions presumably result from differences in strength of the various bonds in the enormous coal molecule, as well as differences in their temperature response. The rate of contribution to devolatilization by a particular reaction is given as

$$\frac{dV_i}{dt} = k_i (V_i^* - V_i) \tag{2.9}$$

subscript i denotes one particular reaction, and unreleased volatile from a particular reaction is given by

$$V_i^* - V_i = V_i^* \exp\left(-\int_0^t k_i dt\right) \tag{2.10}$$

The integral signifies that rate constant is a function of time temperature history. V_i^*, k_0, and E_i are all obtained from experimental data, a problem multiplied by the number of reactions postulated. The problem is simplified if it is assumed that the k_i's differ only in activation energy and that the number of reactions is large enough to permit E to be expressed as a continuous distribution function (example: Gaussian distribution). For the final form equation which relates amount of volatiles released and time-temperature history (heating rate) refer to the subsection 2.4.4.

Infinite parallel reaction model requires only 4 parameters i.e. V^*, k, E_0, and σ when compared to Kobayashi model's 5 parameters. where V^* is the total amount of volatiles from all reactions given by

$$V^* = \Sigma_{i=1}^n V_i^* \tag{2.11}$$

where n is the number of reactions postulated.

Comprehensive codes require a devolatilization model that will produce the composition of the volatile gaseous products and the residual char, as well as the rate of volatiles evolution. All the devolatilization models discussed until now gives only the amount of total volatiles and char released and their rates individually.

In order to know the amounts of different gases in released volatiles, network models which largely relies on coal structure need to be used. Among these models Functional-Group, Depolymerization, Vaporization, Cross-linking (FG-DVC) model explained in section 2.4 predicts the yields and compositions of coal-pyrolysis products(gas, tar, and char). The major difficulty of this model is the relation between coal and model parameters which are coal functional group compositions and rate parameters. Other notable models are DISCHAIN(distributed-energy chain statics) and chemical precolation & devolatilization model(CPD).

The multi-step kinetic model described in the next section postulates the generalized coal devolatilization and combustion model with input parameters as elemental composition of coal.

2.3 Predictive Multi-step model

Multi-step kinetic model[3] is based on the idea that coal is decomposed independently in accordance with different kinetic parameters. Any coal pyrolysis model need to take into account the wide range of experimental conditions which includes heating rates ranging from few K/min to $10^4 - 10^5$ K/s. A very detailed knowledge towards coal structure and reactivity gives insight into coal devolatilization which in turn leads to overcome the above mentioned difficulties. Coal structure and reactivity which are basis to this model are explained in the subsection 1.4.1.

The description of coal pyrolysis process first requires the characterization of the initial structure in terms of atoms, bonds, and average or lumped chemical structure. As a first step of the coal characterization method, the elemental analysis of the coal is corrected and simply normalized to the C,H and O content, on dry, ash (and S, N) free basis. Fig. 2.1 shows the compositions of different coals of interest. Carbon content is always higher than 60 wt% while hydrogen content is usually lower than 7 wt%.

All coals of interest can be included in one of the triangle whose vertexes are pure carbon(CHARC) and two references coals.

1. A reference coal with high oxygen content($COAL_3$).

2. A reference coal without oxygen content($COAL_1$).

A third reference coal($COAL_2$) is selected whose elemental compositions is close to bituminous coals and placed in the middle of the above mentioned triangle. These reference coals are described by lumped monomer structures to save elemental C/H/O compositions. Figure 2.2 gives the structures of reference coals whose monomer formulas are

1. $COAL_1 \rightarrow -C_{12}H_{11}-$

2. $COAL_2 \rightarrow -C_{14}H_{10}O-$
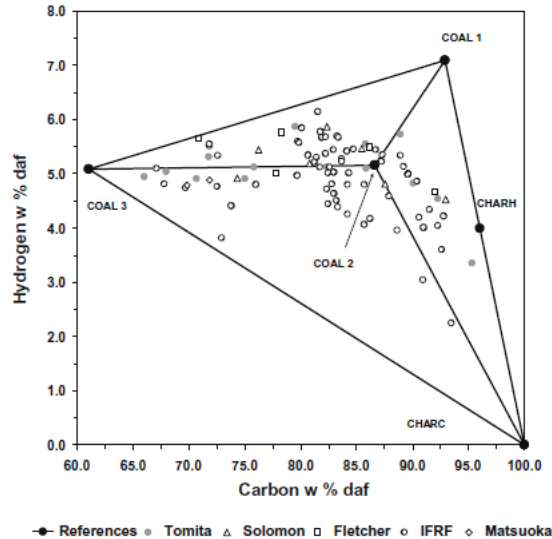
Figure 2.1: Composition of coals[3]

3. $COAL_3 \rightarrow -C_{12}H_{12}O_5-$

4. $CHARH \rightarrow C_2H$(brute formula)

5. $CHARC \rightarrow C$(brute formula)

where $COAL_1$ is considered as a 50/50 mol mixture of $(-C_{12}H_{10}-)$ and $(-C_{12}H_{12}-)$. CHARC is the pure carbon which forms graphite like structure, whereas CHARH is partially hydrogenated char. The compositions of reference coals is given by Table 2.1
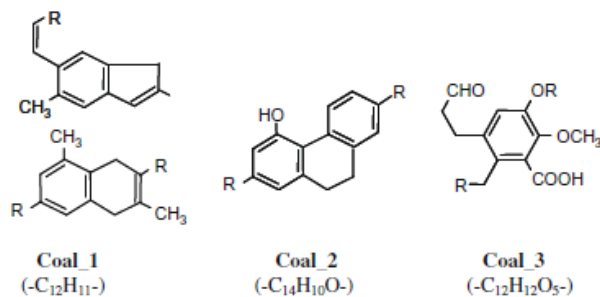
Figure 2.2: Reference coal monomer structures[3]

A coal according to its C, H content lies in one of the triangle formed by reference coals and CHARC, which is then treated as linear combination of three closet reference coals and devolatilization is considered as a straightforward weighted combination of the pyrolysis of the reference coals as discussed in next subsection 2.3.1. Multi-step model works on the principle that "**Blends constituted by similar coals do not show significant deviation from the expected weighted average of the single coals**".

Finally the Table 2.2 gives the elemental composition of given coal and its reference coal fractions.

Table 2.1: Compositions of reference coals[3]

Reference coal	C	H	O	C%	H%	O%
COAL$_1$	12	11	0	92.9	7.1	0.0
COAL$_2$	14	10	1	86.6	5.2	8.2
COAL$_3$	12	12	5	61.0	5.1	33.9
CHARH	2	1	0	96.0	4.0	0.0
CHARC	1	0	0	100.0	0.0	0.0

Table 2.2: Elemental and reference composition of coals[3]

Coal name	C%	H%	O%	COAL$_1$	COAL$_2$	COAL$_3$	CHARC
Morwell	67.94	5.04	27.02	0.0000	0.2522	0.7356	0.0122
Newvale	85.83	5.10	9.07	0.0000	0.9537	0.0356	0.0107
Hongay	95.32	3.36	1.32	0.3566	0.1604	0.0000	0.4830

The reference coals compositions(fractions) for Morwell coal in Table 2.2 is calculated in two steps.

Step 1: Locating the triangle

According to Morwell coal's carbon and hydrogen concentration which are 67.94 and 5.04 respectively, it falls in the triangle whose vertexes are COAL$_2$, COAL$_3$, and CHARC.

Step 2: Carbon, Hydrogen, and Oxygen balance

Carbon, Hydrogen, and Oxygen balance equations are written for the Morwell coal as

$$\text{C,H,O content in Morwell} = \sum_{i=1}^{3} W_i \text{ (C,H,O content in refernce coal of interest).}$$

Here the upper limit of summation is 3 which counts for the vertexes of a triangle. This formula results three linear equations with three unknowns which can be solved for W_1, W_2 and W_3.

Carbon balance:
$$67.94 = W_1\ 86.6 + W_2\ 61 + W_3\ 100 \tag{2.12}$$

Hydrogen balance:
$$5.04 = W_1\ 5.2 + W_2\ 5.1 + W_3\ 0 \tag{2.13}$$

Oxygen balance:
$$27.02 = W_1\ 8.2 + W_2\ 33.9 + W_3\ 0 \tag{2.14}$$

The above equations are solved simultaneously for

W_1 = Fraction of COAL$_2$.

W_2 = Fraction of COAL$_3$.

W_3 = Fraction of CHARC.

which in this case $W_1 = 0.2522$, $W_2 = 0.7356$ and $W_3 = 0.0122$.

2.3.1   Lumped kinetic model of coal pyrolysis

On the basis of the previous characterization a multistep devolatilization mechanism is assumed for each reference coal. Fig. 2.3 shows the schematic of main devolatilization steps.
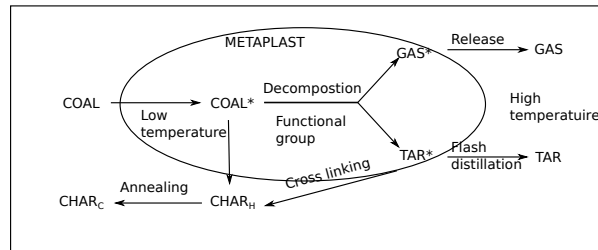
Figure 2.3: Coal decomposition and devolatilization mechanism [4]

The multi-step devolatilization contains 30 reactions with species counting to 27.

The main reactions involved are as follows

1. Low temperature decomposition of reference coals.

2. High temperature decomposition of reference coals.

3. Cross-linking reactions.

4. Annealing reactions.

The complete reaction scheme, with lumped stoichiometries and all the kinetic parameters, is reported in Table 2.3. The mechanism considers the coal to form a matalplastic phase. At low temperatures(or low heating rates) reference coal forms volatiles and char species which will be in metaplast. Later this metaplastic species are released into gas phase which represents devolatilization step. Tar in metaplast phase can be either released with a proper kinetic parameters or it can react with solid residue in cross-linking reactions. At high temperatures(or high heating rates) reference coals directly forms gas, tar, and char.

Light hydrocarbon species are H_2, CH_4 and a lumped pseudo-component with the equivalent formula (-CH_2-), which represents the C_2 - C_5 hydrocarbons. CO, CO_2, and H_2O are main oxygenated compounds. Minor oxygenated compounds with equimolar mixture of formaldehyde and methanol is incorporated using lumped component O_X - C. BTX(benzene, toluene, xylene) formation are also taken into account with single lumped component, where molar B:T:X ratio are 6:3:1. In order to account for annealing effect the reference coals either form $CHAR_H$ which is a partially hydrogenated char and $CHAR_C$ which is completely a carbonaceous structure. Stoichiometric coefficients of the released products evaluated saving the atomic (C,H,O) balances of the initial reference coal.

Table 2.3: Multi-step kinetic model of coal pyrolysis[3]

Reaction mechanism	$A[s, mol, m^3]$	$E[J/mol]$
$COAL_1$		
R_1 $COAL_1 \rightarrow 5\ CHAR_H + 0.1\ CHAR_C + 0.2\ H_2 + 0.9\ CH_4 + C^*_{2-5}$	2.0×10^5	167360
R_2 $COAL_1 \rightarrow TAR^*_1$	1.0×10^5	167360
R_3 $COAL_1 \rightarrow 5\ CHAR_H + 0.25\ CHAR_C + 0.5\ H_2 + 0.75\ CH_4 + C_{2-5}$	1.0×10^{11}	313800
R_4 $COAL_1 \rightarrow TAR^*_1$	1.0×10^{11}	313800
R_5 $TAR^*_1 \rightarrow TAR_1$	2.5×10^9	209200
R_6 $TAR^*_1 + CHAR_H \rightarrow 5.3\ CHAR_H + 3\ CHAR_C + 2.55\ H_2 + 0.4\ CH_4$	2.5×10^1	135980
R_7 $TAR^*_1 + CHAR_C \rightarrow 4.3\ CHAR_H + 4\ CHAR_C + 2.55\ H_2 + 0.4\ CH_4$	2.5×10^1	135980
$COAL_2$		
R_8 $COAL_2 \rightarrow 2\ CHAR_C + 3.94\ CHAR_H + 0.25\ COAL_1 + 0.04\ BTX^* + 0.31\ CH^*_4 + 0.11\ C^*_{2-5} + 0.11\ COH^*_2 + 0.15\ CO^*_2 + 0.41\ H_2O^* + 0.18\ CO^* + 0.265\ H_2$	6.0×10^7	150624
R_9 $COAL_2 \rightarrow 0.61\ CHAR_C + 4.33\ CHAR_H + 0.21\ COAL_1 + 0.16\ BTX^* + 0.27\ CH_4 + 0.7\ CO + 0.1\ H_2O + 0.2\ COH^*_2 + 0.28\ H_2$	4.0×10^{15}	263592
R_{10} $COAL_2 \rightarrow TAR^*_2$	5.0×10^7	150624
R_{11} $COAL_2 \rightarrow TAR^*_2$	4.0×10^{14}	263592
R_{12} $TAR^*_2 \rightarrow TAR_2$	2.4×10^6	163176
R_{13} $TAR^*_2 + CHAR_H \rightarrow 1.5\ CHAR_C + 7\ CHAR_H + H_2O^* + 0.5\ CH_4$	4.5×10^3	125520
$COAL_3$		
R_{14} $COAL_3 \rightarrow 2.73\ CHAR_C + 1.8\ CHAR_H + 0.22\ COAL_1 + 0.08\ BTX^* + 0.1\ CH_2O + 0.1\ CH_2O + 0.1\ CH_4O + 0.11\ CH^*_4 + 0.11\ C^*_{2-5} + 0.2\ H_2 + 0.6\ COH^*_2 + 2.2\ H_2O^* + 0.1\ CO_2 + 0.4\ CO^*_2 + CO^*$	2.0×10^7	138072
R_{15} $COAL_3 \rightarrow COAL^*_3$	5.0×10^{15}	255224
R_{16} $COAL^*_3 \rightarrow 1.5\ CHAR_H + 0.82\ CHAR_C + 2.08\ CO + 0.125\ CH_2O + 0.125\ CH_4O + 0.14\ CH_4 + 0.7\ C_{2-5} + 0.5\ CO_2 + 0.47\ COH^*_2 + 0.16\ BTX^* + 0.25\ COAL_1 + 1.2\ H_2O + 0.29\ H_2$	1.2×10^5	125520
R_{17} $COAL_3 \rightarrow TAR^*_3 + CO^*_2 + H_2O$	1.6×10^6	138072
R_{18} $COAL_3 \rightarrow TAR^*_3 + CO^*_2 + H_2O$	2.0×10^{15}	255224
R_{19} $TAR^*_3 \rightarrow TAR_3$	5.0×10^6	135980
R_{20} $TAR^*_3 + CHAR_H \rightarrow 4\ CHAR_H + 2.5\ CHAR_C + 0.2\ CH^*_4 + 2\ COH^*_2 + 0.8\ H_2 + 0.3\ C_{2-5}$	1.4×10^2	125520
Metaplastic release reactions		
R_{21} $CH^*_4 \rightarrow CH_4$	1.0×10^{00}	71128
R_{22} $C^*_{2-5} \rightarrow C_{2-5}$	1.0×10^{00}	71128
R_{23} $BTX^* \rightarrow 0.6\ C_6H_6 + 0.3\ C_7H_8 + 0.1\ C_8H_{10}$	3.9×10^{09}	200832
R_{24} $CO^* \rightarrow CO$	316.2277×10^{-3}	83680
R_{25} $CO^*_2 \rightarrow CO_2$	1.0×10^{-01}	75312
R_{26} $CO^*_2 \rightarrow CO_2$	5.01×10^8	271960
R_{27} $H_2O^* \rightarrow H_2O$	1.0×10^{00}	75312
R_{28} $H_2O^* \rightarrow H_2O$	5.012×10^{10}	251040
R_{29} $COH^*_2 \rightarrow CO^* + H_2$	5.01×10^6	238488
Annealing reactions		
R_{30} $CHAR_H \rightarrow 2\ CHAR_C + 0.5\ H_2$	1.0×10^9	334720

2.3.2 Annealing effect

Before discussing about char combustion and gasification it is important to know more about annealing process of char and its effect on char reactivity.

Thermal annealing:

Thermal annealing[4] is a chemical phenomena in which char particle undergoes a change in their structure to acquire graphitic domains and parallel decrease in the intrinsic reactivity. Thermal annealing mechanisms acts to destroy active sites before the char begins to react. Chars are annealed during heat-up, devolatilization, and throughout gasification.

Annealing effect is considered in the present coal pyrolysis model which accounts for rearrangement of formed $CHAR_C$ to more graphitic structure $CHAR_G$. Three pseudo components are considered in the residual charcoal matrix which are

1. Hydrogenated species $CHAR_H(C_2H)$ with C/H ratio equal to coronene($C_{24}H_{12}$).

2. Amorphous disordered structure $CHARC_C$.

3. Amorphous ordered structure $CHARC_G$.

Here the reactivity of the of different chars are in the order as $CHAR_H > CHAR_C > CHAR_G$. Kinetic mechanisms for thermal annealing is given by Table 2.4.

Table 2.4: Mechanism of the thermal annealing process[4]

	Annealing reactions	Kinetic expression[*in units m³, s, kJ, kmol]	ΔH_r^0*
R_1	$CHAR_H \rightarrow 2\,CHAR_C + 0.5\,H_2$	$1.0 \times 10^9 \exp(\frac{-3.35 \times 10^5}{RT})[CHAR_H]$	0
R_2	$CHAR_C \rightarrow CHAR_G$	$3.0 \times 10^3 \exp(\frac{-2.10 \times 10^5}{RT})[CHAR_C]$	0
R_3	$CHAR_C \rightarrow CHAR_G$	$1.0 \times 10^{11} \exp(\frac{-4.6 \times 10^5}{RT})[CHAR_C]$	0

The reaction R_1 describes the dehydrogenation of $CHAR_H$ to $CHAR_C$ while reactions R_2 and R_3 describes the progressive ordering of $CHAR_C$ to $CHAR_G$ at low and high temperatures.

2.3.3 Char heterogeneous kinetic mechanism

Char heterogeneous reactions[4] mainly includes

1. Char combustion reaction with O_2.

2. Char gasification reaction with H_2O.

3. Char gasification reaction with CO_2.

The reaction R_4 of table is the partial oxidation of $CHAR_H$ to form $CHAR_C$, H_2, and CO. In order to take into account the selectivity to CO/CO_2, two competitive oxidation reactions are considered for both $CHAR_C$ and for $CHAR_G$.

Finally the coupling of coal pyrolysis and char combustion & gasification includes 43 reactions which includes 32 species.

Table 2.5: Char combustion model [4]

	Reaction mechanism	Kinetic expression[*]	ΔH_r^0*
	O_2 Mechanism		
R_4	$CHAR_H + 0.75\,O_2 \rightarrow 0.5\,H_2O + CO + CHAR_C$	$5.5 \times 10^7 \exp(\frac{-1.20 \times 10^5}{RT})[CHAR_H][O_2]^{0.78}$	-231000
R_5	$CHAR_C + O_2 \rightarrow CO_2$	$7.3 \times 10^7 \exp(\frac{-1.35 \times 10^5}{RT})[CHAR_C][O_2]$	-393700
R_6	$CHAR_C + 0.5\,O_2 \rightarrow CO$	$1.5 \times 10^9 \exp(\frac{-1.60 \times 10^5}{RT})[CHAR_C][O_2]^{0.78}$	-110500
R_7	$CHAR_G + O_2 \rightarrow CO_2$	$2.3 \times 10^7 \exp(\frac{-1.55 \times 10^5}{RT})[CHAR_G][O_2]$	-393700
R_8	$CHAR_G + 0.5\,O_2 \rightarrow 2\,CO$	$6.1 \times 10^7 \exp(\frac{-1.80 \times 10^5}{RT})[CHAR_G][O_2]^{0.78}$	-110500
	H_2O Gasification mechanism		
R_9	$CHAR_H + 0.5\,H_2O \rightarrow H_2 + 0.5\,CO + 1.5\,CHAR_C$	$8.0 \times 10^7 \exp(\frac{-1.75 \times 10^5}{RT})[CHAR_H][H_2O]$	65600
R_{10}	$CHAR_C + H_2O \rightarrow H_2 + CO$	$2.6 \times 10^8 \exp(\frac{-2.03 \times 10^5}{RT})[CHAR_C][H_2O]$	131300
R_{11}	$CHAR_G + H_2O \rightarrow H_2 + CO$	$5.0 \times 10^7 \exp(\frac{-2.07 \times 10^5}{RT})[CHAR_G][H_2O]$	131300
	CO_2 Gasification mechanism		
R_{12}	$CHAR_H + 0.5\,CO_2 \rightarrow 0.5\,H_2 + 0.5\,CO + 2\,CHAR_C$	$6.0 \times 10^7 \exp(\frac{-1.87 \times 10^5}{RT})[CHAR_H][CO_2]$	20500
R_{13}	$CHAR_C + CO_2 \rightarrow 2\,CO$	$8.1 \times 10^7 \exp(\frac{-2.07 \times 10^5}{RT})[CHAR_C][CO_2]$	173000
R_{14}	$CHAR_G + CO_2 \rightarrow 2\,CO$	$2.0 \times 10^7 \exp(\frac{-2.13 \times 10^5}{RT})[CHAR_G][CO_2]$	173000

2.4 Functional group model for coal devolatilization

Pyrolysis model assumes coal to be an ensemble of functional groups organized into a number of aromatic-ring clusters which are connected by aliphatic and ether bridges. As discussed in section 1.4.1 tar and light species are competed for coal donatable hydrogen atoms to stabilize. Thus pyrolysis can be viewed as depolymerization in parallel with thermal decomposition of coal to form tar and gas which compete for donatable hydrogen for stabilization, where chemical changes in pyrolysis products occurs due to the variations in concentration of different functional groups. Observations of pyrolysis studies on different coals have shown that when all conditions are held constant except the coal type, kinetic rate coefficients for individual pyrolysis species which are being produced are insensitive to rank [11]. General trends in coal devolatilization which are observed at different temperatures are as follows.

- At low temperatures there is little change or rearrangement in aromatic-ring clusters and decomposition of aliphatic structures gives CO_2 from carboxyl, H_2O from hydroxyl, hydrocarbon gases from aliphatics, and CO from ethers.

- At high temperatures aromatic-ring clusters do break and produce H_2 from aromatic hydrogen, HCN from ring nitrogen, CO from tightly bound ether groups.

Model for coal pyrolysis takes into account of the findings explained above. The model predicts the time and temperature dependent evolution of product species using

1. Rank independent kinetics.

2. Coal functional group compositions.

3. Time-temperature history of coal.

2.4.1 Model assumptions

Three main assumptions used for modeling coal pyrolysis are [10, 11, 22]

1. The functional groups decomposes independently to produce light gas species whose kinetic rate coefficients are insensitive to coal rank.

2. Coal functional groups are decomposed by parallel competing reactions to produce light gas species and tar, where tar is a representative of coal functional group ensemble in a minimally disturbed way.

3. Tar and light gases species competes for coal donatable hydrogen atoms to stabilize. There yield ceases when donatable hydrogen becomes zero.

Assumption 1 is based on the data from pyrolysis of different types or ranks of coals, which resulted in temperature and time-dependent evolution rate coefficient of a particular species decrease in functional group concentration is similar for all coals. Tar as a minimally disturbed compound of parent coal is proven to be assumption 2 by the similarities in elemental composition of tar and coal from FT-IR spectra and NMR spectra. Since donatable hydrogen to stabilize free radicals generally comes from aliphatic or hydrocarbon portion of coal it is evident from FT-IR spectra that tar evolution ceases when the aliphatic peak of chars goes to zero which proves assumption 3.

Assumptions not considered

- Effect of rank dependent and operating condition variations on the tar rate has not been considered and so amount of tar yield is set as a parameter in this model [21] and its calculation is explained in section 2.4.3.

- Cracking of aromatic nuclei of tar to form smaller molecules is not considered.

2.4.2 Functional group model

The functional groups in coal are depleted because of two parallel independent competing reaction, one with products as gas species and other with tar species. To model these two paths with one yielding a product similar in coal composition to the parent coal, coal is represented as a rectangular area with abscissa as 'X' and ordinate as 'Y' dimension [10] as shown in Fig. 2.4(A).'Y' dimension is divided into fractions according to chemical compositions Y_i^0 as shown in Fig. 2.4(A) which represents initial fraction of particular component and their sum over all components is 1 and these Y_i^0's can be obtained from FT-IR analysis. Fig. 2.4(B) represents the initial stages of devolatilization where the 'X','Y' direction decreases to give tar and gaseous species respectively. End of devolatilization is schematically shown in Fig. 2.4(C). The evolution of each functional group into gas is represented by first order in diminishing of Y_i dimension and it is given by

$$\frac{dY_i}{dt} = -K_i Y_i \tag{2.15}$$

X dimension is divided into potential tar forming fraction X^0 and non-tar forming fraction $1 - X^0$. The calculation of tar forming fraction is explained in sub section: 2.4.3. The evolution of tar is represented by first order diminishing of X dimension and it is given by

$$\frac{dX}{dt} = -K_x X \tag{2.16}$$
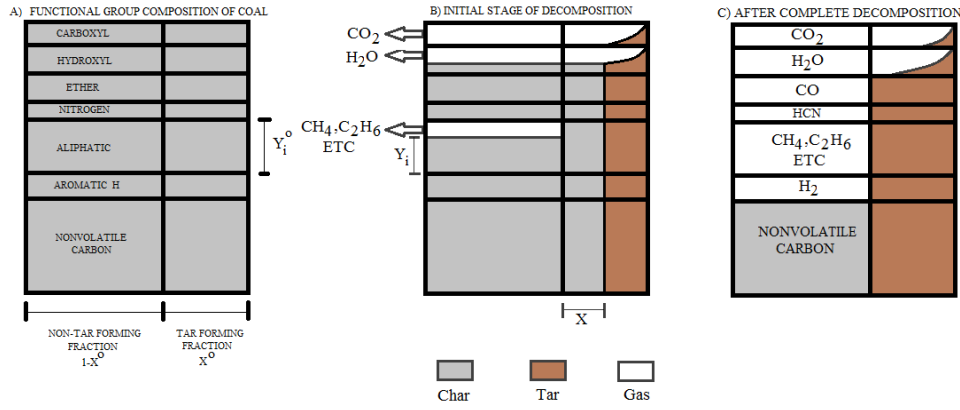
Figure 2.4: Schematic of Functional Group model [10, 11]

Integrating the above Eqs. 2.15 and 2.16 from initial time $t=0$ to time t we get

$$X = X^0 \exp(-K_x t) \tag{2.17}$$

$$Y_i = Y_i^0 \exp(-K_i t) \tag{2.18}$$

The amount of a particular component or functional group in char at any instant is given by

$$W_i(\text{char}) = (1 - X_0 + X)Y_i \tag{2.19}$$

Tar formation from potential tar forming fraction is given by

$$\frac{dW_i(\text{tar})}{dt} = -\frac{dX}{dt} Y_i \tag{2.20}$$

Substituting Eq. 2.16 into Eq. 2.20 and integrating from time $t=0$ to any instant of time t we get amount of a particular component in tar upto specified time t as given below

$$W_i(\text{tar}) = (X^0 Y^0 - X Y_i) \frac{K_x}{K_i + K_x} \tag{2.21}$$

Gas formation from non-tar forming fraction is given by

$$\frac{dW_i(\text{gas})}{dt} = K_i W_i(\text{char}) \tag{2.22}$$

Substituting Eq. 2.19 into Eq. 2.22 and integrating from time $t=0$ to any instant of time t we get amount of a particular component in gas upto specified time t as given below

$$W_i(\text{gas}) = (1 - X^0)(Y_i^0 - Y_i) + W_i(\text{tar}) \frac{K_i}{K_x} \tag{2.23}$$

The equations for amounts of different components in tar,char and gas when summed over all components is equal to 1 and is given by

$$\sum_i^n W_i(\text{char}) + W_i(\text{tar}) + W_i(\text{gas}) = 1 \tag{2.24}$$

The model requires

1. Kinetic rate coefficients of species.

2. Coal's functional group composition.

3. Time-temperature history of coal.

2.4.3 Parametric study on tar yields

Tar yields largely differ depending upon the type of coal and operating pressure of the equipment. In order to account for this variation in tar yields we need to have parameters which considers both coal type and total pressure of the equipment.

A part of coal leads to tar through a mechanism which can be pictured as

$$\text{Coal} \xrightarrow{\text{thermolysis of bridges}} \text{Metaplast} \xrightarrow{\text{transport}} \text{Tar}$$
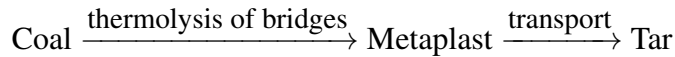
Tar evolution from any type of coal depends upon aliphatic bridges between aromatic structures and the donatable hydrogen atoms to stabilize the radicals formed during pyrolysis. To account for these factors we define three parameters viz. α, β, γ_{tar}.

Where

- α & β $\longrightarrow$ considers the effect of pressure of the equipment.

- γ_{tar} $\longrightarrow$ considers the effect of coal type.

Coal Specific Parameter γ_{tar}:

A coal specific parameter γ_{tar} is used for correlating tar yields with different coal types and it is formulated as.

$$\gamma_{tar} = \frac{\text{Number of liable bridges} * \text{Amount of abstractable hydrogens}}{\text{Number of cross linked bridges}} \tag{2.25}$$

The numerator and denominator terms are given by Table 2.6.

$$
\begin{aligned}
\text{Notations : } [\text{C}] &= \text{the carbon content of coal(wt \% dmmf)} \\
[\text{O}] &= \text{the oxygen content of coal(wt \% dmmf)} \\
[\text{So}] &= \text{the organic sulfur content of coal(wt \% dmmf)} \\
[\text{H}] &= \text{the hydrogen content of coal(wt \% dmmf)} \\
[\text{OH}] &= \text{the hydroxyl group content of coal(wt \% dmmf)} \\
&= 33.2 - 0.35 \, [\text{C}] \\
f_a &= \text{the aromacticity} \\
&= 0.850526 - 2.008147 \left(\frac{[\text{C}]}{100} \right) + 2.241218 \left(\frac{[\text{C}]}{100} \right)^2
\end{aligned}
$$

Table 2.6: Equations and Assumptions to Compute γ_{tar} [5]

Numerator\Denominator	Empirical equation
Number of liable bridges	$\left[\frac{(1-f_a)[C]}{12}\right]^{1.8}$
Assumption:	Liable bridges are aliphatic and its concentration is assumed to be proportional to aliphatic carbon content of coal.
Amount of abstractable hydrogen's	$\frac{[H]}{1} - \frac{[OH]}{17}$
Assumption :	Abstractable hydrogen is the hydrogen attached to aliphatic carbon. Its concentration is proportional is given by amount of elemental hydrogen in coal. OH groups has to be subtracted since they compete for abstractable hydrogen.
Number of cross linked bridges	if $[O] > 3.5$ % dmmf. $\frac{[O]}{16} + \frac{So}{32.066}$ if $[O] \leq 3.5$ % dmmf. $\frac{3.5}{16} + \frac{So}{32.066}$
Assumption	Cross linking bridges consists of ether and thioether structures. Their concentrations are assumed to be proportional to elemental oxygen and organic sulfur of coal.

Pressure dependent parameters α, β:

Tar yield X_{tar} at any given pressure is correlated with γ_{tar} and is given by

$$X_{tar} = \alpha + \beta \gamma_{tar} \tag{2.26}$$

where γ_{tar} is given by Eq. 2.25 and α, β are dependent upon both γ_{tar} and pressure and it is given by Table 2.7.

2.4.4 Distributed Activation Energy Model (DAEM)

Reaction modeling of all heterogeneous substances such as coal and cellulose can be described by Gaussian distribution of activation energies. These are termed as heterogeneous compounds because there are composed of chemically distinct functional groups. This approach assumes that each and every functional group is decomposed by a large number of independent parallel reactions, which are having continuous distribution of activation energies [1, 6, 21] as shown in

Table 2.7: α, β values for different pressures and γ_{tar}[5]

γ_{tar}	values of α, β
$\gamma_{tar} < 15$	$\alpha(10 \text{ Pa - 9 MPa}) = 2$, $\beta(10 \text{ Pa - 9 MPa}) = 0$
$\gamma_{tar} \geq 15$, $\gamma_{tar} \leq 31$	$\alpha(10 \text{ Pa to 100 Pa}) = -30.8$, $\beta(10 \text{ Pa to 100 Pa}) = 2.2$ $\alpha(0.1 \text{ MPa}) = -22.4$, $\beta(0.1 \text{ MPa}) = 1.6$ $\alpha(1 \text{ MPa}) = -16.8$, $\beta(1 \text{ MPa}) = 1.3$ $\alpha(2.5 \text{ MPa to 9 MPa}) = 10.2$, $\beta(2.5 \text{ MPa to 9 MPa}) = 0.8$
$\gamma_{tar} \geq 31$	$\alpha(10 \text{ Pa to 100 Pa}) = 37$ $\alpha(0.1 \text{ MPa}) = 28$ $\alpha(1 \text{ MPa}) = 22$ $\alpha(2.5 \text{ MPa to 9 MPa}) = 15$ $\beta(10 \text{ Pa to 9 MPa}) = 0$

Fig. 2.5. Among the detailed individual volatile product formation models, a growing number employ a Gaussian distribution of activation energies to describe the evolution of individual species.

The main advantage of DAEM is that it accounts for different heating rates (K/s), which are observed in pulverized coal fired furnace. It in turn replaces large no of kinetic parameters to account for different heating rates with standard deviation (σ) of Gaussian distribution. Let F amount is being depleted by an unique activation energy E as shown in Fig. 2.5.

$$\frac{dF}{dt} = -k_0 F \exp(-E/RT) \tag{2.27}$$

Amount of F at any particular instant is is given by integration of Eq. 2.27

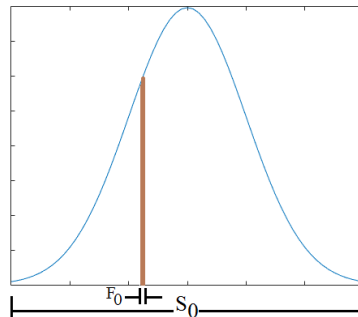$$\frac{F}{F_0} = \exp\left(\int_0^{t_f} -k_0 \exp\left(\frac{-E}{RT}\right) dt\right) \tag{2.28}$$

Figure 2.5: Gaussian distribution

S_0 represents total amount of pyrolyzable material and so F_0 is given by

$$F_0 = S_0 f(E) dE \tag{2.29}$$

The Gaussian distribution function for activation energies is given by

$$f(E) = \frac{1}{\sigma\sqrt{2\pi}} \exp\left(-\frac{(E-E_0)^2}{2\sigma^2}\right) \tag{2.30}$$

The remaining amount of unpyrolyzed material can be represented as

$$S = \int_{-\infty}^{+\infty} F\,dE \tag{2.31}$$

From Equations (2.28) to (2.31) we get

$$\frac{S}{S_0} = \int_{-\infty}^{+\infty} \exp\left(\int_0^{t_f} -k_0 \exp\left(-R/RT\right)\right) f(E)dE \tag{2.32}$$

Eq. 2.32 is the stating point of distributed activation energy analyses which has to be integrated numerically since the integral rarely leads to closed form solution. Any time-temperature can be divided into three periods

1. Heating period.

2. Isothermal period.

3. Cooling period.

For example if the temperature of a substance is increasing which is followed by constant temperature for a certain period and finally decrease in temperature then this profile can be captured by using above mentioned three time periods. This concept of temperature profiles is used to further simply the time integral in Eq. 2.32 by assuming linear approximations of these periods. Therefore, heating rate and cooling rate can be represented as $dT/dt = m_H$ and $dT/dt = -m_C$ respectively.

The time integral in Eq. 2.32 can be expanded by using linear approximations of heating and cooling rates as

$$\int_0^{t_f} -k_0 \exp\left(-R/RT\right) = -\int_0^{T_p} \frac{k_0}{m_H} \exp\left(\frac{-E}{RT}\right) dT - \int_{t_h}^{t_c} k_0 \exp\left(\frac{-E}{RT}\right) dT \tag{2.33}$$

$$-\int_0^{T_p} \frac{k_0}{m_C} \exp\left(\frac{-E}{RT}\right) dT$$

The linear approximations are made in a physical regime of $E/RT >> 1$. The physical significance of this regime is that the temperature ramps up as $T = m \times t$. The closed form solution of first and last integral in Eq. 2.34 can be approximated as

$$\int_0^{T_p} \frac{k_0}{m_H} \exp\left(-\frac{E}{RT}\right) \approx \frac{k_0 RT_p^2}{m_H E} \exp\left(\frac{-E}{RT_p}\right) \tag{2.34}$$

So the final form for the amount of material present at any instant of time is given by Eqs. 2.32,

2.30, 2.34 as

$$\frac{S}{S_0} = \frac{1}{\sigma\sqrt{2\pi}} \int_{-\infty}^{+\infty} \exp\left(\frac{k_0 R T_p^2}{m_H E} \exp\left(\frac{-E}{RT_p}\right)\right) \exp\left(-\frac{(E-E_0)^2}{2\sigma^2}\right) dE \qquad (2.35)$$

Here the cooling rate $m_c = 0$ and isothermal period is zero.

2.4.5 Implementation of DAEM

The implementation of Eq. 2.35 can be simplified by valid assumptions which leads to the removal of double exponential term. Eq. 2.35 can be written as

$$\frac{S}{S_0} = \frac{1}{g\sqrt{\pi}} \int_{-\infty}^{+\infty} \exp\left(\frac{A}{X} \exp\left(-X\right)\right) \exp\left(-\frac{(X-X_0)^2}{g}\right) dX \qquad (2.36)$$

where $A = \frac{k_0 T_p}{m_H}$, $X = \frac{E}{RT_p}$, $dE = RT_p dX$ and $g = \frac{\sqrt{2}\sigma}{RT_p}$

The double exponential shows a steep increase for all values of different parameters. Typically the integral behavior of double exponential term can be approximated as

- $\int_{-\infty}^{+\infty} \exp\left(\frac{A}{X} \exp\left(-X\right)\right) = 0$ when $X < X_C$

- $\int_{-\infty}^{+\infty} \exp\left(\frac{A}{X} \exp\left(-X\right)\right) = 1$ when $X > X_C$

Where X_C is the approximation that we need to make in-order to satisfy the above conditions.

By applying following conditions of double exponential term to Eq. 2.36 we get

$$\frac{S}{S_0} = \frac{1}{g\sqrt{\pi}} \int_{X_c}^{+\infty} \exp\left(-\frac{(X-X_0)^2}{g}\right) dX \qquad (2.37)$$

Which can be written as

$$\frac{S}{S_0} = \frac{1}{\sqrt{\pi}} \int_{Y_c}^{+\infty} \exp\left(Y\right) dX \qquad (2.38)$$

where $Y = (X-X_O)/g$ and $Y_c = (X_c-X_O)/g$

Eq. 2.38 can be evaluated by finding the complementary error function of Y_c as given below

$$\frac{S}{S_0} = \frac{1}{2}\text{erfc}(Y_c) = \frac{1}{2}\left[1 - \text{erf}(Y_c)\right] \qquad (2.39)$$

The accuracy of estimating Eq. 2.35 by this approximation depends upon the estimated value of X_c. Estimation of X_c can be done by three ways using the equation

$$D = \frac{A}{X_c} \exp(X_c) \qquad (2.40)$$

where D is the argument of first exponential term of Eq. 2.36, calculation of D value is given by Table 2.8. The third condition of Table 2.8 gives the best approximation of Eq. 2.36.

Table 2.8: Estimation of X_c [6]

Condition	D value
When double exponential shows maximum slope	1
When double exponential has a value of 0.5	0.693
When argument of double exponential has value of 0.5	0.5

2.4.6   Estimation of initial functional group compositions

As we know that the input parameters for the functional group model are the initial compositions of functional groups Y_i^0's. It's calculation is based on the FT-IR analysis. Even then the estimation of this parameters is not straight forward [13], so it needs a way to predict these parameters for coals whose initial functional group compositions are not known. Using the ultimate analysis of the given coal and the functional group compositions for known coals we should be able to predict these unknown input parameters. This led to develop a correlation approach, which follows the coalification process using the coal's oxygen to carbon and hydrogen to carbon atomic ratios as indicated in the Fig. 2.6 . The basis for this correlation approach is to assume that a relationship exists between the rank and elemental composition of a coal. This conclusion has been drawn form the fact that vitrinite reflectance index (v.r.i) is a function of O/C and H/C [12], moreover v.r.i is also used as rank indicator.

Using the correlation approach, a parameter for unknown coals can be drawn by using the data of extensively studied coals and making a comparison of elemental compositions. The coals upon which this approach is built are called as library coals [23].
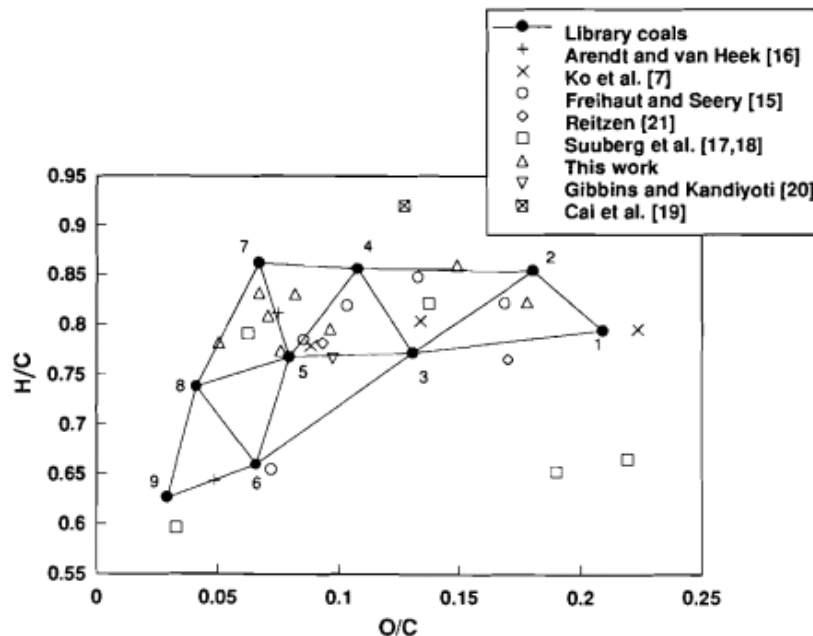

Figure 2.6: van Krevelen diagram [12]

Interpolation technique is used to find the unknown parameters with O/C and H/C as rank indicators. The library coals are positioned in the van Krevelen diagram and joined to form triangular mesh as shown in Fig. 2.6 . Let x^0(i) (i = 1,N) be the parameter for known coal, while

its corresponding parameter for unknown coals be x. Here "N" represents the no of library coals in this case N = 9. Each triangle formed is called as an element and each element consists of three nodes(coals). For finding the unknown parameter of coal, first it is to identified that in which element does it falls. Let that a coal has fallen in k^{th} element, whose nodal numbers are $n_k^{(1)}$, $n_k^{(2)}$ and $_k^{(3)}$. Then the unknown parameter x is given by

$$x = (1 - r - s) \, x^0 \left(n_k^{(1)} \right) + r \, x^0 \left(n_k^{(2)} \right) + s \, x^0 \left(n_k^{(3)} \right) \quad (0 \leq r, s \leq 1) \qquad (2.41)$$

Here r, s are the local coordinates of the unknown coal in the kth element. Their values are evaluated by using the area of the 3 triangles formed by joining the position (P) of unknown coal with that of three nodes. Let the areas of three triangles be $\triangle \, (n_k^{(1)}, n_k^{(2)}, n_k^{(3)})$, $\triangle \, (n_k^{(1)}, P, n_k^{(3)})$ and $\triangle \, (n_k^{(1)}, n_k^{(2)}, P)$ whose vertices are $(n_k^{(1)}, n_k^{(2)}, n_k^{(3)})$, $(n_k^{(1)}, P, n_k^{(3)})$ and $(n_k^{(1)}, n_k^{(2)}, P)$. Finally the values of r, s is given by Eqs. 2.42 and 2.43 respectively.

$$r = \frac{\triangle(n_k^{(1)}, P, n_k^{(3)})}{\triangle(n_k^{(1)}, n_k^{(2)}, n_k^{(3)})} \qquad (2.42)$$

$$s = \frac{\triangle(n_k^{(1)}, n_k^{(2)}, P)}{\triangle(n_k^{(1)}, n_k^{(2)}, n_k^{(3)})} \qquad (2.43)$$

The van Krevelen diagram consists of nine coals out of which six are Argonne premium coals while three are PSOC coals (PSOC 1474, PSOC 1448, and PSOC 1521). The six Argonne premium [13] coals x^0(i)'s are given in Appendix-I, while the 3 PSOC coals x^0(i)'s are unavailable in literature. Out of 8 Argonne premium coals only six are used and they are Beulah-Zap, Wyodak, Illinois 6, Blind Canyon, Pittsburgh 8 and Upper Freeport.

2.4.7 Difference between multi step kinetic and functional group model

The reaction pathway that leads to the formation of primary gases and secondary gases from functional group analysis and devolatilization model based on ultimate analysis is shown in Fig. 2.7
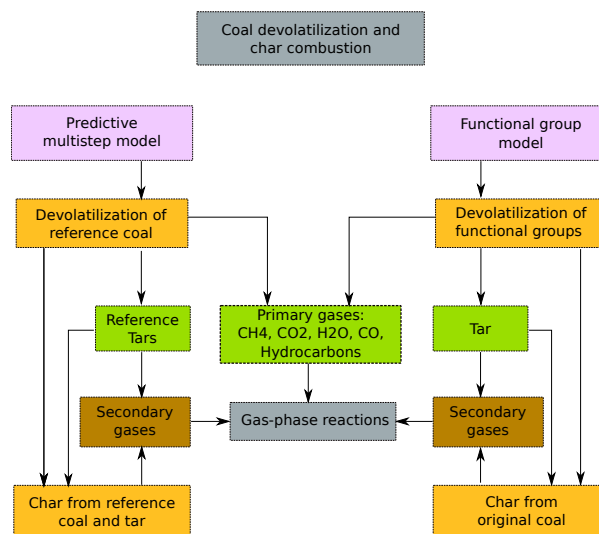

Figure 2.7: Reaction pathway

Chapter 3

Mathematical Modelling

The current work is targeted in developing a coal devolatilization and char combustion model, which can be integrated with furnace module developed for pulverized coal furnace. Furnace module is built on reactor network model, which assumes that entire furnace is divided into number of horizontal sections and each horizontal section is further divided into four halves. This essentially forms four zones, which are treated as continuously stirred tank reactor(CSTR) and each CSTR will have uniform composition and temperature. The detailed kinetics and thermodynamics library accounts for the gas phase reactions happening in each CSTR. So, the numerical model for pulverized coal furnace consists of three main modules. They are

- The furnace model

- The detailed kinetics and thermodynamics library

- The coal devolatalization and char combustion kinetics

Explanation of furnace module is out of the scope of this project, instead furnace module is explained interms of a single CSTR integrated with detail kinetic library and coal kinetics. The following sections explain how the detailed kinetics and thermodynamics library implemented for gas phase reactions and modelling approach adopted for coal devolatalization and char combustion. Fundamental aspects involved in implementing detail kinetic library is explained first followed by its detailed introduction.

3.1 Chemical kinetics - Rate expressions [14]

Consider a set of elementary reactions. In general the set of reactions can be written as

$$\sum_{k=1}^{K} v'_{ki} C_k \Leftrightarrow \sum_{k=1}^{K} v''_{ki} C_k, \quad i = 1, \dots, R \tag{3.1}$$
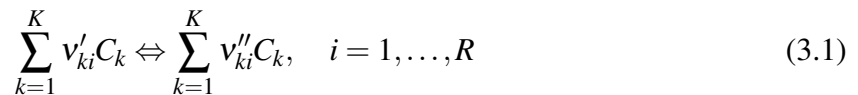
The molar production rate of a species k is then

$$\dot{g}_k = \sum_{i=1}^{R} v_{ki} q_i, \quad k = 1, \dots, K \tag{3.2}$$

where

$$v_{ki} = v''_{ki} - v'_{ki}. \tag{3.3}$$

The rate of progress variable q_i is given by the difference in the forward and reverse reaction rate as

$$q_i = k_{fi} \prod_{k=1}^{K} [X_k]^{v'_{ki}} - k_{ri} \prod_{k=1}^{K} [X_k]^{v''_{ki}},\tag{3.4}$$

where $[X_k]$ is the molar concentration of species k.

3.1.1 Temperature dependence of rate coefficients

The rate coefficients of chemical reactions depend strongly on temperature in a non linear way. Arrhenius described this temperature dependence as

$$k = A_0 \exp\left(-\frac{E}{RT}\right).\tag{3.5}$$

More recent studies however have shown the temperature dependence of pre-exponential factor as well. However this is small in comparison to the exponential dependence

$$k = A_0 T^{\beta} \exp\left(-\frac{E}{RT}\right).\tag{3.6}$$

3.1.2 Relation for forward and reverse reactions

$$K_p = \frac{k_f}{k_r} = \exp(-\Delta_R \overline{G}^0/RT)\tag{3.7}$$

$$\frac{k_f}{k_r} = \exp\left(\frac{-\Delta_R \overline{H}^0 + T\Delta_R \overline{S}^0}{RT}\right)\tag{3.8}$$

$$\frac{k_f}{k_r} = \exp\left(\frac{-\Delta_R \overline{H}^0}{RT}\right) \exp\left(\frac{\Delta_R \overline{S}^0}{R}\right)\tag{3.9}$$

The forward and reverse rate constants k_f and k_r can be expressed in terms of Arrhenius expression, i.e.,

$$k_f = A_f \exp(-E_f/RT) \quad \text{and} \quad k_r = A_r \exp(-E_r/RT)\tag{3.10}$$

Substituting Eq. 3.10 into Eq. 3.9 gives

$$\frac{A_f}{A_r} \exp\left(\frac{E_r - E_f}{RT}\right) = \exp\left(\frac{-\Delta_R \overline{H}^0}{RT}\right) \exp\left(\frac{\Delta_R \overline{S}^0}{R}\right)\tag{3.11}$$

i.e.,

$$E_f - E_r = \Delta_R \overline{H}^0 \quad \text{and} \quad \frac{A_f}{A_r} = \exp\left(\Delta_R \overline{S}^0/R\right)\tag{3.12}$$

3.1.3 Third body reactions

In certain reactions a "third body" is required for the reaction to proceed, for instance is dissociation and recombination reactions such as
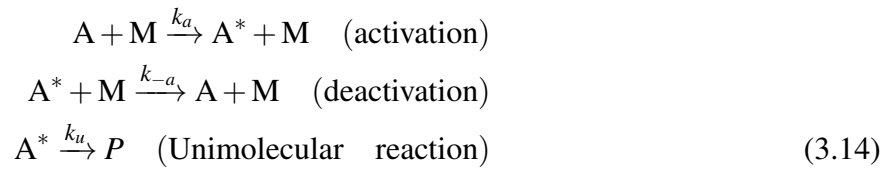
$$H + O_2 + M \Leftrightarrow HO_2 + M$$

When a third body is needed the concentration of the effective third body must appear in the rate of progress variable

$$q_i = \left(\sum_{k=1}^{K} \alpha_{ki}[X_k] \right) \left(k_{fi} \prod_{k=1}^{K} [X_k]^{v'_{ki}} - k_{ri} \prod_{k=1}^{K} [X_k]^{v''_{ki}} \right) \tag{3.13}$$

If all species contribute equally as third bodies then $\alpha_{ki} = 1$ for all k and the first factor is the total concentration of the mixture. However, in reality some species act more efficiently as third bodies and α_{ki} differs from 1 for those species.

3.1.4 Pressure dependence of rate coefficients

The apparent pressure dependence of rate coefficient is an indication that those reactions are not elementary and they are infact sequence of reactions. In the simplest case pressure dependence can be understood using *Lindemann model*. According to this model, for a unimolecular dissociation to occur energy needs to be added to the molecule by collision with other molecules M so that the energy in the molecule is sufficient to break the bond. The excited molecule may decompose into products or deactivates through collision.

$$A + M \xrightarrow{k_a} A^* + M \quad \text{(activation)}$$
$$A^* + M \xrightarrow{k_{-a}} A + M \quad \text{(deactivation)}$$
$$A^* \xrightarrow{k_u} P \quad \text{(Unimolecular} \quad \text{reaction)} \tag{3.14}$$

The rate of formation of P is written as

$$\frac{d[X_P]}{dt} = k_u[X_{A^*}] \tag{3.15}$$

$$\frac{d[X_{A^*}]}{dt} = k_a[X_A][X_M] - k_{-a}[X_{A^*}][X_M] - k_u[X_{A^*}] \tag{3.16}$$

Assuming that the concentration of reaction intermediates are in quasi steady state

$$[X_A^*]\left[k_{-a}[X_M] + k_u\right] = k_a[X_A][X_M] \tag{3.17}$$

$$[X_A^*] = \frac{k_a[X_A][X_M]}{k_{-a}[X_M] + k_u} \tag{3.18}$$

$$\frac{d[X_P]}{dt} = \frac{k_a k_u[X_A][X_M]}{k_{-a}[X_M] + k_u} \tag{3.19}$$

Two extremes can be identified

- Reactions at very low pressure

- Reactions at very high pressure

In the low pressure range the concentration of collision partner is very small, i.e $k_{-a}[X_M] \ll k_u$. In that case the rate of formation of P is

$$\frac{d[X_P]}{dt} = k_a[X_A][X_M] = k_0[X_A][X_M] \tag{3.20}$$

i.e, the rate is proportional to the concentration of the reactants and the collision partner M and k_0 is the low pressure rate coefficient given by

$$k_0 = A_0 T^{\beta_0} \exp(-E_0/RT) \tag{3.21}$$

In the high pressures range the collision partner has large concentration and $k_{-a}[X_M] \gg k_u$:

$$\frac{d[X_P]}{dt} = \frac{k_u k_a [X_A]}{k_{-a}} = k_\infty [X_A]. \tag{3.22}$$

k_∞ is the rate coefficient at high pressure given by

$$k_\infty = A_\infty T^{\beta_\infty} \exp(-E_\infty/RT) \tag{3.23}$$

There are more accurate theories available for the pressure dependent reactions. The appropriate treatment of pressure dependent reactions is necessary since many combustion reaction are carried out at elevated pressures. If the rate law for a unimolecular reaction is written as $d[X_P]/dt = k[X_A]$ then the rate coefficient depends on the temperature and pressure. The theory of unimolecular reaction yields fall off curves that describes the pressure dependence of k for different temperatures. At any pressure the rate coefficient k is given by

$$k = k_\infty \left[\frac{Pr}{1+Pr} \right] F. \tag{3.24}$$

The reduced pressure Pr is given by

$$Pr = \frac{k_0 [X_M]}{k_\infty} \tag{3.25}$$

If F in Eq. 3.24 is unity, then it is Lindemann form. More complex expressions for F are available in the literature. A widely used formalism is the F center treatment of Troe, where 10 parameters are used to determine the rate coefficient at given pressure and temperature.

$$\ln F = \ln F_{\text{cent}} \left[1 + \left[\frac{\ln Pr + C}{n - d(\ln Pr + C)} \right]^2 \right]^{-1} \tag{3.26}$$

$$c = 0.4 - 0.67 \ln F_{\text{cent}} \tag{3.27}$$

$$n = 0.75 - 1.27 \ln F_{\text{cent}} \tag{3.28}$$

$$d = 0.14 \tag{3.29}$$

and

$$F_{\text{cent}} = (1 - \alpha) \exp(-T/T^{***}) + \alpha \exp(-T/T^*) + \exp(-T^*/T) \tag{3.30}$$

3.1.5 Chemically activated bimolecular reaction

In the case of chemically activated bimolecular reaction the rate constant is calculated according to

$$k = k_0 \left[\frac{1}{1+Pr} \right] F \tag{3.31}$$

The calculation of Pr and F remains the same as that in the case of fall of reactions

3.2 Detailed kinetics & thermodynamics library

The detailed kinetics and thermodynamics library lets one to calculate the rate of production (consumption) of various chemical species participating in gas-phase reactions as well as the thermodynamic properties mentioned in section 3.5. There are two input files that are required for the calculation of molar production rates for the gas-phase species and thermodynamic properties and they are

1. chem.inp

2. therm.dat

3.2.1 The *chem.inp* file

The chem.inp file must contain the list of elements and chemical species participating in the reaction mechanism. This file essentially follows the format specification of CHEMKIN software. The listing of elements start with the keyword "elements" and end with the keyword "end". The listing of species starts with the keyword "species" and ends with "end". The listing of reaction mechanism starts with the keyword "reactions" and ends with the keyword "end". The reaction rate constants are assumed to have the units of cm-mol-sec and the activation energies can be mentioned in cal/mol or J/mol. If no units are specified then they are assumed to be in cal/mol. However, while reading *chem.inp*, the program converts all units into SI units. *chem.inp* file used is GRI mech version 3.0 [24].

Simple reactions

Some of these reactions are simple reactions, whose rates are calculated according to Arrhenius expression, where as some reactions are third-body reactions and other are pressure dependent. For example reaction on line 26 is a simple elementary reaction whose pre-exponential factor is given as $A_0=3.87\times10^4$ and the temperature dependence is given by $\beta=2.7$ and $E_a= 6260$. After converting the units to SI, the forward reaction rate constant for this reaction is calculated according to Eq. 3.6. The reverse reaction rate constant is calculated from the thermodynamic properties according to Eq. 3.9, and then the net rate of reaction is given by Eq. 3.4.

While specifying the reactions, each reaction can contain a maximum of six chemical species, and the reactants and products must be separated by the descriptors "=", "<=>", or "=>". The first two descriptors specify reversible reactions and the last one specifies a forward reaction.

```
26)  O+H2<=>H+OH        3.870E+04   2.700    6260.00
```

Third body reactions

If a reaction contains M as reactant, then that represents a third body reaction. Auxiliary information line about collision efficiencies follow the reaction description. For instance reaction on line 22 is a third body reaction with collision efficiencies specified on line 23. The species name is the keyword and the data following the species name is the enhanced efficiency factor. Since the reaction contains the descriptor "<=>", this is a reversible reaction and the net reaction rate is calculated according to Eq. 3.13. The forward and reverse reaction rate constants are still calculated according to Eq. 3.6 and Eq. 3.9 respectively. The collision efficiency of all species that are not present in the auxiliary information line is zero.

```
22)  2O+M<=>O2+M                                   1.200E+17   -1.000        .00
23)  H2/ 2.40/ H2O/15.40/ CH4/ 2.00/ CO/ 1.75/ CO2/ 3.60/ C2H6/ 3.00/ AR/  .83/
```

Pressure dependent reactions

A particular reaction may follow the construct of simple reaction in the high pressure limit and may require a third body collision in the low pressure limit. At either limits the reaction rate can be calculated according to the rate expressions explained above. However, the rate equation becomes more complicated when the pressure conditions are such that the reaction is in between the limits. In order to denote that a reaction occur in the fall of region, a parenthesis is provided for the species or third body. A pressure dependent reaction may also be a chemically activated bimolecular reaction. For fall of reactions, the Arrhenius parameters listed on the reaction line corresponds to the high pressure limit and the low pressure limit Arrhenius parameters must follow the keyword LOW. For chemically activated bimolecular reactions, the low pressure limit parameters appear in the reaction line and the high pressure limit parameters are given with the keyword HIGH in the auxiliary information. The troe parameters may also be provided as auxiliary information and the parameters follow the keyword TROE. For fall of reactions, the reaction rates are constants are calculated according to Eq. 3.24 and the F is calculated according to Eq. 3.26.

In the case of chemically activated bimolecular reactions, the reaction rate constants are calculated according to Eq. 3.31.

3.2.2 The *therm.dat* file

The various thermodynamic properties are evaluated based on the NASA polynomials generally containing 14 coefficient. The first 7 set of coefficients are used for the calculation of properties in the high temperature region and the second set of seven coefficients are used for the calculation at low temperature region. An example of the file format is given in Appendix-I.

3.3 Modelling approach towards coal devolatilization and char combustion

In this section and the upcoming ones the modelling approach adopted for coal devolatilization and char combustion based on the predictive multi-step model as explained in section 2.3 is presented. Detailed explanation of framing governing equations, different phases involved and calculation of unknown properties of different species required for energy balance are presented.

The model consists of two phases i.e, solids and gases as represented in Table: 3.1 , where solids in-turn are divided into reference coal species and metaplast. It is evident form the the Tables 2.3 and 2.4 that coal devolatilization, and gases evolution are mainly dependent upon the solid species concentration. Some amount of evolved gas species such as H_2O and CO_2 reacts with different char species given by Table 2.5, while the remaining gas species participates in the gas phase reactions. Complete devolatilization and combustion model consists of 17 solid species and 11 gas species. Combustion model does not include the diffusion effects for the transportation of gas species to the surface and into the pores of char.

Table 3.1: Phases and species involved in coal devolatilization and char combustion

Solid Species		Gas species
Metaplast	Reference Coal species	
C_{2-5}^*	$COAL_1$	H_2
Tar_1^*	$COAL_2$	CH_4
BTX^*	$COAL_3$	CO_2
CH_4^*	$CHAR_H$	CO
COH_2^*	$CHAR_C$	H_2O
CO_2^*	$CHAR_G$	Tar_1
H_2O^*	ASH	Tar_2
CO^*		CH_2O
Tar_2^*		C_{2-5}
Tar_3^*		Tar_3
$COAL_3^*$		CH_4O
		C_6H_6
		C_7H_8
		C_8H_{10}

3.3.1 Governing equations

The governing equations presented in this section are used for calculating the mass production terms for the species participating in devolatilization and combustion inside a **single continuous stirred tank reactor** for no flow condition. The mass production terms of all species are solved simultaneously for calculating the mass of species. The mass production term for a species is given by

$$\frac{dm_i}{dt} = (\dot{\omega}_i V_s + \dot{g}_i V) M_i \tag{3.32}$$

where

m_i = mass of the species i (Kg).

$\dot{\omega}_i$ = molar production rate of species i from solid phase reactions (mol/m^3-s).

$\dot{g}$ = molar production rate of species i from gas phase reactions (mol/m^3-s).

M_i = molecular weight of species i (Kg/mol).

V_s = volume of solids (m^3).

V = volume of reactor (m^3).

The molar production rate of species depends upon the concentration of solid phase species as discussed earlier and it is calculated by multiplying the reaction rates with the respective stoichiometric coefficients of the species and coal concentration as follows

$$\dot{\omega}_i = \sum_{r=1}^{n} v_i^r k_r \exp(-E_r/RT) \prod [X_k]. \tag{3.33}$$

where

v_i^r = stoichiometric coefficient of i$^{\text{th}}$ species in r$^{\text{th}}$ reaction.

r = total no of reactions.

$[X_k]$ = concentration of k$^{\text{th}}$ solid species.

Calculation of solid species concentration

The input required for calculating the solid species concentration $[X_k]$ are the individual masses. From the individual masses the weight fraction of solid components are calculated as follows

$$x_k = \frac{m_k}{\sum_{k=1}^{k=N_s} m_k}, \quad k = 1, \ldots, N_s \tag{3.34}$$

where

m$_k$ = individual mass.

N$_s$ = no of solid species from Table: 3.1

From the calculated solid component mass fractions the individual solid component concentrations is calculated as follows

$$[X_k]_{mol/m^3} = \rho_{\text{coal}} \frac{x_k}{M_k} \tag{3.35}$$

ρ_{coal} is taken as a constant value in kg/m^3, which is calculated using Eq. 1.8 .

Finally the solid volume in Eq. 3.32 is calculated by using the total solid mass(M_{total}) and coal density(ρ_{coal}), which is given by

$$M_{\text{total}} = \sum_{k=1}^{N_s} m_k, \quad k = 1, \ldots, N_s \tag{3.36}$$

$$V_s = \frac{M_{\text{total}}}{\rho_{\text{coal}}} \tag{3.37}$$

Sample calculations

The sample calculations for detailed understanding of how the mass production values for different species are calculated is explained by considering two different order reactions form Table 2.3 is given in this part of section.

For reaction 1 in Table 2.3

$$R_1 = k_1 \exp(-E_1/RT) [X_{COAL_1}] \qquad mol/m^3-s \qquad (3.38)$$

$$\dot{\omega}_{COAL_1} = -R_1 \qquad (3.39)$$

$$\dot{\omega}_{COAL_H} = 5\,R_1 \qquad (3.40)$$

$$\dot{\omega}_{COAL_C} = 0.1\,R_1 \qquad (3.41)$$

$$\dot{\omega}_{H_2} = 0.2\,R_1 \qquad (3.42)$$

$$\dot{\omega}_{CH_4} = 0.9\,R_1 \qquad (3.43)$$

$$\dot{\omega}_{C_{2-5}^*} = 1\,R_1 \qquad (3.44)$$

$$(3.45)$$

For reaction 7 in Table 2.3

$$R_7 = k_7 \exp(-E_7/RT) [X_{Tar_1^*}] [X_{CHAR_C}] \qquad mol/m^3-s \qquad (3.46)$$

$$\dot{\omega}_{Tar_1^*} = -R_7 \qquad (3.47)$$

$$\dot{\omega}_{CHAR_C} = -R_7 + 4\,R_7 \qquad (3.48)$$

$$\dot{\omega}_{CHAR_H} = 4.3\,R_7 \qquad (3.49)$$

$$\dot{\omega}_{H_2} = 2.55\,R_7 \qquad (3.50)$$

$$\dot{\omega}_{CH_4} = 0.4\,R_7 \qquad (3.51)$$

$$(3.52)$$

3.4 Flow reactors

In previous section the governing equations for single zone batch CSTR is presented. Extension of that case to normal CSTR with mass flow across it is presented in this section.

3.4.1 Species conservation

$$\frac{dm_i}{dt} = \dot{m}_i^{in} - \dot{m}_i^{out} + \dot{\omega}_i M_i V_s + \dot{g}_i M_i V \quad i = 1,\ldots,N_s+N_g \quad Kg/s \qquad (3.53)$$

where

$\dot{\omega}_i$ = molar production rate of species i from solid phase reactions (mol/m^3-s).

$\dot{g}_i$ = molar production rate of species i from gas phase reactions (mol/m^3-s).

M_i = molecular weight of species i (kg/mol).

V_s = volume of solids (m^3).

V = volume of solids (m^3).

N_s = no of solid species.

N_g = no of gas species.

The last two terms in Eq. 3.53 are the source terms for solid phase and gas phase species respectively. If " i " is a solid species then the last term will be zero.

3.4.2 Energy balance

The enthalpy balance can be written as

$$\frac{dh}{dt} = -Q + \sum_{\text{in}} \dot{m}_{\text{in}} h_{\text{in}} - h \sum_{\text{out}} \dot{m}_{\text{out}}. \tag{3.54}$$

Here h_{in} is the enthalpy of an incoming stream in J/kg and h is the enthalpy of the mixture at any given time t in J/kg. The enthalpy of the mixture can be expressed in terms of individual species enthalpies. i.e.,

$$h = m \sum_{k} h_k Y_k \tag{3.55}$$

Taking the derivative of the above equation w.r.t time gives

$$\frac{dh}{dt} = \left(\sum_{k} h_k Y_k \right) \frac{dm}{dt} + m \left[\sum_{k} \left(h_k \frac{dY_k}{dt} + Y_k \frac{dh_k}{dt} \right) \right] \tag{3.56}$$

identifying $\sum_k h_k Y_k = h$, the specific enthalpy of the mixture

$$\frac{dh}{dt} = h \frac{dm}{dt} + m \sum_{k} h_k \frac{dY_k}{dt} + m \sum_{k} Y_k \frac{d(c_{pk}T)}{dt} \tag{3.57}$$

Assuming c_{pk} to be constant w.r.t t

$$\frac{dh}{dt} = h \frac{dm}{dt} + m \sum_{k} h_k \frac{dY_k}{dt} + m \sum_{k} Y_k c_{pk} \frac{dT}{dt} \tag{3.58}$$

identifying $\sum_k Y_k c_{pk} = c_p$ as the specific heat of the mixture

$$\frac{dh}{dt} = h \frac{dm}{dt} + m \sum_{k} h_k \frac{dY_k}{dt} + m c_p \frac{dT}{dt} \tag{3.59}$$

i.e.,

$$h \frac{dm}{dt} + m \sum_{k} h_k \frac{dY_k}{dt} + m c_p \frac{dT}{dt} = \sum_{\text{in}} \dot{m}_{\text{in}} h_{\text{in}} - h \sum_{\text{out}} \dot{m}_{\text{out}} \tag{3.60}$$

i.e.,

$$h \sum_{\text{in}} \dot{m}_{\text{in}} - h \sum_{\text{out}} \dot{m}_{\text{out}} + \sum_{k} h_k \left[\sum_{\text{in}} \dot{m}_{\text{in}} \left(Y_{k,\text{in}} - Y_k \right) + (\dot{\omega}_{k,\text{gen}} + \dot{g}_{k,\text{gen}}) M_k V + \right] + \tag{3.61}$$

$$m c_p \frac{dT}{dt} = \sum_{\text{in}} \dot{m}_{\text{in}} h_{\text{in}} - h \sum_{\text{out}} \dot{m}_{\text{out}}$$

i.e.,

$$h \sum_{\text{in}} \dot{m}_{\text{in}} + m c_p \frac{dT}{dt} = -\sum_{k} h_k (\dot{\omega}_k + \dot{g}_k) M_k V + \sum_{\text{in}} \dot{m}_{\text{in}} h_{\text{in}} - \sum_{k} h_k \left[\sum_{\text{in}} \dot{m}_{\text{in}} \left(Y_{k,\text{in}} - Y_k \right) \right] \tag{3.62}$$

$$h \sum_{\text{in}} \dot{m}_{\text{in}} + m c_p \frac{dT}{dt} = -\sum_{k} h_k (\dot{\omega}_k + \dot{g}_k) M_k V + \sum_{\text{in}} \dot{m}_{\text{in}} \left(h_{\text{in}} - \sum_{k} h_k Y_{k,in} \right) + \sum_{\text{in}} \dot{m}_{\text{in}} \left(\sum_{k} h_k Y_k \right) \tag{3.63}$$

identifying the last terms in the bracket as mixture enthalpy, the energy balance equation finally translates into

$$mc_p \frac{dT}{dt} = -\sum_k h_k(\dot{\omega}_k + \dot{g}_k)M_k V + \sum_{in} \dot{m}_{in}\left(h_{in} - \sum_k h_k Y_{k,in}\right) - Q \tag{3.64}$$

The final form of energy balance equation consists of molar production of species form coal devolatilization, gas phase reactions, char combustion and gasification. In-order to solve the Eq. 3.64 for energy balance terms such as c_{pk} and h_k of individual species needs to be known. From Table 3.1 we can infer that certain species thermodynamic data need to be calculated, as the species are

- Lumped components to represent certain mixture of species.

- Metaplast species to account for transport resistances during devolatilization.

- Solid phase species.

The calculation of missing thermodynamic properties of certain species are calculated on simplifying assumptions based on devolatilization theory explained in section 2.3 and on available literature as explained in the below section.

3.5 Thermodynamic data

The thermodynamic properties such as specific heat(c_p) and enthalpy(h) of species can be calculated form 7-coefficient NASA polynomials. Molar properties such as specific heat, enthaply and enthropy of species can be calculated form 7-coefficient NASA polynomials as follows

Specific heat

The standard state heat capacity may be evaluated as a function of temperature and are given in terms of arbitrary number of polynomial fits according to

$$C_{pk}^0 = R \sum_{n=1}^N a_{nk} T^{(n-1)}. \tag{3.65}$$

The superscript '0' refers to standard stat of 1 atm. For perfect gases the heat capacities are independent of pressure and the standard-state values are the actual values. Using NASA polynomials the molar specific heat is calculated as

$$\frac{C_{pk}^0}{R} = a_{1k} + a_{2k}T_k + a_{3k}T^2 + a_{4k}T^3 + a_{5k}T^4 \tag{3.66}$$

Enthalpy

The standard state values of other thermodynamic properties may be written in terms of Eq. 3.65 as

$$\Delta H_k^0 = \int C_{pk}^0 dT \tag{3.67}$$

i.e

$$\frac{H_k^0(T)}{RT} = \sum_{n=1}^{N} \frac{a_{nk}T^{(n-1)}}{n} + \frac{a_{N+1,k}}{T}. \tag{3.68}$$

The constant of integration ($a_{N+1,k}R$) is the standard heat of formation at 0K. However, this constant is normally evaluated from the knowledge at 298K. Using NASA polynomials the molar enthalpy is calculated as

$$\frac{H_k^0}{RT_k} = a_{1k} + \frac{a_{2k}}{2}T + \frac{a_{3k}}{3}T^2 + \frac{a_{4k}}{4}T^3 + \frac{a_{5k}}{5}T^4 + \frac{a_{6k}}{T} \tag{3.69}$$

3.5.1 NASA polynomials calculation

As explained in the above section the thermodynamic data for species who's NASA polynomials are not known calculated based on simplifying assumptions drawn from devolatilization theory and available literature. The NASA polynomials for all species presented in Table 3.2 are calculates as part of this work.

Table 3.2: Species for which NASA polynomials will be calculated

Solid Species		Gas species
Metaplast	Reference Coal species	
C_{2-5}^*	$COAL_1$	Tar_1
Tar_1^*	$COAL_2$	Tar_2
BTX^*	$COAL_3$	Tar_3
CH_4^*	$CHAR_H$	C_{2-5}
COH_2^*	$CHAR_C$	
CO_2^*	$CHAR_G$	
H_2O^*	ASH	
CO^*		
Tar_2^*		
Tar_3^*		
$COAL_3^*$		

Assumptions: Following are the assumptions made to find the NASA polynomials for species.

1. Coal enthalpy is calculated based on the Einstein specific heat theory. In the model we are considering that $COAL_1$, $COAL_2$, $COAL_3$ and $COAL_3^*$ encompass the coal molecule.

2. $CHAR_H$ is assumed to have NASA polynomials of Coronene($C_{24}H_{12}$), while $CHAR_C$ and $CHAR_G$ will have NASA polynomials of carbon and graphite respectively.

3. New NASA polynomials are calculated for Tar compounds form their composition details[4]

   - Tar_1: 52% wt of $C_{12}H_8$ and 48% wt of $C_{10}H_{12}$

   - Tar_2: 100% wt of $C_{14}H_{10}O$

   - Tar_3: 28% wt of $C_9H_{10}O_2$, 43% wt of $C_{14}H_{10}O$ and 29% wt of $C_{11}H_{12}O_4$

- As all hydrocarbons from C_2-C_5 are released as a lumped species C_{2-5} and it consists of 15-20 % of ethylene[3], it is considered that C_{2-5} will have the same NASA polynomials of ethylene.

4. All activated(metaplast) species will have same NASA polynomials as of gas phase species and this is due to the fact that they are trapped in metaplast before they get released into the gas phase, which means CO_2^* will have the NASA polynomials of CO_2. The exceptional cases are

   - Since $COAL_3^*$ is a part of solid coal and will never exists in gas phase, it is clubbed with $COAL_1$, $COAL_2$ and $COAL_3$ to account for coal enthalpy.
   - New NASA polynomials are calculated for Tar_1^*, Tar_2^*, Tar_3^*, BTX^* and COH_2^*.
     - Tar_1^*, Tar_2^* and Tar_3^* are equated to calculated Tar_1, Tar_2 and Tar_3 NASA polynomials respectively.
     - BTX consists of Benzene, Toluene and Xylene in molar ratio of B:T:X = 6:3:1. So, form this data new polynomials will be calculated for BTX and equated to BTX^*.
     - Similar argument is used for COH_2^* by treating it as a equi-molar mixture of CO^* and H_2.

5. Finally the enthalpy of ash is calculated using an empirical equation, which is of form h = f(T).

For calculating NASA polynomials, mixture average properties are used, which is represented below

Mixture average enthalpy:

$$\overline{H} = \sum_{k=1}^{K} H_k X_k \tag{3.70}$$

Where
$\overline{H}$ = Mixture average enthalpy.
H_k = Individual species enthalpy.
X_k = Mole fraction or mass fraction of species.

3.5.2 Ash

The variable composition of ash and its little experimental data available makes it difficult to calculate the specific enthalpy of ash. Correlations drawn from very little available data makes the model to generate a large errors when applied to a wide range of coal ranks. Considering the above facts a correlation has been drawn for specific enthalpy of ash as function of several oxide components and their concentrations.

Assumptions

Calculation of ash specific enthalpy is based on concentration of major oxide components present in it[7]. The major ten oxide components considered in ash are represented in Table 3.3 with their mean, minimum and maximum weight percentages.

Table 3.3: The Mean, Minimum and Maximum Wt% of ten oxide components in ash[7]

Wt%	SiO_2	CaO	K_2O	P_2O_5	Al_2O_3	MgO	Fe_2O_3	SO_3	Na_2O	TiO_2
Mean	51.68	7.0	1.93	0.25	24.54	1.92	8.22	2.62	0.76	1.08
Minimum	29.38	0.43	0.29	0.10	11.32	0.31	0.79	0.10	0.09	0.53
Maximum	68.35	30.2	4.16	1.77	37.04	3.98	21.74	14.42	2.90	2.65

Calculation

From the above table the specific enthapy(KJ/Kg) of ash is calculated as

$$h_{ash} = \sum m_i \left(h_i - h_{0,i} \right)$$ (3.71)

Where
m_i = mass fraction of components i.
h_i = Specific enthaply of component i at current state(T,P).
$h_{0,i}$ = Specific enthaply of component i at reference state(T_0,P_0).

From the calculated values of h_{ash} using Eq. 3.71 a correlation[7] has been deduced between specific enthalpy(kJ/Kg) and Temperature(K) by using least square method, which is given by Eq. 3.72

$$h_{ash} = 0.0002155 \, T^2 + 0.7618 \, T - 254.20.$$ (3.72)

3.5.3   Coal

The specific heat of coal correlations considering the effect of coal rank and carbonization temperatures plays a major role in modelling coal devolatilization. Model which treats coal as entity of coke(char+ash), primary volatile matter and secondary volatile matter has been reported in literature. The disadvantage of the above mentioned model is that it lacks the ability to account for variable compositions of these mixture. Van Krevelen [25] proposed the coal specific correlation as function of its rank at ambient temperatures. The model assumes that each atom i.e., C, H, O, N and S oscillate only in the direction normal to the plane where the binding forces are week. The specific heat(C) of daf coal given by Van Krevelen depends upon the mean atomic weight(a) of coal, which is given below

$$c = \frac{R}{a} \qquad J/Kg/K$$ (3.73)

The definition of mean atomic weight comes from ultimate analysis of coal

$$\frac{1}{a} = \sum_{i=1}^{5} \frac{y_i}{\mu_i}$$ (3.74)

where
y_i = weight fractions of C, H, O, N and S on daf basis.
μ_i = atomic weights of C, H, O, N and S.

In the present work specific heat model for coal is implemented on the basis of Einstein quantum theory on solids, which is explained below

Specific heat model

This model assumes that solid state atoms oscillates independently in three dimensions[25]. The correlations for instantaneous specific heat and specific enthalpy is as follows

$$c = 3\,R\,g_1(\Theta/T) \qquad\qquad J\,Kg - atom^{-1}\,K^{-1} \qquad\qquad (3.75)$$

$$h = 3\,R\,\Theta\,g_0(\Theta/T) \qquad\qquad J\,Kg - atom^{-1} \qquad\qquad (3.76)$$

where $g_1 = \dfrac{\exp(z)}{\left(\frac{(\exp(z)-1)}{z}\right)^2}$ and $g_0 = \dfrac{1}{\exp(z)-1}$.

Θ = Einstein characteristic temperature.
T = Temperature in K.

when applied Einstein model to coal assuming that all each atom has same characteristic frequency i.e., having same temperature in all three directions, we have for coal specific heat and enthalpy equations as follows.

$$c = 3\,(R/a)\,g_1(1200/T) \qquad\qquad J\,Kg^{-1}\,K^{-1} \qquad\qquad (3.77)$$

$$h = 3600\,(R/a)\,g_0(\Theta/T) \qquad\qquad J\,Kg^{-1} \qquad\qquad (3.78)$$

A characteristic temperature of 1200 reduces Eqs. 3.77 and 3.78 to Eqs. 3.75 and 3.76. A very accurate representation of experimental fit is observed by using two characteristic temperatures[25] one within the layer planes where binding forces are strong and the other normal to planes where binding forces are weak. Equations 3.77 and 3.78 finally becomes

$$c = (R/a)\,[g_1(380/T) + 2\,g_1(1800/T)] \qquad\qquad J\,Kg^{-1}\,K^{-1} \qquad\qquad (3.79)$$

$$h = (R/a)\,[380\,g_0(380/T) + 3600\,g_0(1800/T)] \qquad\qquad J\,Kg^{-1} \qquad\qquad (3.80)$$

3.6 NASA polynomials

The thermodynamic data needed for implementing the energy balance Eq. 3.64 is presented in this section. Implementing the theory explained in the above section resulted in thermodynamic data to calculate the heat capacity and enthalpy. Normal curve fitting techniques are used to find the NASA polynomials for the species whose data are to be calculated based on mixture compositions and also to those species whose data is calculated based on empirical equations.

The results presented here in the form of Tables 3.4, 3.5 and 3.6 are used as the basis for finding the thermodynamic data for unknown species. Table 3.4 is the representation of already available literature data, while Tables 3.5 and 3.6 data has been calculated based on theory explained in the above sections. Calculation of a_7 coefficient in Tables 3.5 and 3.6 are avoided as it is only required for calculating entropy. Instead of calculating reference coals NASA polynomials for both low and high temperatures, it has been calculated for a wide range of temperatures and coefficients are represented in Table 3.5 .

Finally the molar specific heat and enthalpy calculated with the developed new NASA polynomials of Tables 3.5 and 3.6 is compared with the mixture molar enthalpy and specific heat for those species whose calculation is based on mixture properties, while comparison is made with empirical equation for those species whose calculation is based on empirical equation.

Results are given in Figs. 3.1 - 3.14 . In Fig. 3.6 comparison is provided only for specific heat given by simple Einstein model and Einstein model with two characteristic temperatures. Its comparison with experimental data is provided in [25].

3.6.1 NASA polynomials taken from literature

Table 3.4: NASA polynomials known for the following species

Coeff	Low Temperatures			High Temperatures		
	Tar_2	$CHAR_C$	$CHAR_G$	Tar_2	$CHAR_C$	$CHAR_G$
a_1	1.86060189E+01	2.49858500e+00	-6.70566100e-01	2.95530459E+01	2.60208700e+00	1.49016600e+00
a_2	-3.63716443E-02	8.08577700e-05	7.18150000e-03	4.04155118E-02	-1.78708100e-04	1.66212600e-03
a_3	3.08794896E-04	-2.69769700e-07	-5.63292100e-06	-1.60091642E-05	9.08704100e-08	-6.68720400e-07
a_4	-3.89835106E-07	3.04072900e-10	2.14229900e-09	2.91497737E-09	-1.14993300e-11	1.29088000e-10
a_5	1.55168865E-10	-1.10665200e-13	-4.16856200e-13	-1.99585707E-13	3.31084400e-16	-9.20533400e-15
a_6	-1.99286775E+03	8.54587800e+04	-7.33949800e+01	-1.01792833E+04	8.54215400e+04	-7.07401900e+02
a_7	-5.40624758E+01	4.75345900e+00	2.60159600e+00	-1.36141567E+02	4.19517700e+00	-8.71778500e+00
$T_1(K)$	298.150	300	300	1000	1000	1000
$T_2(K)$	1000	1000	1000	5000	5000	5000

3.6.2 NASA polynomials calculated

Table 3.5: NASA polynomials calculated for low temperatures

Coeff	Low Temperature								
	Tar_1	Tar_3	COH_2^*	BTX^*	ASH	$Coal_1$	$Coal_2$	$Coal_3$	$Coal_3^*$
a_1	-9.69349309e+00	6.04492978e+00	3.45378473e+00	1.08338198e+00	6.52270614e+00	2.21882498e-01	2.77651563e-01	3.37677480e-01	3.37677480e-01
a_2	1.19927847e-01	5.72369166e-02	6.63574899e-05	1.95464451e-02	3.69032074e-03	9.16663330e-02	1.14706210e-01	1.39504722e-01	1.39504722e-01
a_3	-9.77173923e-05	6.31251400e-05	1.11746950e-08	7.97701712e-05	-3.73147676e-18	-5.28240975e-05	-6.61011721e-05	-8.03916858e-05	-8.03916858e-05
a_4	3.99534041e-08	-1.30823668e-10	7.15360064e-10	-1.25273455e-07	3.36900707e-21	1.32080493e-08	1.65278269e-08	2.01010031e-08	2.01010031e-08
a_5	-6.46391840e-12	5.81091264e-11	-4.38977754e-13	5.32421834e-11	-1.05196019e-24	-1.19624013e-12	-1.49690915e-12	-1.82052824e-12	-1.82052824e-12
a_6	1.48586071e+04	-2.60475685e+04	-7.68055071e+03	6.33905785e+03	-2.17651864e+03	-4.69979175e+02	-5.88106108e+02	-7.15249668e+02	-7.15249668e+02
a_7	0.0	0.0	0.0	0.0	0.0	0.0	0.0	0.0	0.0
T_1(K)	300	300	300	200	300	273.15	273.15	273.15	273.15
T_2(K)	1430	1300	850	1000	1400	4273.15	4273.15	4273.15	4273.15

Table 3.6: NASA polynomials calculated for high temperatures

Coeff	High Temperature								
	Tar_1	Tar_3	COH_2^*	BTX^*	ASH	$Coal_1$	$Coal_2$	$Coal_3$	$Coal_3^*$
a_1	2.49656771e+01	2.85674439e+01	3.20852958e+00	1.19157225e+01	6.52270614e+00	0	0	0	0
a_2	2.95323628e-02	3.81263628e-02	6.19078757e-04	2.37466371e-02	3.69032074e-03	0	0	0	0
a_3	-8.85444862e-06	-1.53847817e-05	3.86914450e-08	-8.60788662e-06	-2.14316386e-17	0	0	0	0
a_4	9.32526805e-10	2.96012020e-09	-6.44054590e-11	1.39833471e-09	6.50529908e-21	0	0	0	0
a_5	-6.79403070e-15	-2.23332079e-13	9.77063465e-15	-8.40810209e-14	-7.38783210e-25	0	0	0	0
a_6	4.17296556e+03	-3.46511548e+04	-7.61543848e+03	1.86327935e+03	-2.17651864e+03	0	0	0	0
a_7	0.0	0.0	0.0	0.0	0.0	0	0	0	0
T_1(K)	1430	1300	850	1000	1400	0	0	0	0
T_2(K)	3500	3500	3500	6000	3000	0	0	0	0
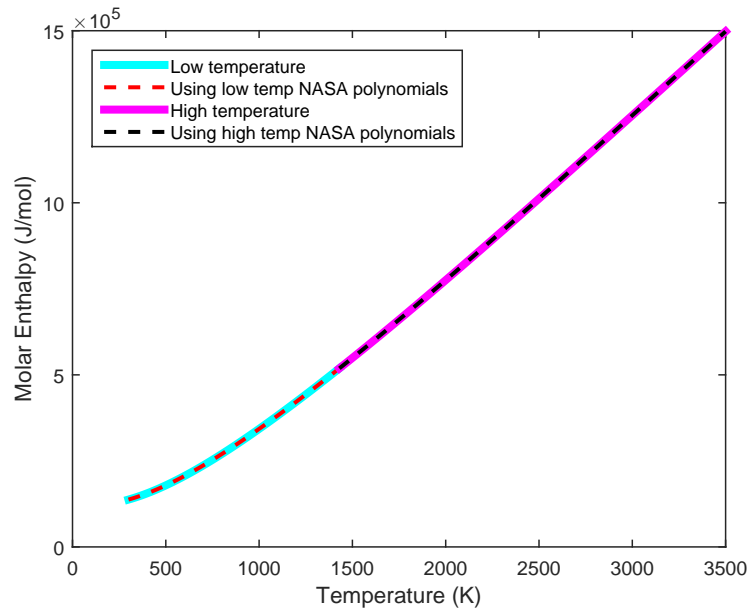
Figure 3.1: Comparison of Tar$_1$ molar enthalpy with calculated NASA polynomials
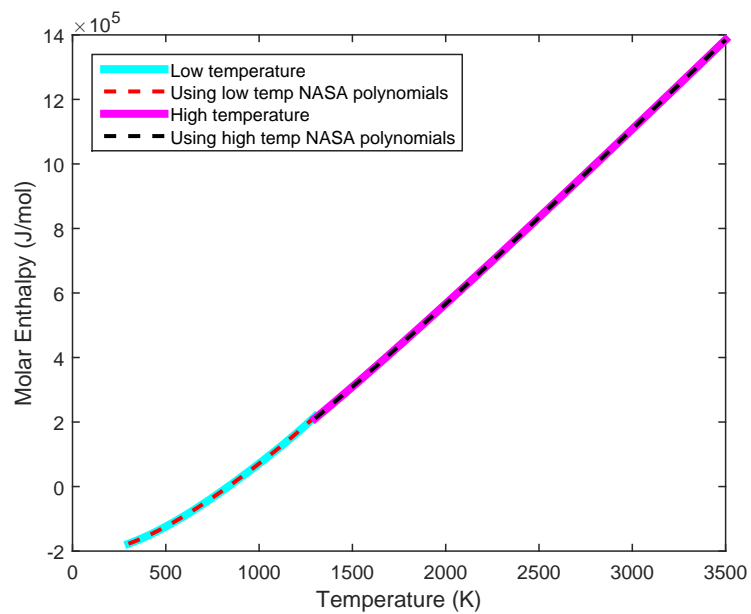
Figure 3.2: Comparison of Tar$_3$ molar enthalpy with calculated NASA polynomials
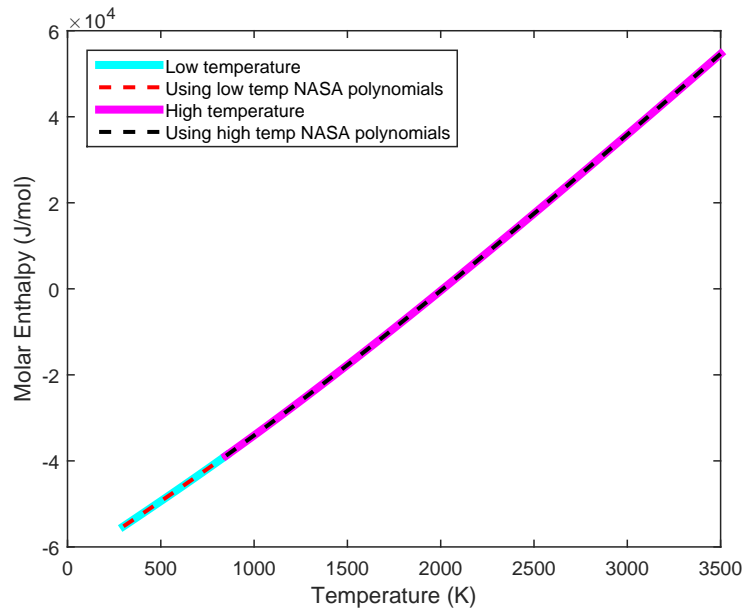
Figure 3.3: Comparison of COH_2^* molar enthalpy with calculated NASA polynomials
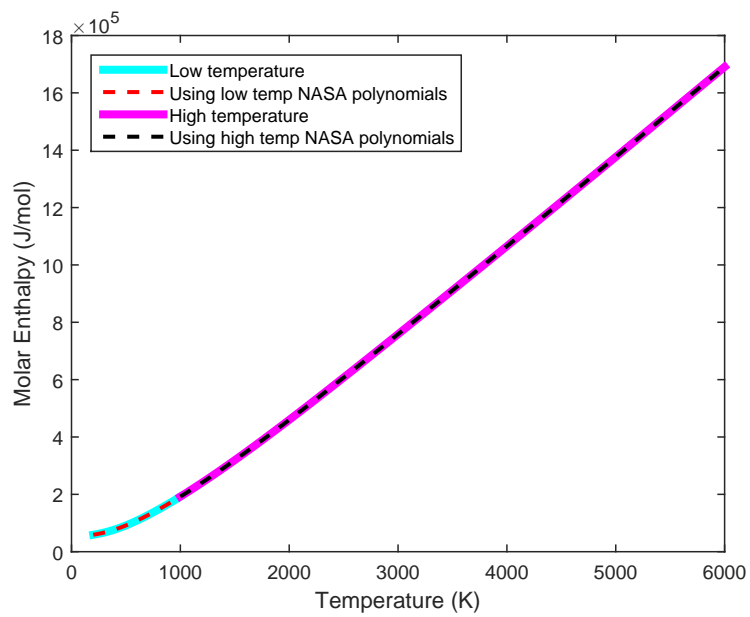

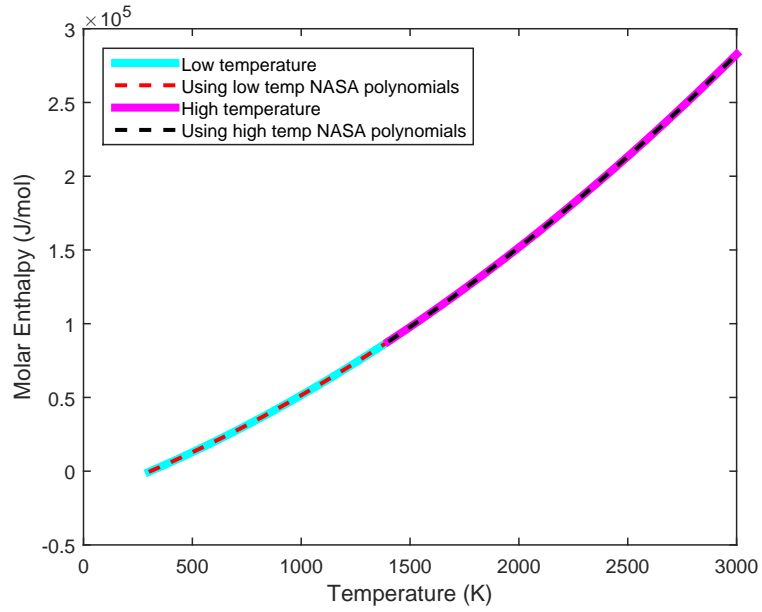Figure 3.4: Comparison of BTX^* molar enthalpy with calculated NASA polynomials

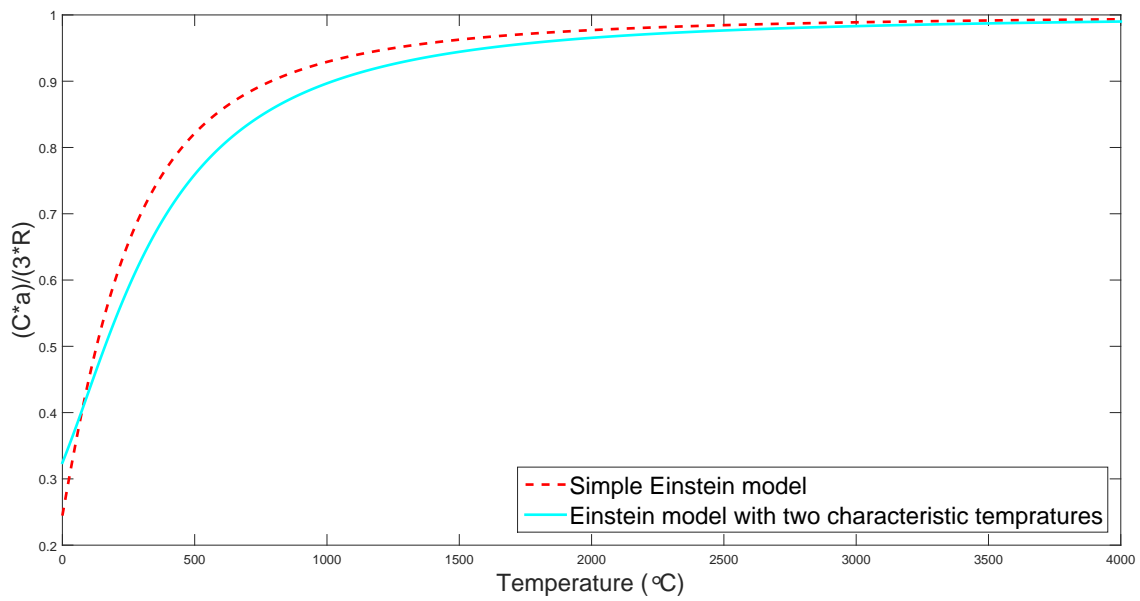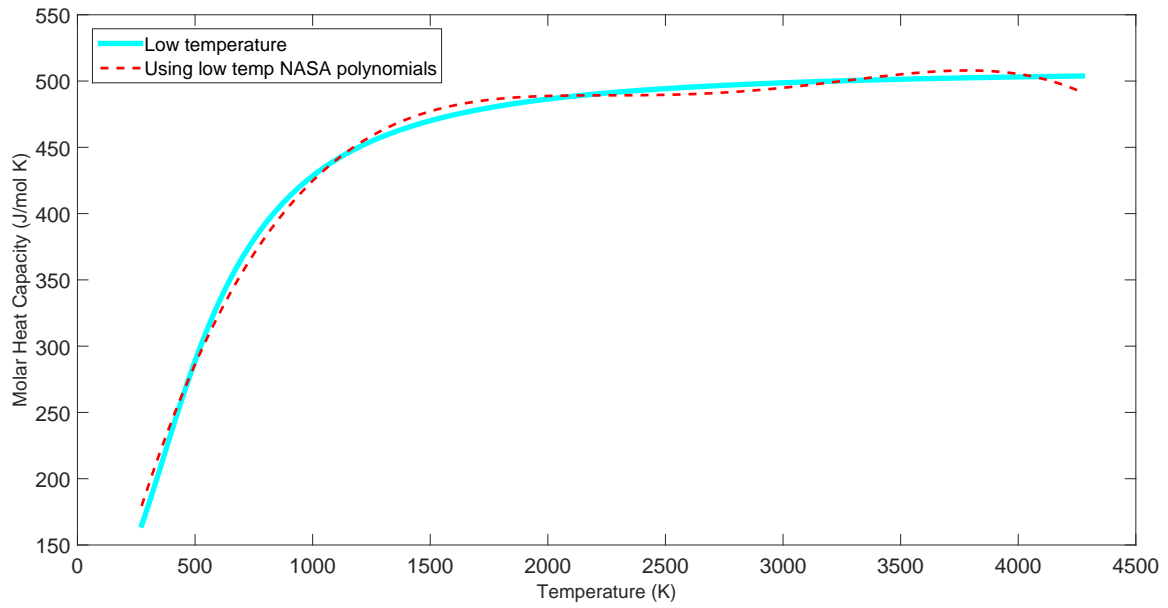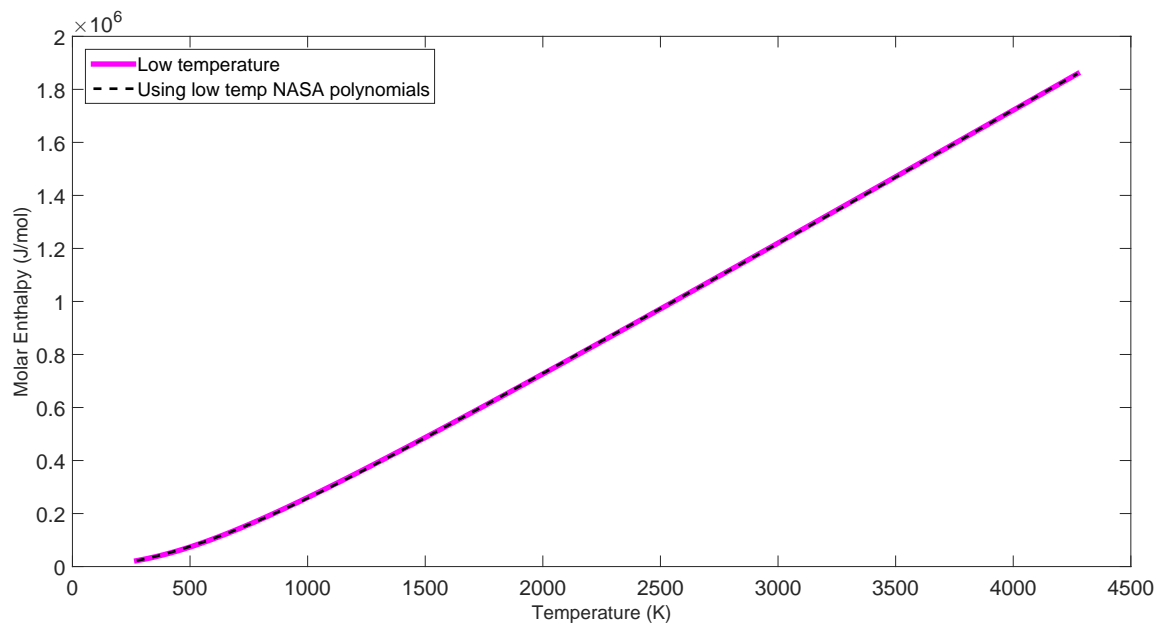Figure 3.5: Comparison of ASH molar enthalpy with calculated NASA polynomials

Figure 3.6: Comparison of Merrick molar enthalpy with calculated NASA polynomials

Figure 3.7: Comparison of Coal$_1$ molar heat capacity with the values calculated using NASA polynomials

Figure 3.8: Comparison of Coal$_1$ molar enthalpy with the values calculated using NASA polynomials
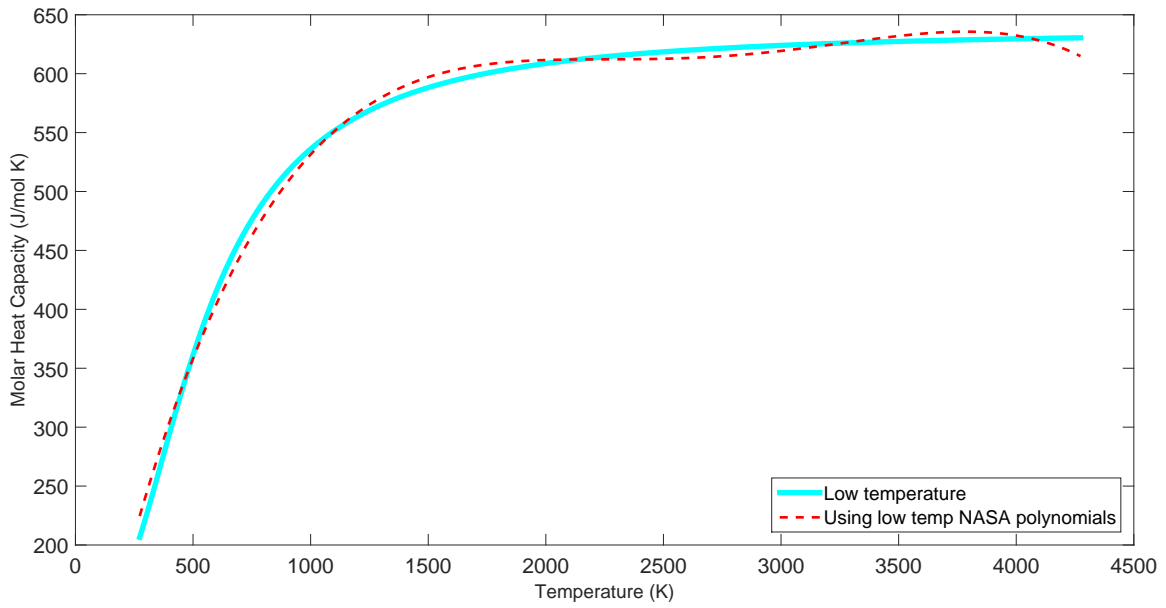
Figure 3.9: Comparison of Coal$_2$ molar heat capacity with the values calculated using NASA polynomials
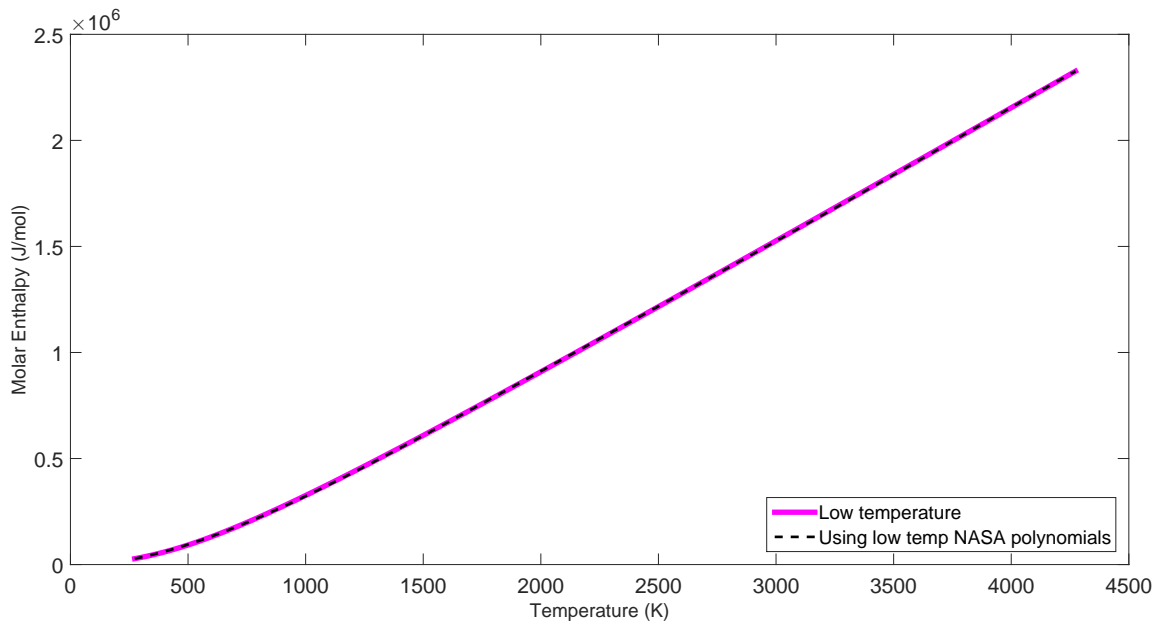
Figure 3.10: Comparison of Coal$_2$ molar enthalpy with the values calculated using NASA polynomials
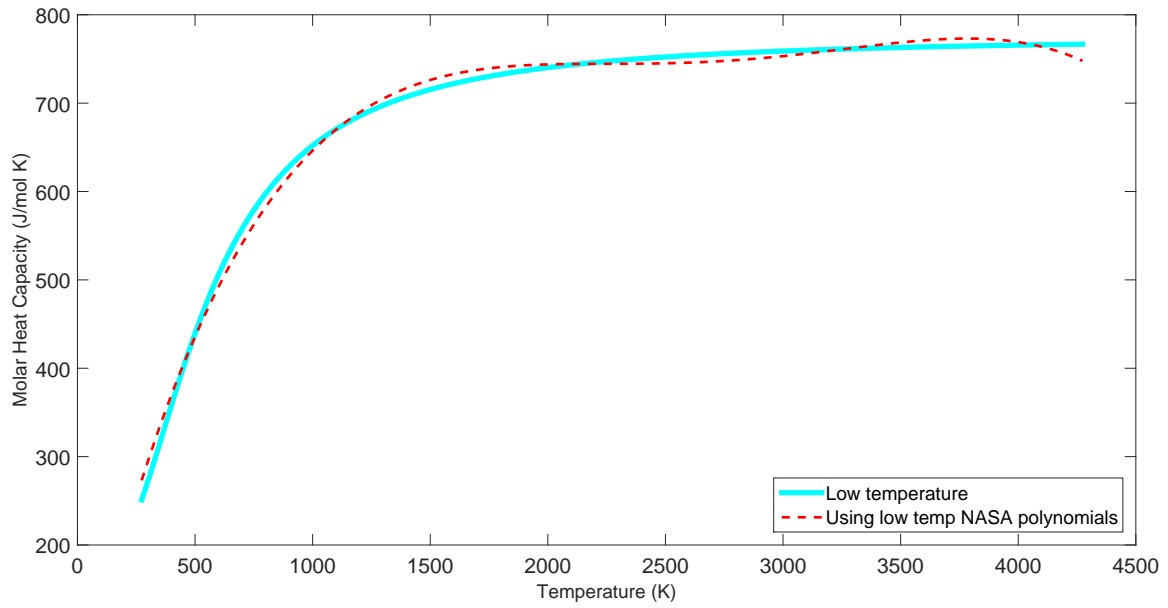
Figure 3.11: Comparison of Coal$_3$ molar heat capacity with the values calculated using NASA polynomials
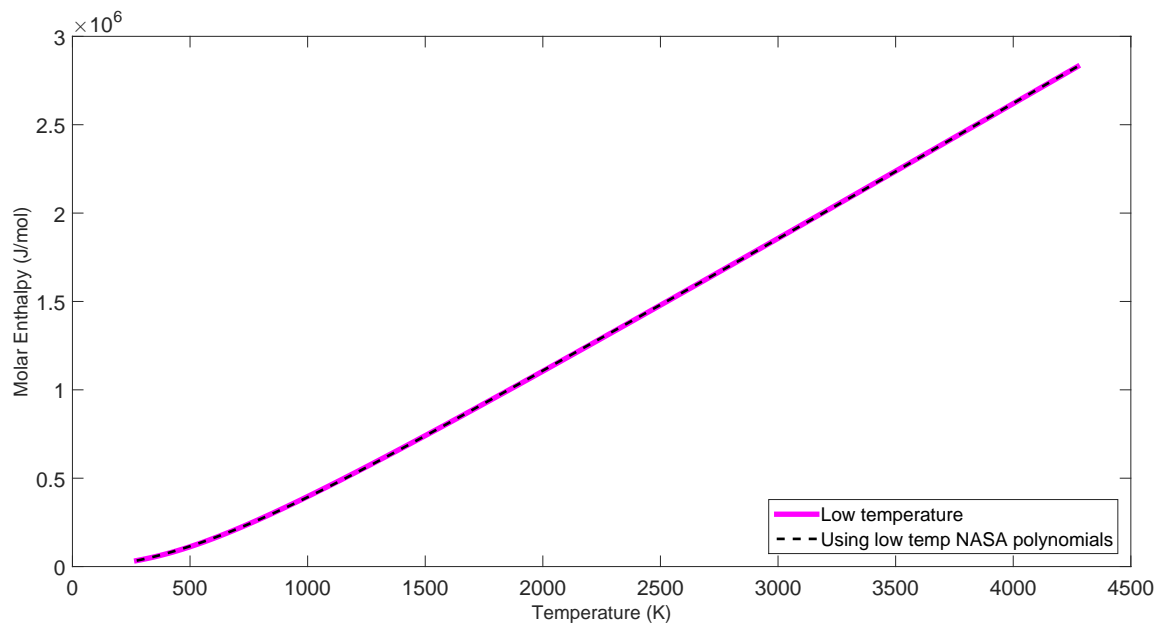
Figure 3.12: Comparison of Coal$_3$ molar enthalpy with the values calculated using NASA polynomials
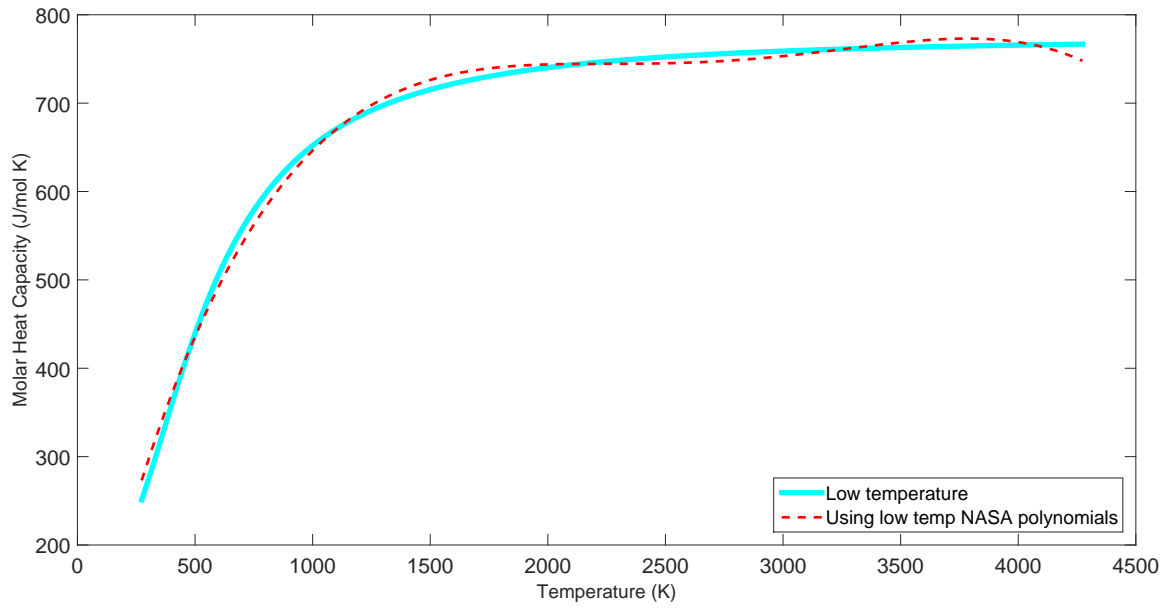
Figure 3.13: Comparison of Coal$_3^*$ molar heat capacity with the values calculated using NASA polynomials
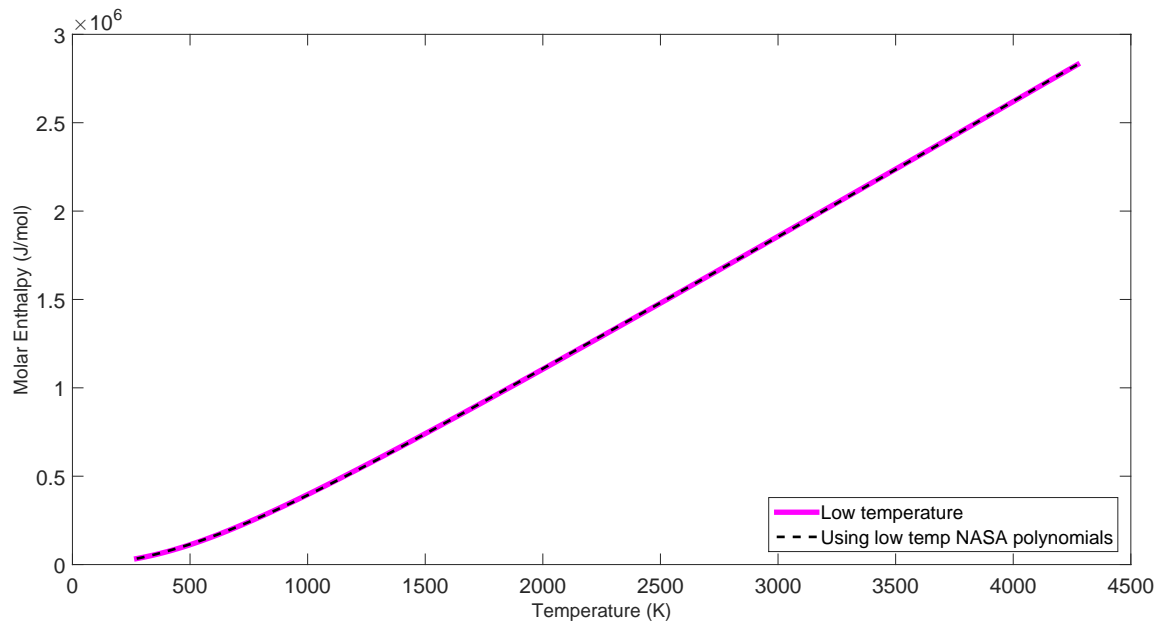
Figure 3.14: Comparison of Coal$_3^*$ molar enthalpy with the values calculated using NASA polynomials

Chapter 4

Results and Discussion

4.1 Experimental data

Results form thermogravimetric analysis (TGA) coupled with in-line FTIR are used to validate the model. Seven coals with different ultimate analysis as mentioned in Table 4.1 are tested for a predefined time-temperature history. Complete experimental setup and its description is provided by Solmon et al. The temperature history for which the experimental data obtained is as follows,

1. Sample coal is heated at 30 K/min in the He sweep gas to 150 °C as a part of drying process.

2. Devolatilization process is continued with a heating rate of 30 K/min upto 900 °C.

Table 4.1: Ultimate analysis of coals used for model validation.

S.No	Coal name	C	H	O	N	S
1	Beluah Zap	72.90	4.83	20.34	1.15	0.70
2	Wyodak	75.00	5.35	18.02	1.12	0.47
3	Illinois 6	77.70	5.00	13.51	1.37	2.38
4	Blind Canyon	80.70	5.76	11.58	1.57	0.37
5	Pittsburgh 8	83.20	5.32	8.83	1.64	0.89
6	Upper Freeport	85.50	4.70	7.51	1.55	0.74
7	Pocahontas	91.10	4.44	2.47	1.33	0.50

4.2 General trends and model comparisons

The model explained in section 3.3 is tested for seven different coals as indicated in Table 4.1. A predefined temperature history is assumed to compare the results with those of experiments. Model predicts the devolatilization behavior by discarding the drying period i.e., coal sample is heated from 150 °C to 900 °C without incorporating the drying phenomena. This is due to the fact that the ultimate analysis indicted in the Table 4.1 is on dry-ash-free basis. So, the model uses a heating rate of 30 K/min to heat the coal sample from 423 K to 1173 K

for a period of 50 min. Based on the coal structure and its changes during aging process it is know that for an increase in coal rank(described by the reflectance of vitrinite in Table 1.2) the carbon and aromaticity increases, while the oxygen content decreases. On this grounds it is expected that the content of oxygenated compounds should decrease with increase in rank, while hydrocarbons should increase. An another important trend in coal devolatilization process is the dependency of volatile matter on available hydrogen atoms to stabilize the formed radicals. Thus devolatilization stops when the abstractable hydrogen atoms found in aromatic compounds or in functional groups ceases.

The goal of any mathematical model is to predict the general trends of the system. To account for the above mentioned trends seven different coals are tested. Figure 4.1 depicts our thoughts on the residue left over for different coal ranks. Model shows deviations from residue predictions for certain coals, which is discussed in upcoming section but the Fig. 4.1 bounds to the rule of coal devoltilization as a function of abstractable hydrogen atoms. Exceptional cases are Illinois 6 and Pocahontas coals for which next section will give the answers for their deviations from devoltilization behavior.
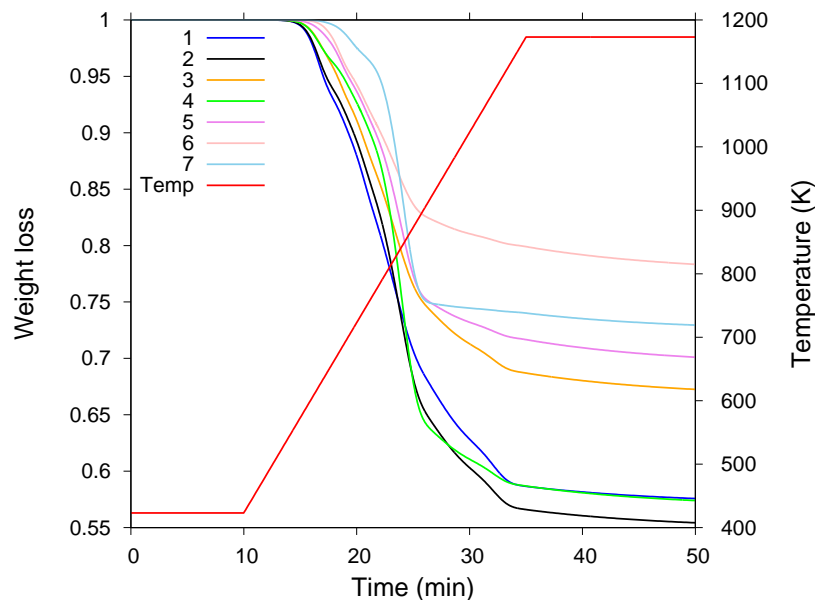
Figure 4.1: Residual curve for seven different coals [no's indicate the S.No in Table 4.1].

Similarly tests are conducted for major oxygenated compounds and hydrocarbon species. Figure 4.2 represents the ability of the model to capture the evolution of species with rank as a parameter. All oxygenated compounds quantity decreases during devolatilization for different coals, while methane shows a peak quantity for blind canyon coal. Since hydrogen content shows a peak for increasing rank, blind canyon coal exhibits maximum CH_4 content among seven coals tested. Similar trends appeared for hydrocarbon lumped species C_{2-5} as indicated in Fig. 4.3 with exceptional cases for Illinois 6 and Pocahontas coals. Predicting the exact trends of major gas species with rank as parameter during devolatilization makes the heat transfer model more accurate, when the primary objective is modelling of boiler. This is due to the fact that major species which are accounted in any radiation module are CO_2 and H_2O.
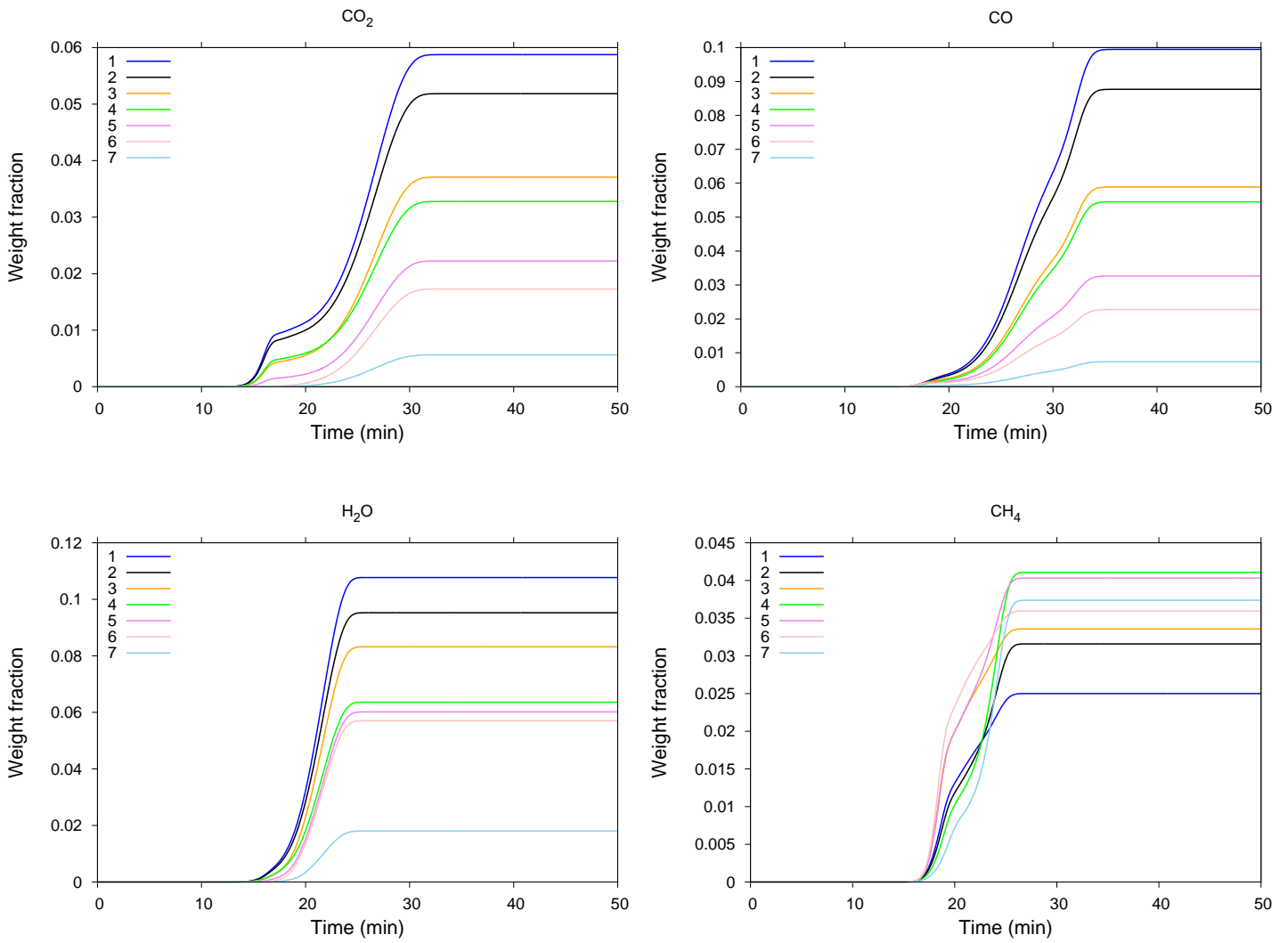
Figure 4.2: Gas profiles for seven different coals [no's indicate the S.No in Table 4.1].
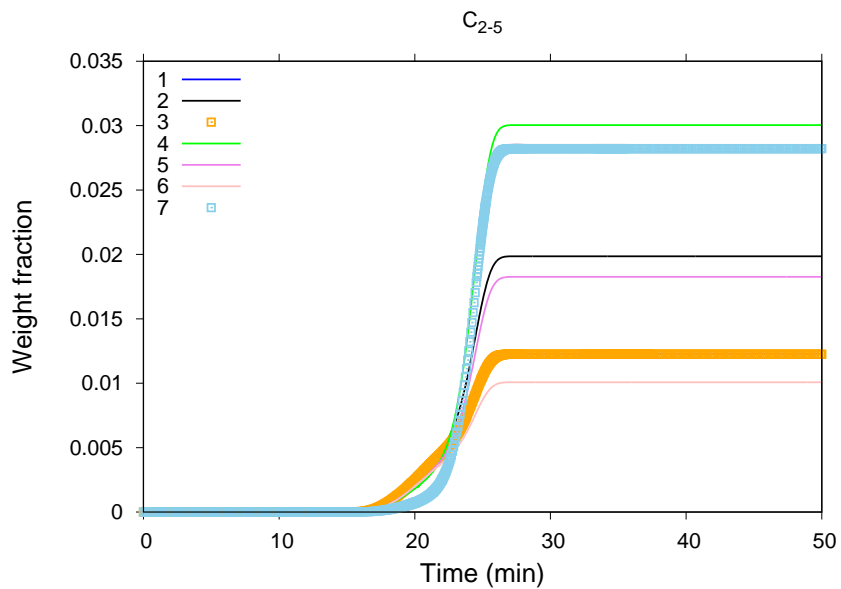

Figure 4.3: Lumped compound for hydrocarbon species[no's indicate the S.No in Table 4.1].

4.3   Experimental data and model comparison

As explained in the above sections model validation has been conducted for 7 different coals with a predetermined temperature history. Here comparative study of current model predictions and available experimental data has been presented only for the coal devolatilization and represented in the form of solid residue left over and major gas phase species (CO_2, CO, H_2O and CH_4). For understanding how the devolatilization and combustion processes could effect the release of major gas phase species Fig. 4.4 represents the breakdown of Pittsburgh coal devolatilization and combustion processes. Figure 4.4 represents that the summation of gas species quantity such as H_2O, CO_2, SO_2, Tar, CO, C_2H_4 and CH_4 will be enough to keep track of weight loss curve. Similar argument can be used for other coals except the contribution of other gas species can be expected. For example the Illinois No. 6 coal's residual curve major contributors are H_2O, CO_2, SO_2, Tar, CO, C_2H_4, CH_4, NH_3 and COS.
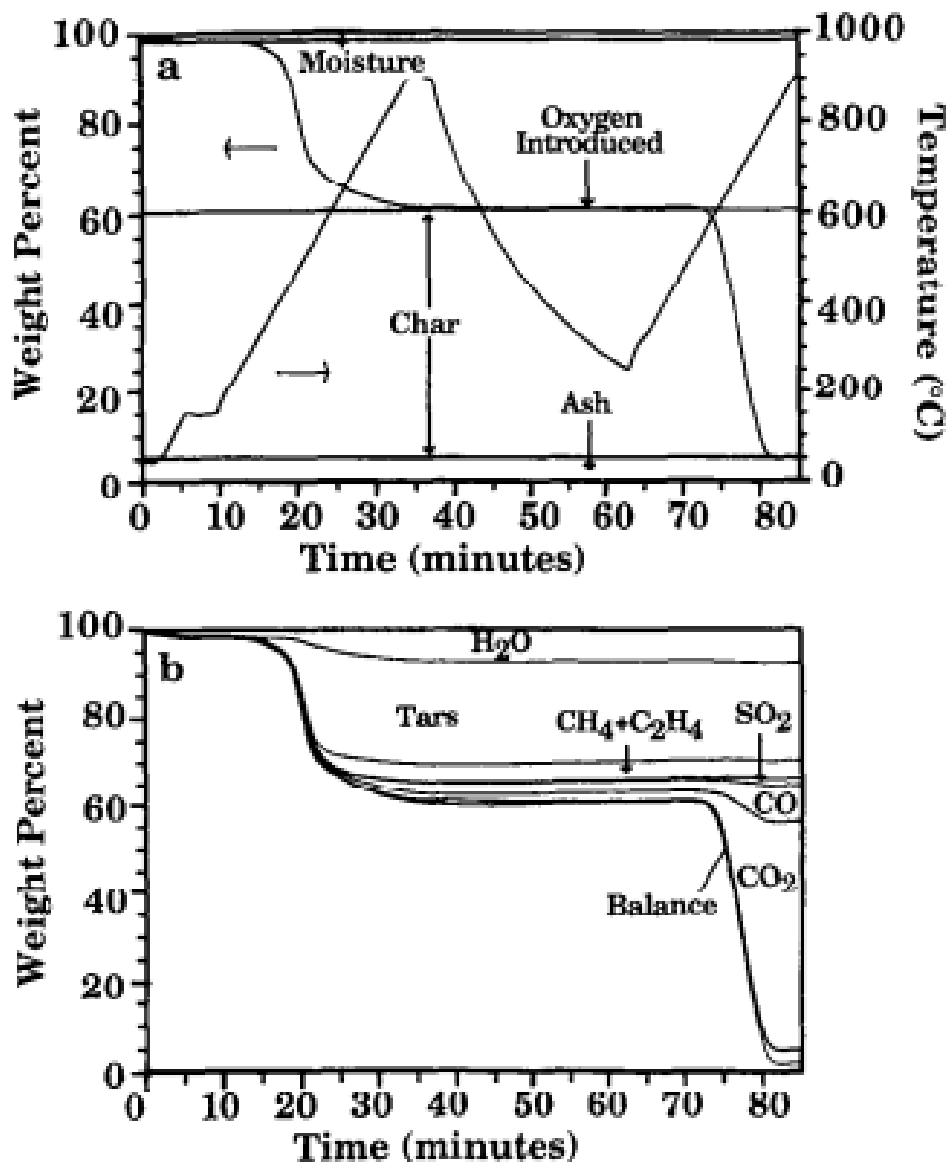
Figure 4.4: Devolatilization and combustion processes breakdown[13]

Residual plot of all Figs. 4.5 - 4.11 represents the amount of solid species left over or the amount of volatile matter released as a progress of time. The upper part of the weight loss curve is the volatile matter, while the lower area represents the amount of solid remaining.

Figure 4.5 represents the model validation for Beluah ZAP coal, which indicates the slight deviations of residual curve predicted by the current model with that of experiments. Predictions of gases CO and H_2O has been validated, however, CO_2 and CH_4 are under and over predicted respectively in Fig. 4.5 . Model results are also in reasonable agreement with the literature cited model [3]. Similarly Fig. 4.6 shows the capability of model in predicting the gas species fractions except in the case of CO_2 and CH_4, which are under and over predicted as in the case of Beluah ZAP coal but close match is observed in the residual plot.

Comparison of weight loss curves with experimental data has been provided for other coals in Figs. 4.7 - 4.9. Large deviations are observed in residual curve for the Illinois 6, Pittsburgh, Upper Freeport and Pocahontas coals represented by Figs. 4.7, 4.9, 4.10 and 4.11 respectively. Even the model lacks the capability in predicting the experimental weight loss curve for coals represented in the Figs. 4.7 - 4.9, it follows the trends to match the major gas species subjected to both rank as parameter and in quantitative terms. For each coal type (S.No 3 - 5 as indicate in Table 4.1) it has been observed that certain gas species predictions are in well agreement with those of experiments, while certain cases deviate but not to a large extent. A summary for these coals can be indicated as

1. For Illinois coal (Fig. 4.7) accurate predictions in H_2O, while slight under prediction of CO_2, CO and CH_4.

2. For Blind Canyon Utah coal (Fig. 4.8) accurate predictions in CO_2, slight over predictions in H_2O and marginal under prediction in CO and CH_4 with a close match in residual curve.

3. For Pittsburgh coal (Fig. 4.9) predictions in CH_4 and CO_2 are accurate, while CO and H_2O shows slight under and over predictions respectively.

Acute understanding of these trends indicates that a shift in close predictions of oxygenated compounds (CO_2, H_2 and CO) to hydrocarbons (CH_4) is observed from Fig. 4.9 . As explained above, Fig. 4.10 which is associated with Upper freeport coal indicates the close prediction of CH_4 gas and slight under prediction of oxygenated compounds. Similar nature is associated with the Pocahontas coal (Fig. 4.11) except that the oxygenated compounds are over predicted.

Other gas species such as C_2H_4 and other hydrocarbons are not used to validated the model. The reason can be explained as follows for hydrocarbon species, since all hydrocarbon species from C_2 - C_5 are lumped into a single compound (C_{2-5} indicated in Table 3.1) their quantity can be expressed as fraction of this lumped species to fit the experimental curve as close as possible if experimental data is available. This fitting process is based on trail and error. For ethylene, experimental data is available in literature cited by Ranzi et al [3], which represents the ethylene fraction formed for all coals is in the range of 0.0025 - 0.0035 weight fraction of overall gas species. When it comes to ethylene, considering a weight fraction of 15 -20% [3] of C_{2-5} species gives reasonable estimate of ethylene quantity during devolatilization. So, in this way the model developed is capable of predicting the higher hydrocarbons (C_2 - C_5), which again participate in the gas phase combustion processes.

When it comes to the reasons for deviations in residual curve for different coals, answer lies in the inaccuracy of tar predictions. The closest match in residual curve of Wyodak coal given by Fig. 4.6 is accompanied by accurate predictions in tar species as indicated in Fig. 4.12. Similarly for Beluah ZAP and Blind Canyon Utah coals close predictions in residual curves are achieved because of reasonable predictions in tar species quantity. From Figs. 4.5 - 4.13 a relation ship can be drawn between residual curve and tar species predicted by the model, which can be generalized as

- The accuracy in prediction of volatile matter largely depends on the predicted tar species quantity.

The above statement can be explained as, when a residual curve is under determined (or volatile matter under determined) it will have the same effect on tar species quantity i.e., tar species will also be under determined in that case. Similarly argument can be applied for explaining the case of over determined volatile matter, which happened for Beluah ZAP and Pocahontas coal form 7 test cases. From Figs. 4.5, 4.11, 4.12 and 4.13 we can infer that over prediction in volatile matter in supported by over predictions in tar quantity.
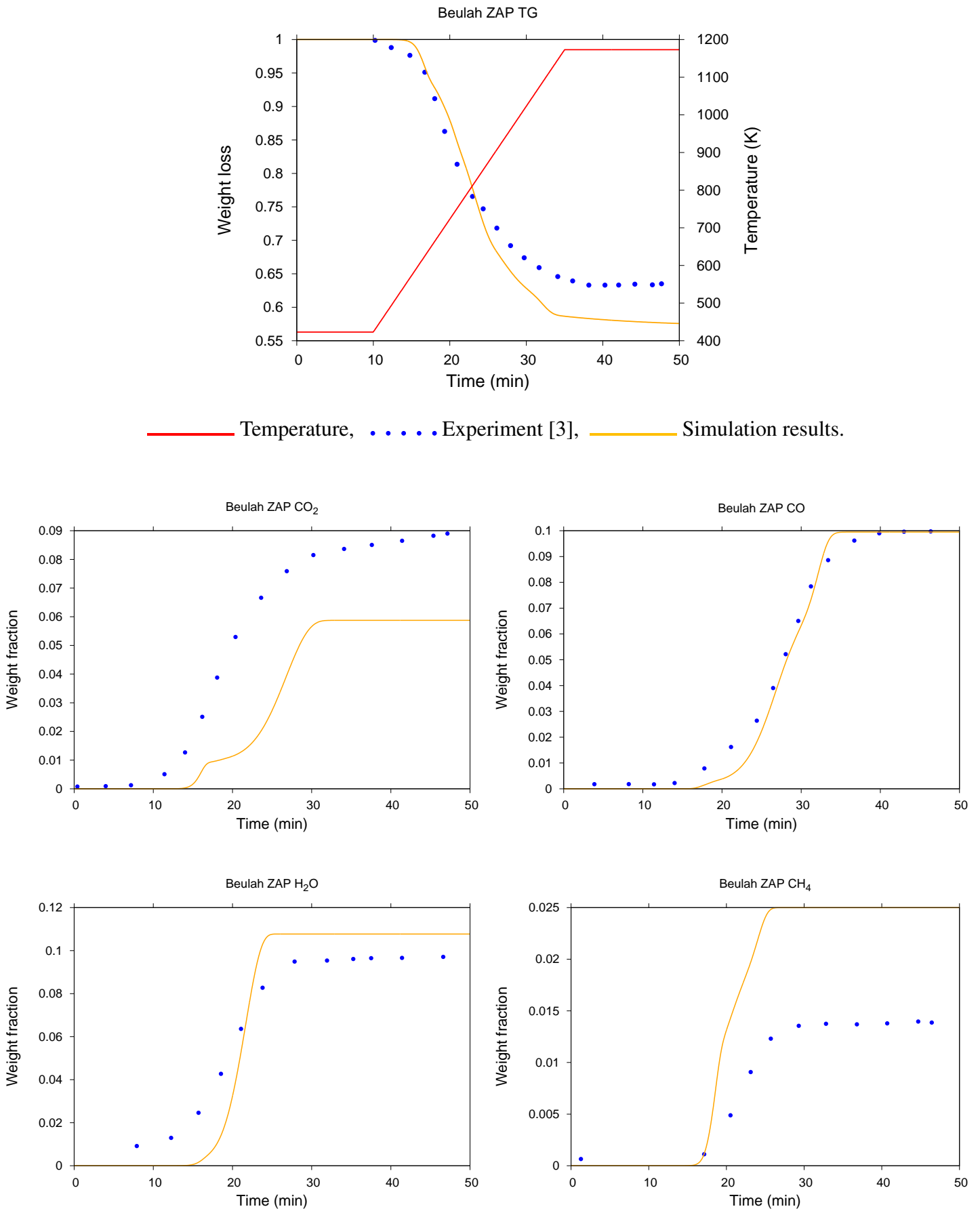
Figure 4.5: Model validation for thermogravimetric analysis(TG) of Beluah ZAP coal.
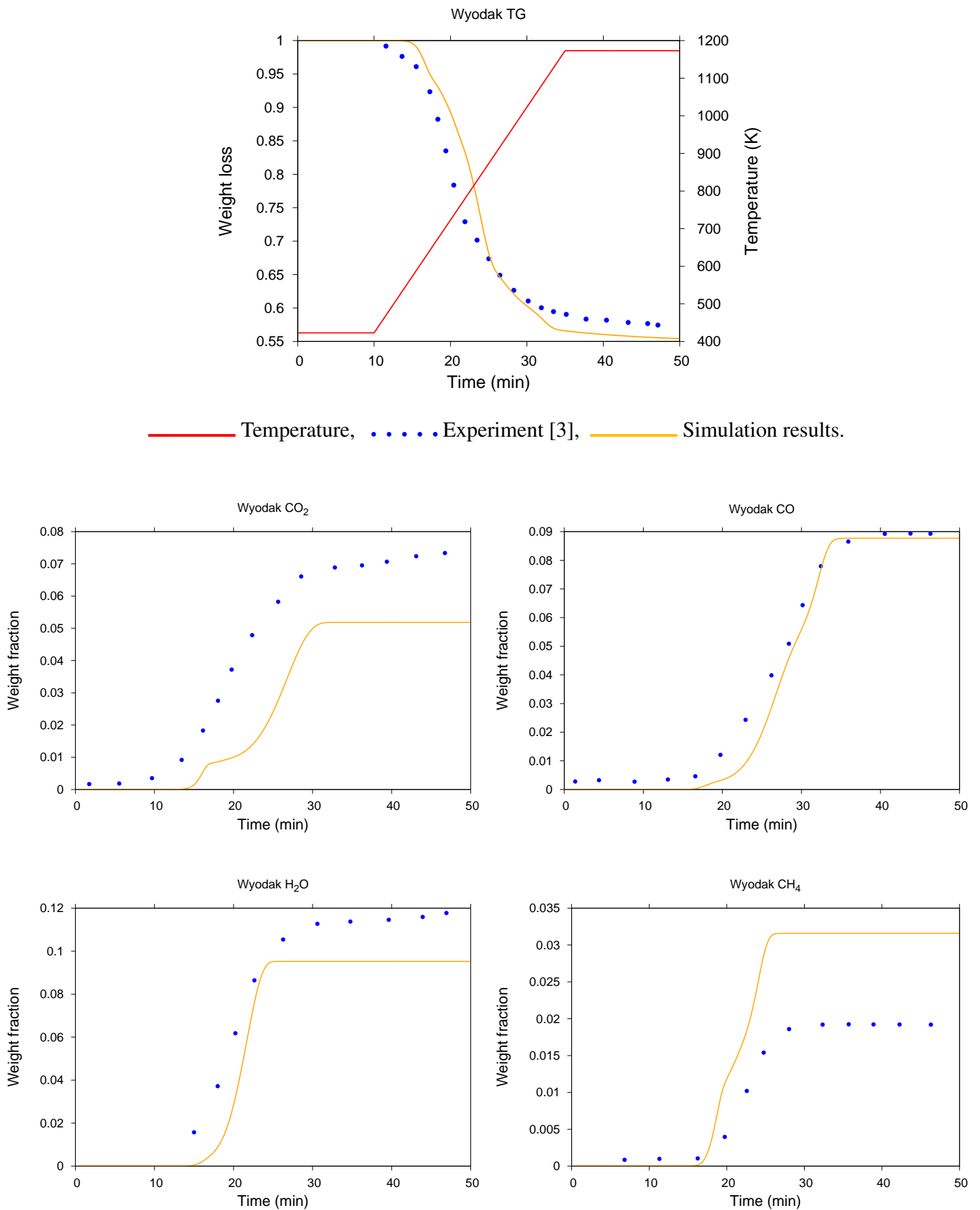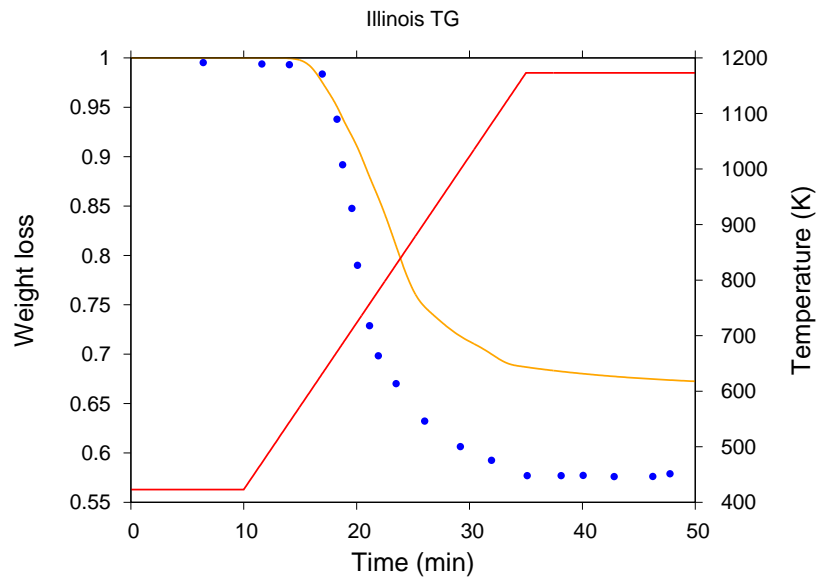
Figure 4.6: Model validation for thermogravimetric analysis(TG) of Wyodak coal.
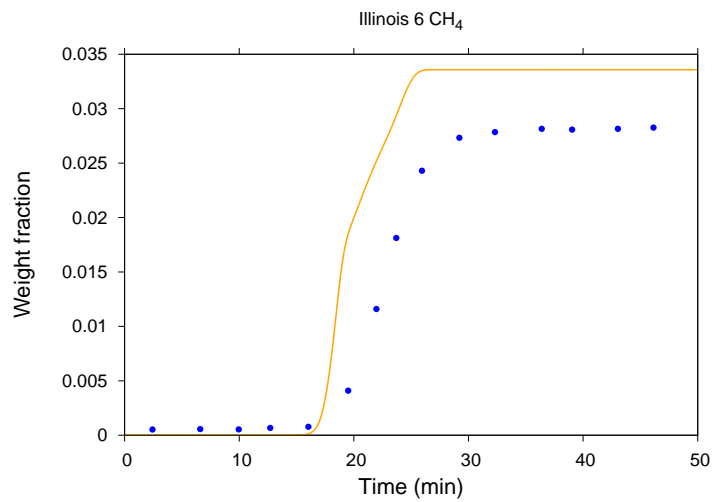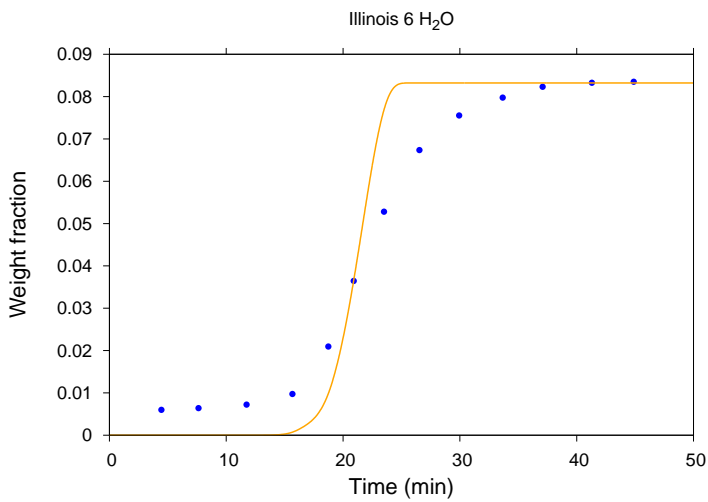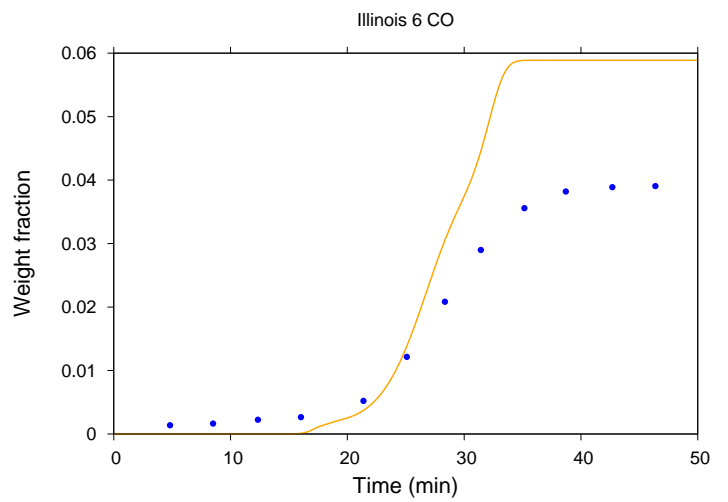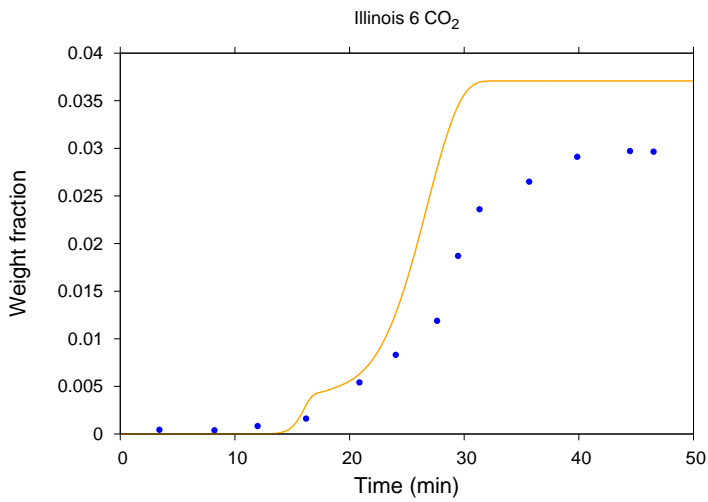
Figure 4.7: Model validation for thermogravimetric analysis(TG) of Illinois 6 coal.
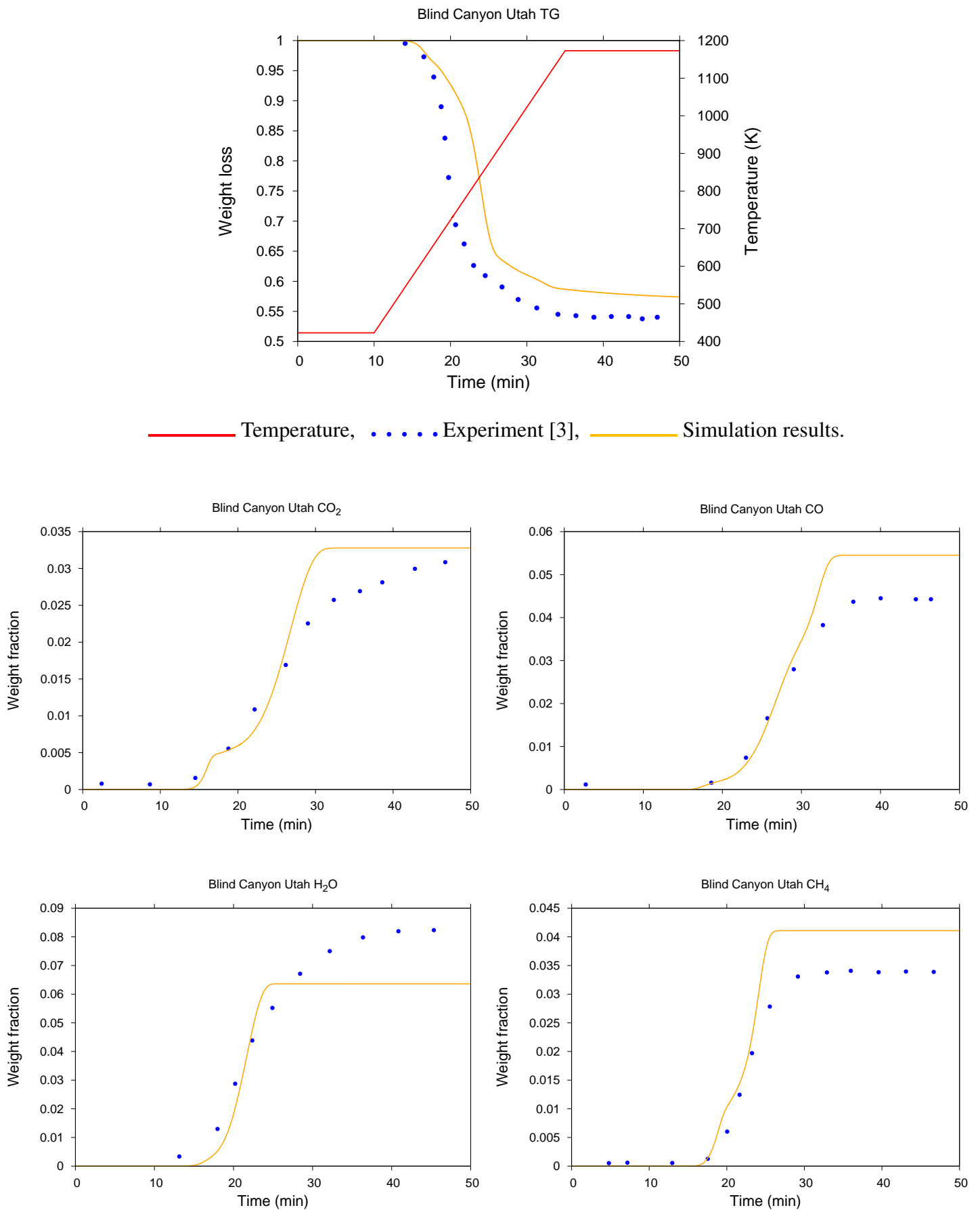
Figure 4.8: Model validation for thermogravimetric analysis(TG) of Blind Canyon Utah coal.
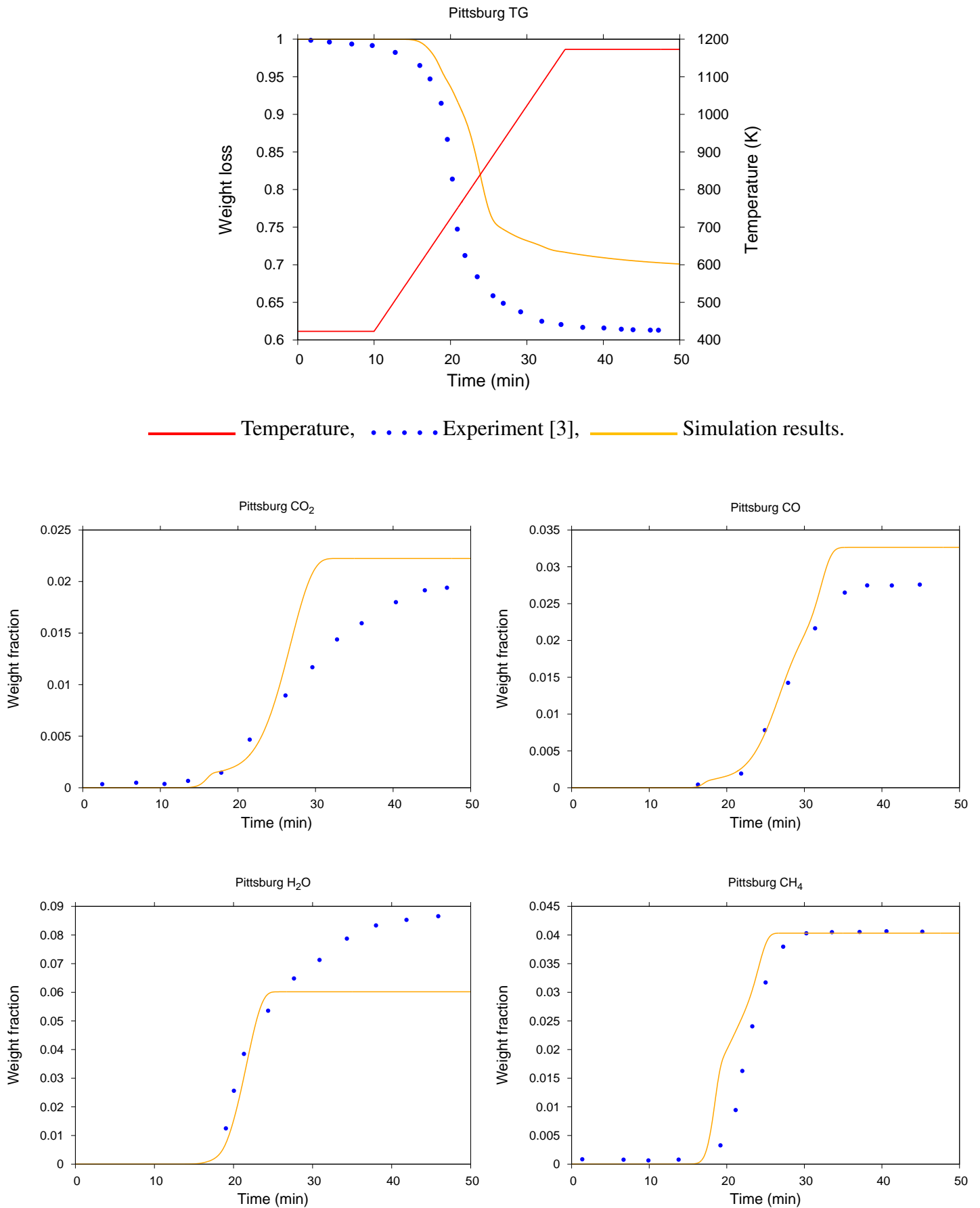
Figure 4.9: Model validation for thermogravimetric analysis(TG) of Pittsburg coal.
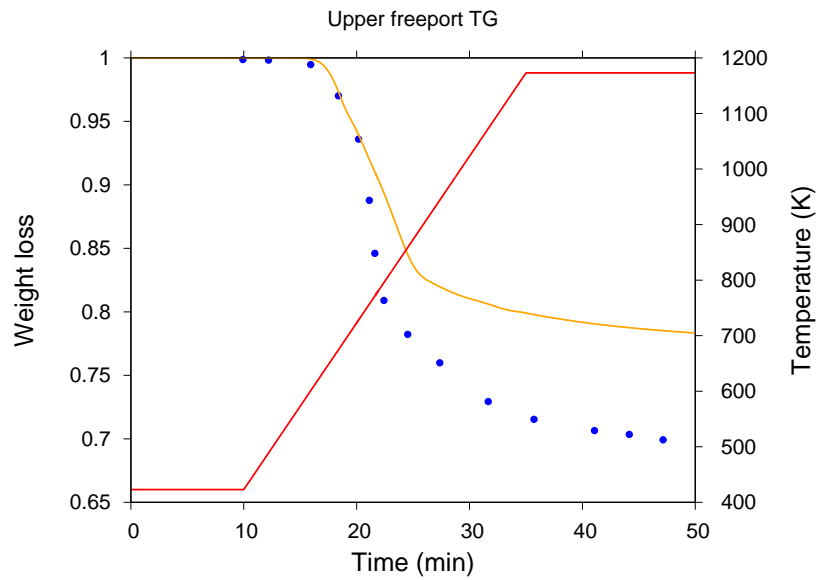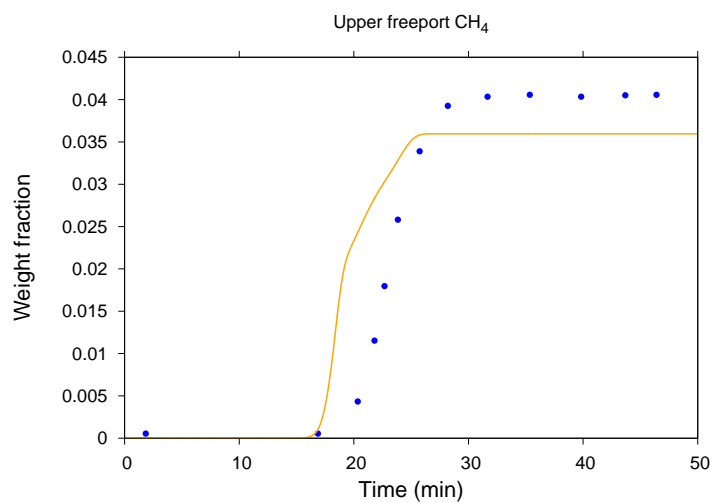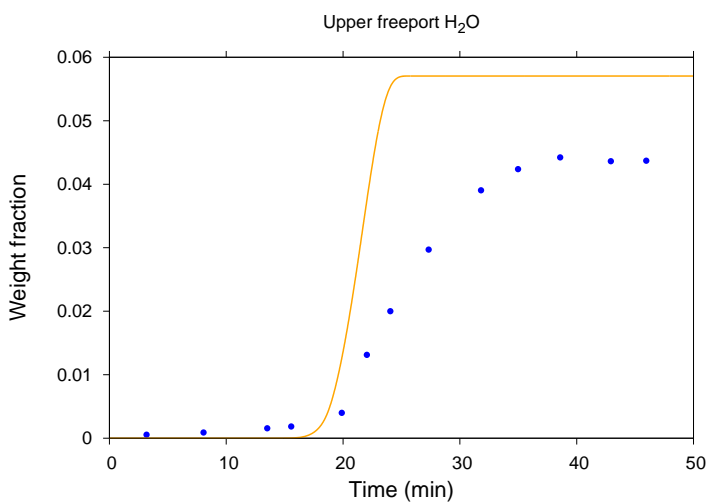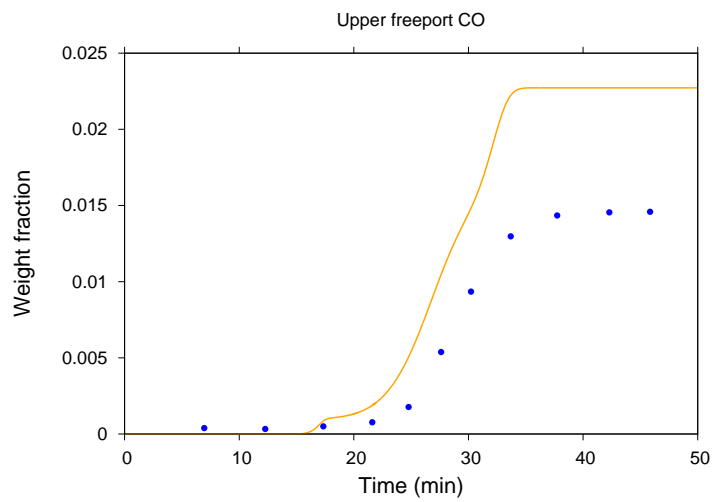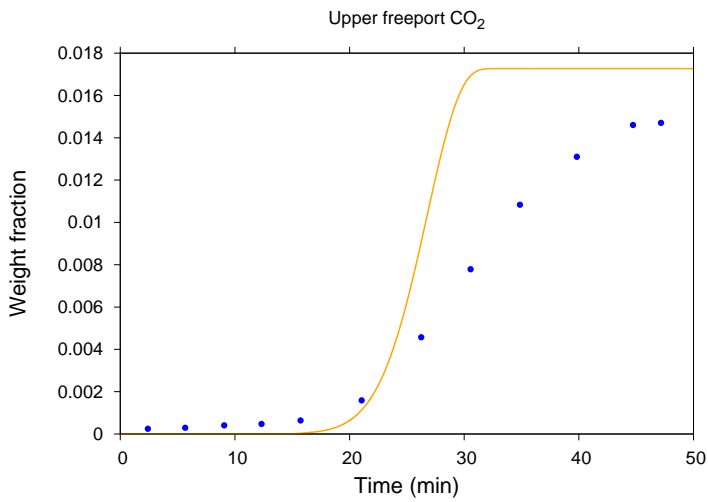
Figure 4.10: Model validation for thermogravimetric analysis(TG) of Upper Freeport coal.
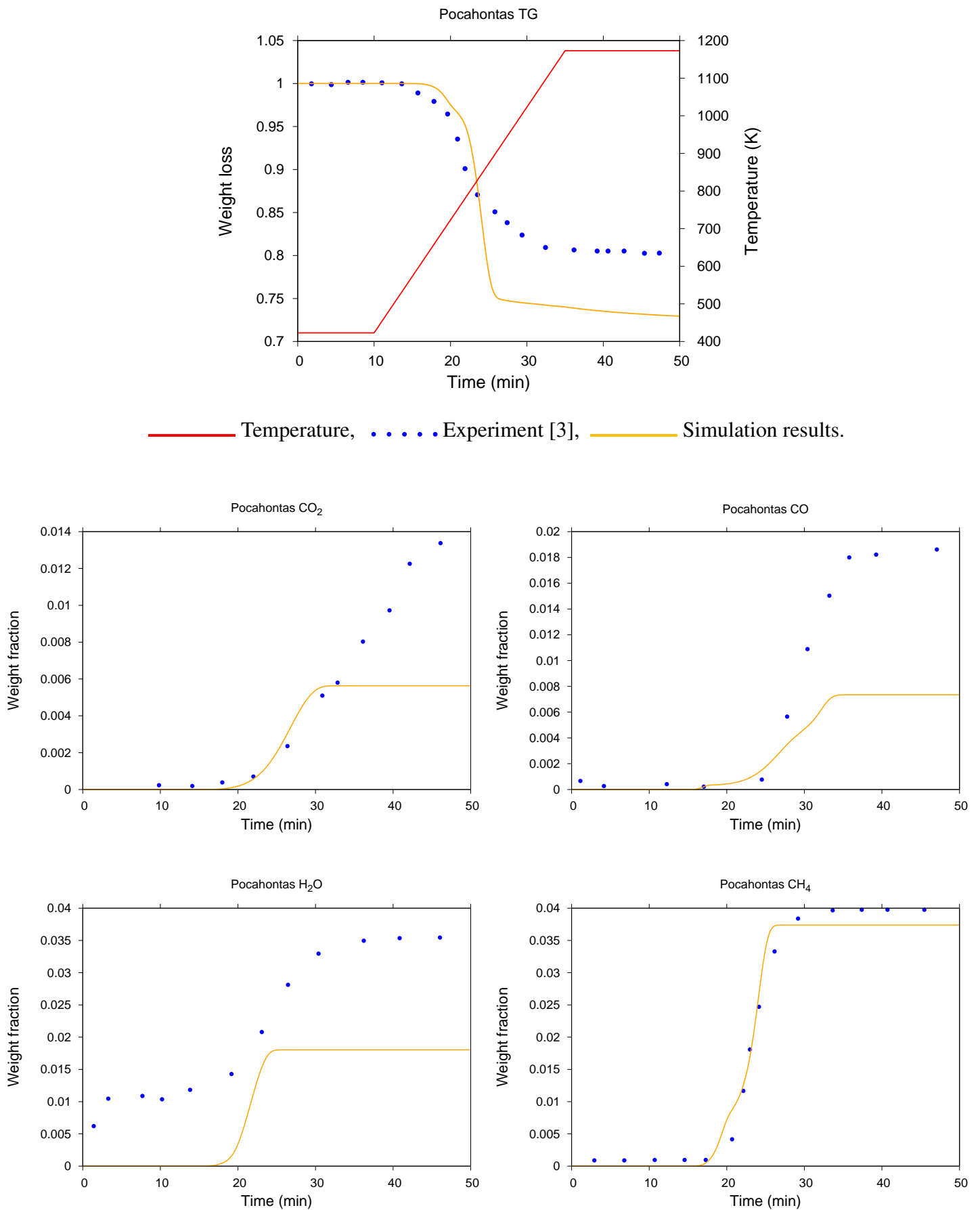
Figure 4.11: Model validation for thermogravimetric analysis(TG) of Pocahontas coal.

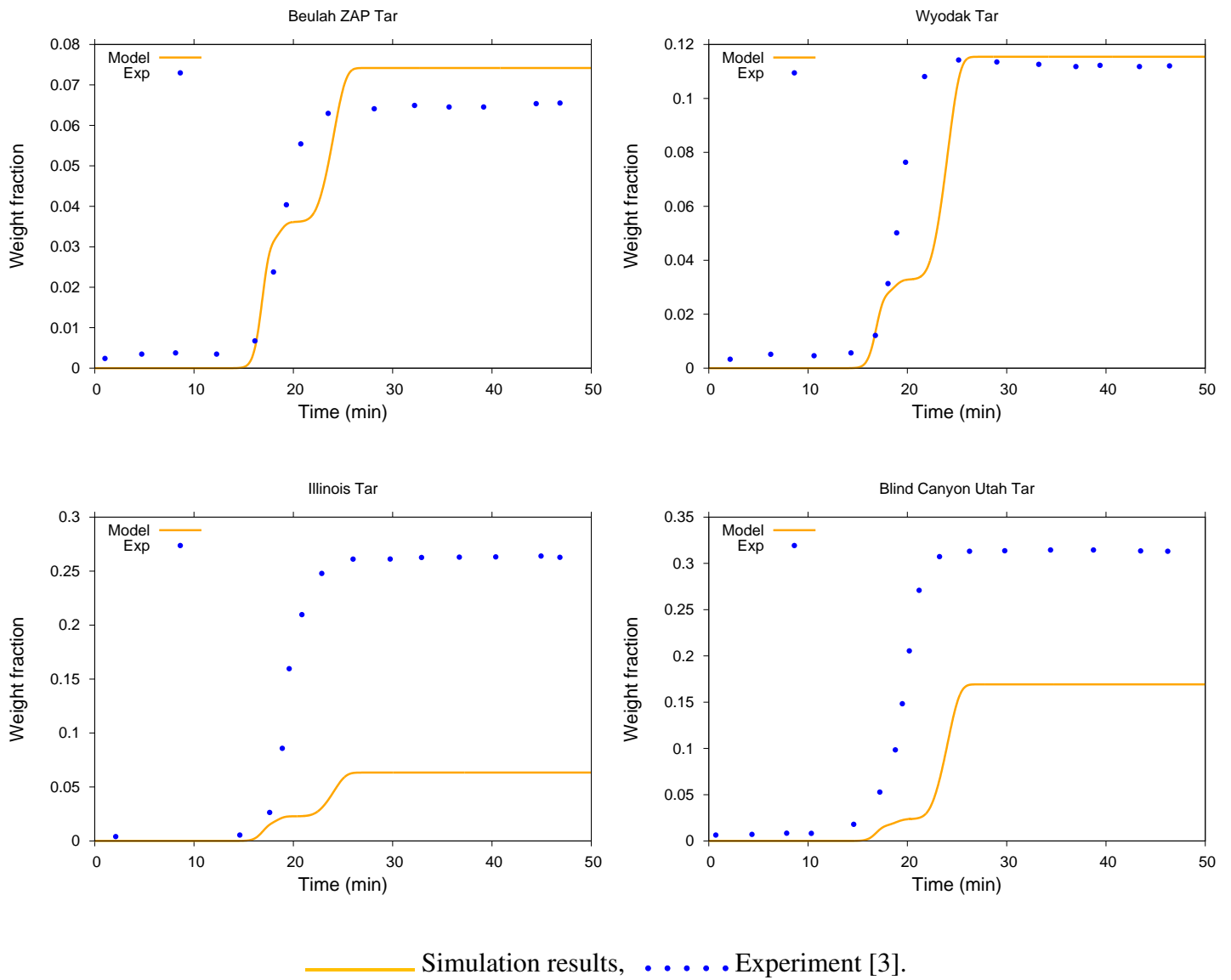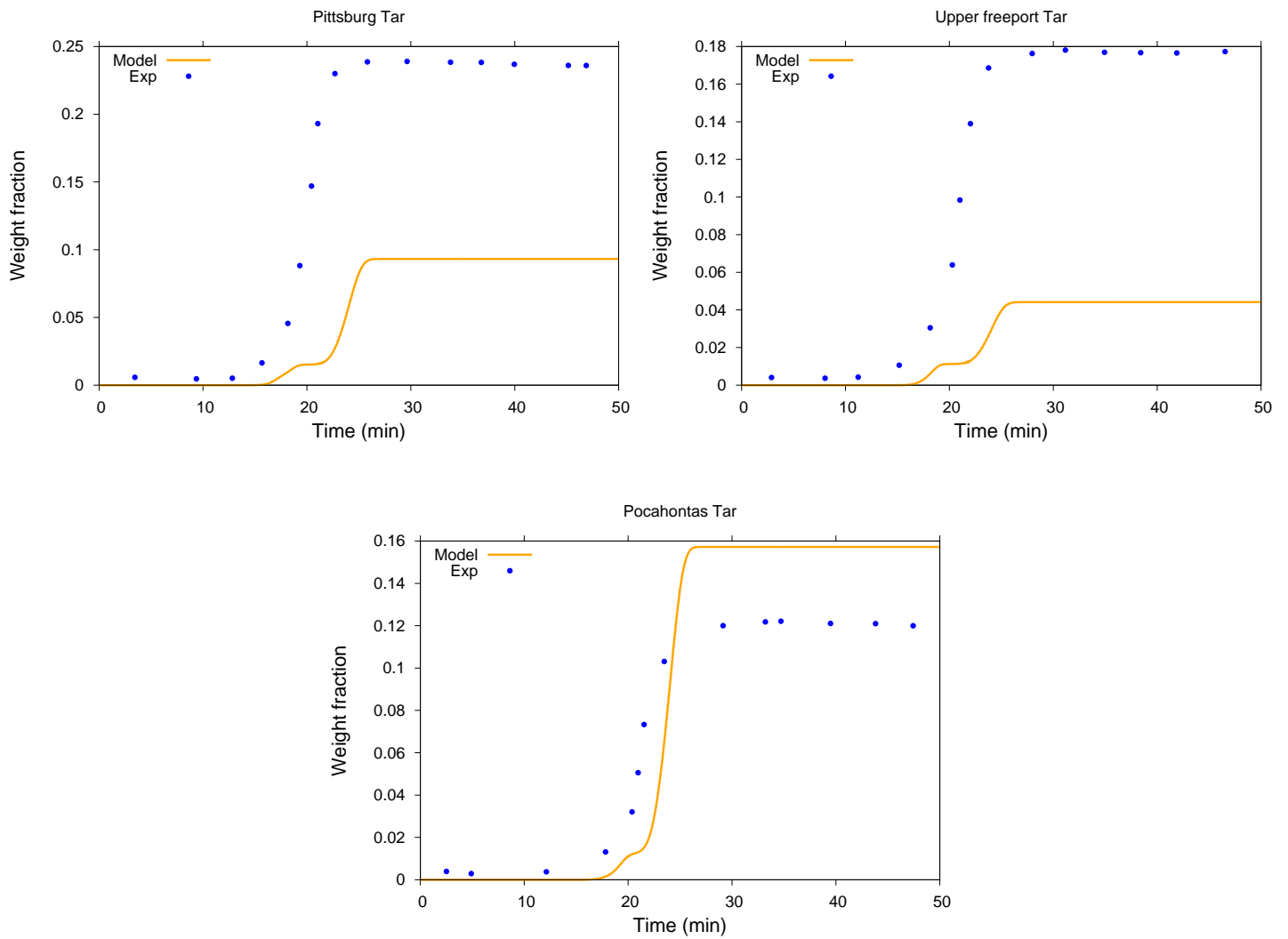Figure 4.12: Model validation for thermogravimetric analysis(TG) of 4 different coals for tar species.

Figure 4.13: Model validation for thermogravimetric analysis(TG) of 3 different coals for tar species.

Chapter 5

Conclusions

A predictive multi-step kinetic model has been implemented for the coal pyrolysis and as part of this work. Initial coal characterization is done using its ultimate analysis to different reference coals. These reference coals fractions are subjected to pyrolysis using a multi-step kinetic mechanism, which accounts for species behavior at low and high temperatures. Model validation has been conducted for different experimental data obtained form wide operating ranges (heating rate, coal rank, time and temperature). Reasonable fits are obtained for major gas species such as CO, CO_2, H_2O and CH_4. Model is able to predict the release of gas species with rank as parameter, which includes less oxygenated compounds for high rank coals while low quantity of hydrocarbons for low rank coals. Prediction in other hydrocarbons from C_2 to C_5 is accounted in the model provided if experimental data is available.

The deviations in predictive capabilities of the model for high rank coals is observed due the inaccuracies in the tar quantities predicted by the model. As the model is based on kinetic mechanism which are tested for certain stoichiometric coefficients, improvements in predictions of tar species can be obtained by tuning the coefficients of reactions and the kinetic parameters for the best fit towards experimental data.

Bibliography

[1] J. Lahaye, G. Prado, Fundamentals of the Physical-Chemistry of Pulverized Coal Combustion, 1987.

[2] W. Fuchs, A. G. Sandhoff, Theory of coal pyrolysis, Industrial & Engineering Chemistry (1942) 567–571.

[3] S. Sommariva, T. Maffei, G. Migliavacca, T. Faravelli, E. Ranzi, A predictive multi-step kinetic model of coal devolatilization, Fuel 89 (2) (2010) 318–328. doi:10.1016/j.fuel.2009.07.023.

[4] T. Maffei, P. D. I. Milano, Kinetic Model of Coal Combustion (753429) (2013) 189.

[5] T. H. F. K. Lee Smith, L. Douglas Smoot, R. J. Pugmire, The Structure and Reaction Processes of Coal, 1994.

[6] E. Suuberg, Approximate Solution Technique for Nonisothermal, Gaussian Distributed Activation Energy Models, COMBUSTION AND FLAME 50 (1983) 243–245.

[7] G. Song, L. Shen, J. Xiao, L. Chen, Estimation of Specific Enthalpy and Exergy of Biomass and Coal Ash, Energy Sources, Part A: Recovery, Utilization, and Environmental Effects 35 (9) (2013) 809–816. doi:10.1080/15567036.2011.586983.

[8] D. Genetti, An advanced model of coal devolatilization based on chemical structure, Master's thesis (1999).

[9] P. R. Solomon, M. A. Serio, E. M. Suuberg, Coal pyrolysis: Experiments, kinetic rates and mechanisms, Progress in Energy and Combustion Science 18 (2) (1992) 133–220.

[10] P. R. Solomon, D. G. Hamblen, R. M. Carangelo, M. A. Serio, G. V. Deshpande, General Model of Coal Devolatilizationt, Energy & Fuels 2 (4) (1988) 405–422.

[11] M. A. Serio, D. G. Hamblen, J. R. Markham, P. R. Solomon, Kinetics of Volatile Product Evolution in Coal Pyrolysis : Experiment and Theory, Energy & Fuels 1 (21) (1987) 138–152.

[12] Y. Zhao, M. a. Serio, R. Bassilakis, P. R. Solomon, A method of predicting coal devolatilization behavior based on the elemental composition, Symposium (International) on Combustion 25 (1) (1994) 553–560. doi:10.1016/S0082-0784(06)80685-5.

[13] P. R. Solomon, M. a. Serio, A characterization method and model for predicting coal conversion behaviour. Reply to Herod, A. and Kandiyoti, R. Fuel 1993, 72, 469, Fuel 73 (8) (1994) 1371. doi:10.1016/0016-2361(94)90318-2.

[14] R. J. Kee, M. E. Coltrin, P. Glarborg, Chemically reacting flow: Theory and Practice, John Wiley & Sons, 2003.

[15] K. C. S. D. Jennifer M.K.O'Keefe, A Bechtel, On the fundamental difference between coal rank and coal type, International Journal of Coal Geology 118 (2013) 58–87.

[16] G. James, The chemistry and technology of coal. Second edition, Vol. 36, 1995.

[17] A. W. Scaroni, M. R. Khan, S. Eser, L. R. Radovic, Coal Pyrolysis, 2000.

[18] J. P. Mathews, V. Krishnamoorthy, E. Louw, A. H. N. Tchapda, F. Castro-Marcano, V. Karri, D. a. Alexis, G. D. Mitchell, A review of the correlations of coal properties with elemental composition, Fuel Processing Technology 121 (2014) 104–113. doi:10.1016/j.fuproc.2014.01.015.

[19] D. A. Bell, B. F. Towler, M. Fan, Coal Gasification and its Applications, William Andrew, 2011.

[20] L. D. Smoot, P. Smith, Coal Combustion and Gasification, 1985. doi:10.1007/978-1-4757-9721-3.

[21] D. B. Anthony, J. B. Howard, H. C. Hottel, H. P. Meissner, Rapid devolatilization of pulverized coal, Symposium (International) on Combustion 15 (1) (1975) 1303–1317.

[22] R. H. Schlosberg (Ed.), Chemistry of Coal Conversion, 1985th Edition, Springer Science+Business Media, LLC, 1985.

[23] P. M. B. P. Williains, A, J. Norman, Keynote address to the Coal Utilization and the Environmenatal Conference (May 18-20, 1993).

[24] M. F. N. W. M. Gregory P. Smith, David M.Golden, GRI-MECH 3.0, http://combustion.berkeley.edu/gri-mech/version30/text30.html.

[25] D. Merrick, Mathematical models of the thermal decomposition of coal 62 (1982) 540–546. doi:10.1016/0016-2361(83)90223-5.

Appendix-I

```
THERMO
 500.000  1000.000  5000.00
O2                TPIS89O  2                G   200.000  3500.000  1000.000     1
 3.28253784E+00 1.48308754E-03-7.57966669E-07 2.09470555E-10-2.16717794E-14    2
-1.08845772E+03 5.45323129E+00 3.78245636E+00-2.99673416E-03 9.84730201E-06    3
-9.68129509E-09 3.24372837E-12-1.06394356E+03 3.65767573E+00                   4
CN                HBH92 C   1N   1          G   200.000  6000.000  1000.000     1
 0.37459805E+01 0.43450775E-04 0.29705984E-06-0.68651806E-10 0.44134173E-14    2
 0.51536188E+05 0.27867601E+01 0.36129351E+01-0.95551327E-03 0.21442977E-05    3
-0.31516323E-09-0.46430356E-12 0.51708340E+05 0.39804995E+01                   4
N2                121286N   2                G   300.000  5000.000  1000.000     1
 0.02926640E+02 0.14879768E-02-0.05684760E-05 0.10097038E-09-0.06753351E-13    2
-0.09227977E+04 0.05980528E+02 0.03298677E+02 0.14082404E-02-0.03963222E-04    3
 0.05641515E-07-0.02444854E-10-0.10208999E+04 0.03950372E+02                   4
END
```

Format specifications for NASA polynomials

There are four lines for specifying the thermodynamic data for any given chemical species, which are listed in Table 5.1.

Table 5.1: Format specification for species data in the thermodynamic data

Line No.	Content	Column reserved
line 1	Species name (must start from column 1)	1-18
	Data (not used)	19-24
	Atomic symbols 4(2A,3I)	25-44
	Species phase (S,L,G, or)	45
	Low temperature (Fortran scientific notation)	46-55
	High temperature (Fortran scientific notation)	55-65
	Common temperature	66-73
	Comment (not used)	74-78
	Line number 1	80
line 2	Coefficients (upper temperature) a_1 to a_5 (5E15.0)	1-75
	line number 2	80
line 3	Coefficients a_6 to a_7 upper temperature (2E15.0)	1-75
	Coefficients a_1 to a_3 lower temperature (2E15.0)	
	Line number 3	80
line 4	Coefficients a_4 to a_7 (4E15.0) lower temperature	1-60
	Line number 4	80

Values of E/R (K) (upper figure) and σ/R (K) (lower figure)[b]

Group–pool[a]; A (s^{-1})	Beulah Zap lignite	Wyodak Anderson subbit.	Illinois No. 6 hvb	Blind Canyon hvb	Lewiston Stockton hvb	Pittsburgh No. 8 hvb	Upper Freeport mvb	Pocahontas No. 3 lvb
CO_2–XL	18 000	18 000	20 500	21 000	21 250	21 500	22 000	23 000
5.0×10^{12}	1500	1500	3000	4000	3500	3600	2000	2500
CO_2–L	23 500	24 000	24 750	25 000	26 000	26 500	27 000	28 000
5.0×10^{13}	2000	2500	1750	1250	3000	3000	3000	2500
CO_2–T	31 000	32 000	32 000	32 000	32 000	32 000	32 000	33 500
7.5×10^{12}	3000	2800	2750	5000	3200	2500	2500	2700
CO–L	24 500	24 750	25 000	25 000	25 500	26 000	28 000	29 000
5.0×10^{12}	3000	2500	1000	1250	1100	1250	750	1250
CO–T	30 000	30 250	30 500	30 500	30 500	30 750	31 500	32 000
5.0×10^{12}	3000	3000	2000	2000	1600	1900	1400	1500
CO–XT	39 000	39 750	40 000	40 000	40 000	40 000	40 000	40 000
2.0×10^{14}	2500	2500	3000	2500	3000	2800	2250	3200
CH_4–L	28 000	28 000	28 000	28 000	28 000	28 000	28 750	29 500
3.0×10^{13}	2500	2250	1800	1500	1200	1300	800	750
CH_4–T	32 000	32 000	32 000	32 000	32 000	32 000	32 000	33 000
6.0×10^{13}	2200	2000	2200	2200	2200	2200	2000	1700
H_2O–XL	16 500	17 000	18 000	0	0	0	0	0
5.0×10^{12}	1500	1500	1800	0	0	0	0	0
H_2O–L	23 000	24 250	25 000	25 000	25 500	26 000	27 500	28 000
5.0×10^{12}	2700	2500	1500	1250	1250	1250	1250	1250
H_2O–T	31 000	31 000	32 000	32 000	32 000	32 000	34 000	35 000
2.0×10^{14}	3500	3500	2800	2500	2500	2500	4000	3000
Tar–BB	26 000	26 000	26 000	27 000	27 250	27 500	28 250	29 000
1.0×10^{14}	1000	1000	750	1250	1000	1250	1250	750

[a]BB, bridge breaking; L, loose; T, tight; XL, extra-loose; XT, extra-tight
[b]R is the gas constant

Figure 5.1: Argonne premium coals [13]